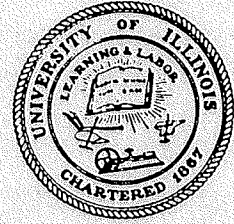


Metals Process Simulation Laboratory
Department of Mechanical and Industrial Engineering
University of Illinois
1206 West Green Street
Urbana, IL 61801
217-333-6919
217-244-6534 (FAX)



Single Crystal Process Modeler Program

David D. Goettsch

and

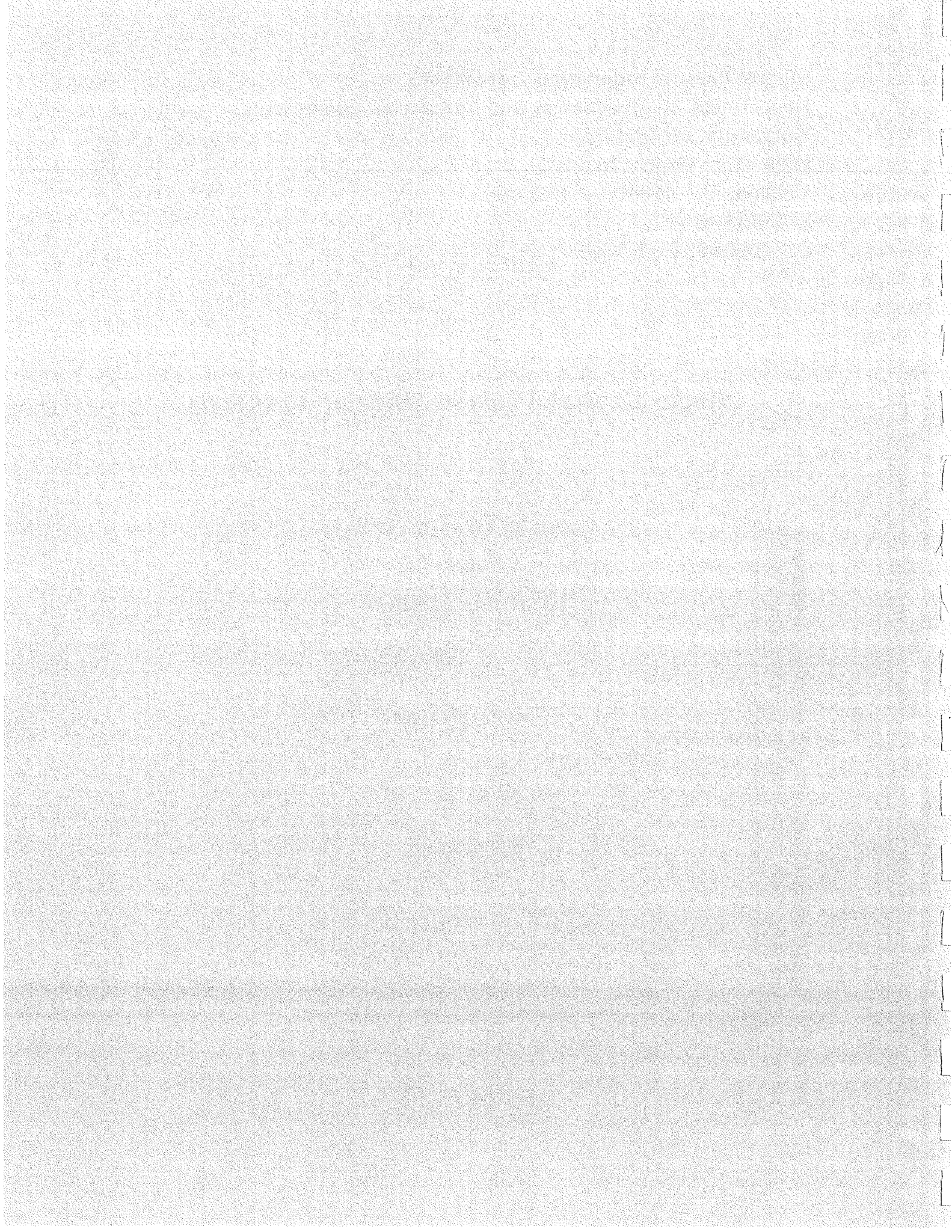
Brian G. Thomas

Final Report

submitted to

PCC Airfoils, Inc.
Signature Square Suite 290
25201 Chagrin Blvd.
Beachwood, Ohio 44122

February, 1989



Metals Process Simulation Laboratory
Department of Mechanical and Industrial Engineering
University of Illinois
1206 West Green Street
Urbana, IL 61801
217-333-6919
217-244-6534 (FAX)



Single Crystal Process Modeler Program

David D. Goettsch
and
Brian G. Thomas

Final Report

submitted to

PCC Airfoils, Inc.
Signature Square Suite 290
25201 Chagrin Blvd.
Beachwood, Ohio 44122

February, 1989

1.0 PROJECT OBJECTIVES

The overall objective of the University of Illinois for this project was to develop, with the assistance of PCC Airfoils and SDRC, a mathematical modeling facility to accurately simulate the solidification of a single crystal airfoil. The finite-element model to be developed would accept three-dimensional mesh data of a turbine blade or vane, gating, and mold material, and processing conditions and simulate temperature development during the solidification process. This program could then be used to predict defect development and assist designers to optimize the investment casting process for new blade designs. Specific objectives of the University of Illinois are as follows:

1.1 Establishment of computational facility

Establish a computational facility (computer workstation) at the University of Illinois at Urbana-Champaign that is capable of running FACET, and TOPAZ through an interface with I-DEAS.

1.2 Development of moving boundary capability

Add the ability to handle the moving boundary conditions of the single crystal process to the TOPAZ/FACET program. This includes the adaptation of FACET to generate appropriate view factors for each surface location at appropriate times. It also includes the modification of TOPAZ to accept this information and run the moving boundary simulation.

1.3 Determination of heat transfer mechanisms

Determine which heat transfer mechanism(s) in the single crystal casting process are most important, and incorporate these into the model.

1.4 Experimental verification of model

Use the data generated from experiments casting simple geometries at PCC Airfoils to verify the accuracy of the simulation procedure.

2.0 SUMMARY OF WORK COMPLETED

2.1 Development of moving boundary capability

A computational facility has been established at UIUC that is capable of running realistic heat flow simulations of the directional solidification process for single crystal airfoils using versions of FACET, and TOPAZ. The facility is part of the Metals Process Simulation Laboratory in 223C M.E.L. and consists of a MicroVax II GPX computer workstation. It is networked to Macintosh II microcomputers (as graphics terminals), a laser printer, and an ethernet link to the UIUC campus network, which has access to networks and computers throughout the country, including the Cray X/MP supercomputer at UIUC.

2.2 Development of moving boundary capability

The ability to handle the moving boundary conditions of the single crystal process has been added into the TOPAZ/FACET program. This includes the adaptation of FACET to generate appropriate view factors for each surface location at appropriate times. It also includes the modification of TOPAZ to accept this information and to adjust view factors and temperatures at each time to simulate the furnace environment observed by each portion of the blade.

This was achieved through the development of two separate methods. The first method, referred to as the "simple wall method", is a fast, simple procedure capable of economical moving boundary simulations, but lacks accuracy when realistic baffle configurations and furnace temperatures are modelled.

A second procedure, the novel "view factor exchange method", has also been developed and implemented into FACET/TOPAZ as part of this project. Its name derives from its unique methodology for determining appropriate view factors at each time step in TOPAZ with results from just a single FACET run, with considerable savings in computation and storage over other proposed methods. This

method has been tested against analytical results (using another view factor program developed in this project) and been proven to be an accurate modeling method for simulating directional solidification in industrial furnaces. The remaining chapters of this report give details regarding the theory behind these methods, modifications made to FACET and TOPAZ, the procedure used to run the programs, verification simulations against an analytical solution method, and three separate heat flow simulations.

2.3 Determination of heat transfer mechanisms

The most important heat transfer mechanism governing temperature development in the directionally solidifying blade has been determined to be radiation. To achieve an accurate simulation, research with the model has proven that the entire interior of the furnace must be modelled as accurately as possible. The final simulation, described in Chapter 5.3, includes the effects of:

- 1) the presence of the feeding system including pour cup and runners,
- 2) occasional obstruction of mold surfaces caused by the two separate baffles, (inner and outer)
- 3) radiation from the furnace interior into both baffles, and model simulation of temperature development in both baffles,
- 4) varying withdrawal rate over time to match experimental conditions,
- 5) independent variation of susceptor and cooling chamber emissivity, using emissivity of less than one in the cooling chamber, and
- 6) simulation of the collapse and disappearance of the inner baffle after it hits the cup.

2.4 Experimental verification of model

The model was used to simulate the temperature data generated from thermocouples placed in experimental castings of simple cylindrical blades cast in clusters at PCC Airfoils. The predicted temperatures (using the simulation that incorporated the effects described above and in Chapter 5.3), show remarkable correlation

with the experimental results, considering the uncertainties in the data, and the over-simplifications made in this two-dimensional model simulation.

Prepared by:

David D. Goettsch
Research Assistant

and

Dr. Brian G. Thomas
Principal Investigator

Date _____

TABLE OF CONTENTS

	PAGE
INTRODUCTION.....	1
1. LITERATURE REVIEW.....	7
2. THEORY.....	13
2.1 FACET VIEW FACTOR INTEGRATION.....	13
2.2 TOPAZ3D ENCLOSURE RADIATION.....	15
2.2.1 Radiosity Matrix Solver.....	16
2.2.2 Iterative Radiosity Solver.....	17
2.3 SIMPLE WALL METHOD.....	18
2.4 VIEW FACTOR EXCHANGE METHOD.....	19
3. PROCEDURE.....	28
3.1 MODIFICATIONS TO FACET.....	28
3.1.1 Intercept Elements.....	28
3.1.2 Baffle Surface Elements.....	29
3.2 MODIFICATIONS TO TOPAZ3D.....	29
3.3 SIMULATION PROCEDURE.....	34
3.3.1 Simple Wall Method.....	34
3.3.2 View Factor Exchange Method.....	36
4. VERIFICATION SIMULATIONS.....	51
4.1 BAFFLE ANALYSIS.....	51
4.2 2-D ANALYTICAL MODEL.....	54
4.3 ANALYTICAL SENSITIVITY STUDY.....	58
4.4 SIMPLE WALL MODEL.....	63
4.5 VIEW FACTOR EXCHANGE MODEL.....	71
5. EXPERIMENTAL CASTING SIMULATIONS.....	77
5.1 AXI-SYMMETRIC MODEL.....	79

5.2 FURNACE SLICE MODEL.....	94
5.3 FURNACE SLICE MODEL WITH FEEDING SYSTEM.....	104
6. CONCLUSIONS.....	116
REFERENCES.....	118
APPENDICES	
A: MODIFIED FACET SUBROUTINE DATAIN.....	120
B: MODIFIED FACET SUBROUTINE VIEW3D.....	126
C: MODIFIED FACET SUBROUTINE OBSTR.....	128
D: MODIFIED FACET SUBROUTINE SECTN.....	130
E: NEW FACET SUBROUTINE HEIGHT.....	133
F: NEW FACET SUBROUTINE HWRITE.....	134
G: MODIFIED TOPAZ3D SUBROUTINE RADIN3.....	136
H: MODIFIED TOPAZ3D SUBROUTINE APLYBC.....	143
I: ANALYTICAL 2D VIEW FACTOR CODE.....	158
J: ANALYTICAL 2D HEAT FLUX CODE.....	164

INTRODUCTION

The aerospace industry is continually trying to make jet engines operate more efficiently by operating the engines at higher and higher temperatures. The most advanced turbine engines used today use directionally solidified airfoils to achieve their high operating temperatures. Conventionally cast polycrystal blades are still widely used, but in critical areas directionally solidified columnar and single crystal blades make the difference. To illustrate this point, Figures 1 and 2 show that columnar grain and single crystal blades are a significant improvement over polycrystal blades in fuel efficiency and overall service life. Directional solidification shows such an improvement in high temperature properties because there are no grain boundaries (a weak point in the casting), perpendicular to the principal stress axis in a turbine blade (See Figure 3). A single crystal is a further improvement over columnar grain because it eliminates all grain boundaries. Therefore, the alloying elements usually needed as grain boundary strengtheners can be eliminated, which increases the melting point of the nickel alloy used and thus increases the service temperature of the airfoil. However, directional solidification is more complex and costly process than with blades cast with the conventional polycrystal casting process.

Most turbine blades are investment cast in a groups of 10 to 30 in a circular arrangement, called a cluster. The thin ceramic mold is placed in a special vacuum furnace with a hot zone and a cold zone, as shown in Figure 4. In the process, superheated alloy is poured into the mold situated on a water cooled chill plate and surrounded by an induction heated graphite susceptor. The mold is withdrawn at a programmed rate from the hot susceptor into the cooling chamber. Crystal growth is initiated at the bottom and spreads slowly upward through the airfoil as the mold is

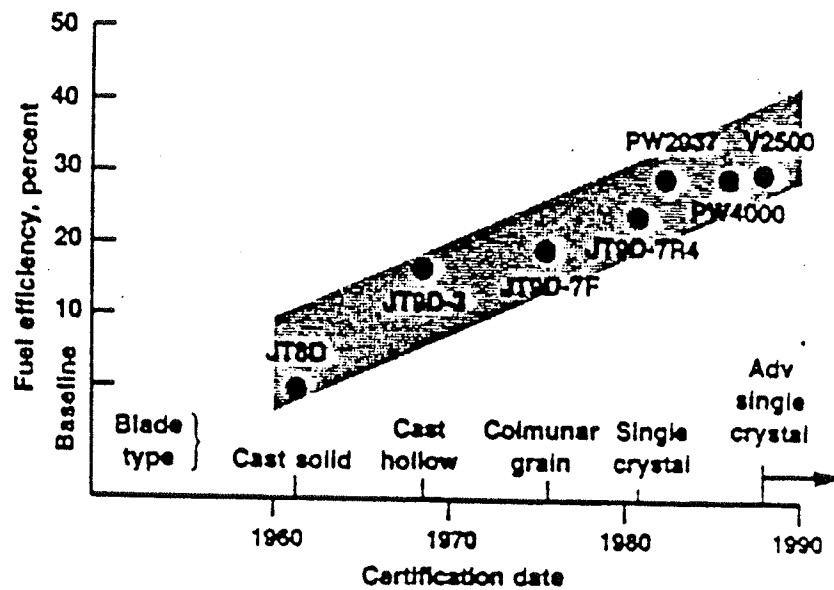


Figure 1. The improvement in fuel efficiency with engine model and the contributions made by cast superalloy technology. [6]

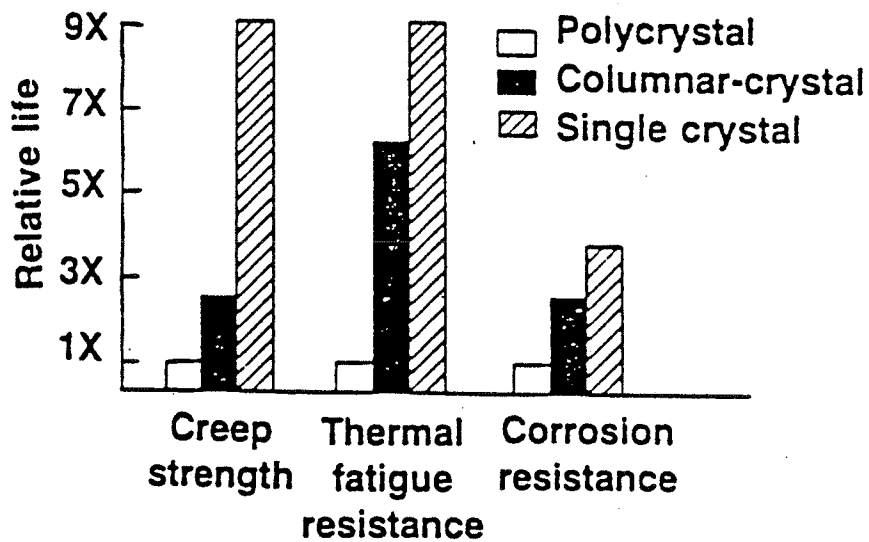


Figure 2. Comparative properties of polycrystal, columnar crystal and single crystal superalloys. [6]

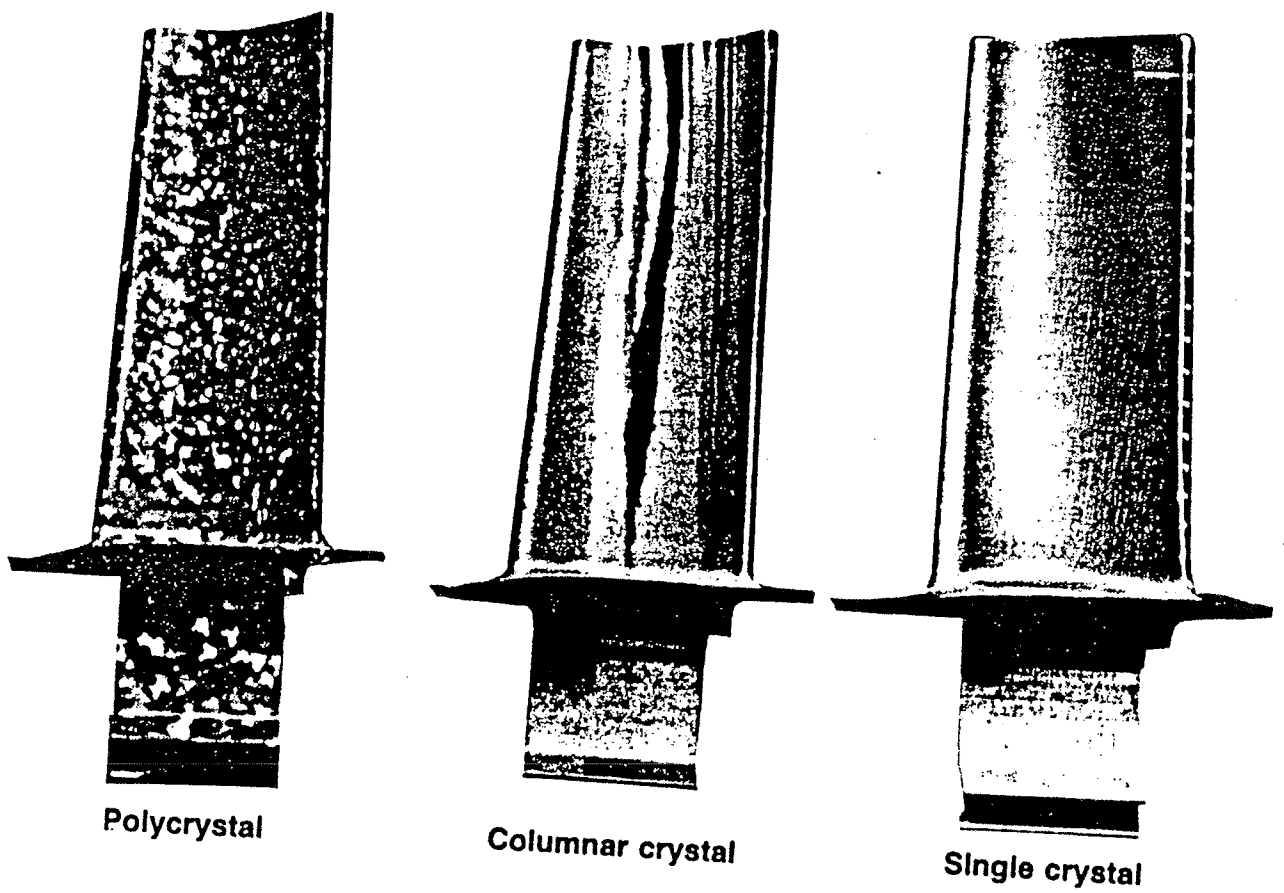


Figure 3. Advances in turbine airfoil technology from polycrystal to columnar crystal to single crystal castings. [6]

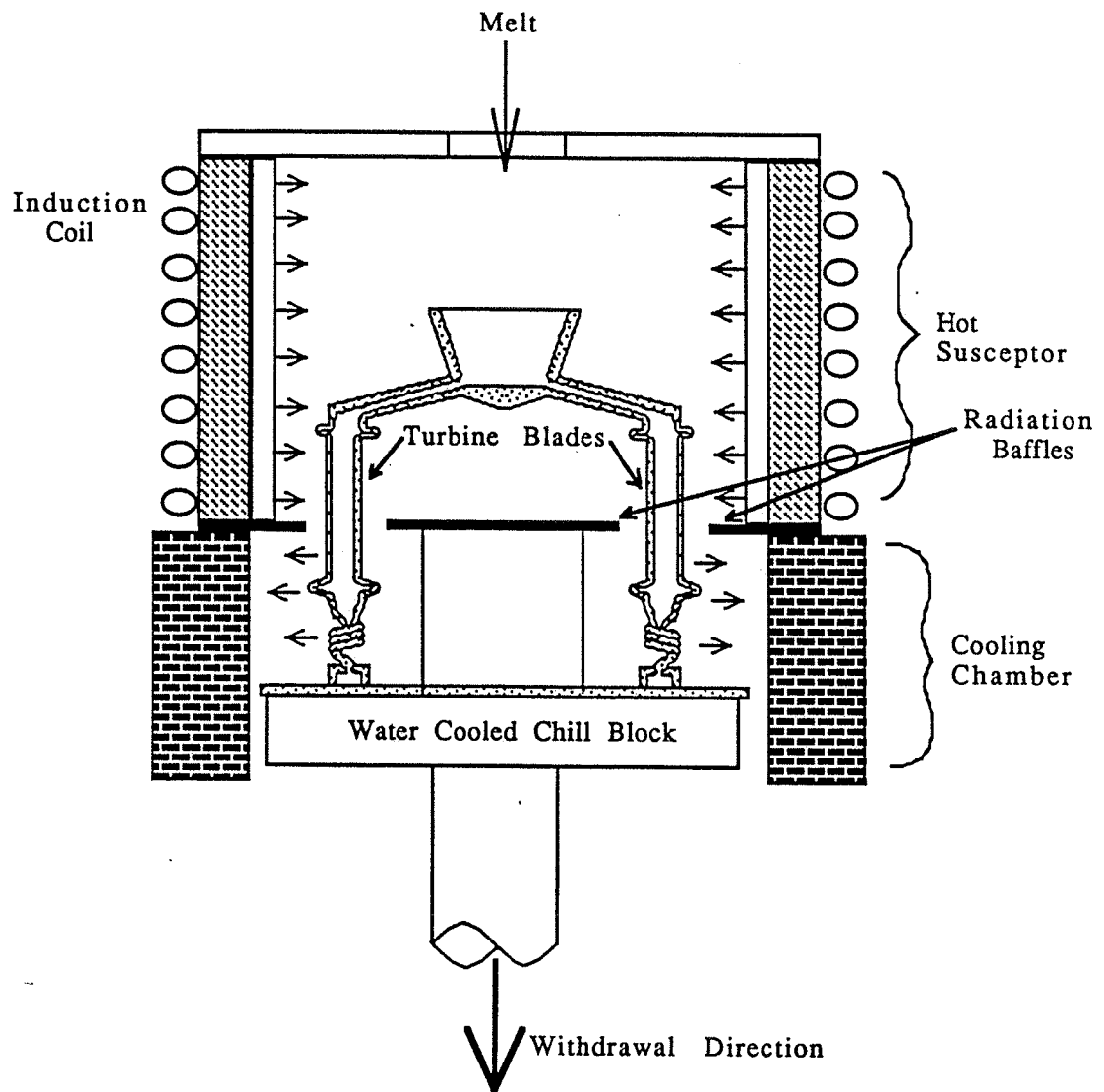


Figure 4. Schematic of single crystal airfoils being directional solidified in a cluster arrangement.

lowered. A single crystal casting has a grain selector below the airfoil which permits only one crystal with a $\langle 100 \rangle$ orientation to enter the airfoil portion of the mold.

Research has established that refined microstructure resulting from higher gradient processes have superior properties [1]. In order to create the maximum thermal gradient across the individual airfoil castings, radiation baffles are used. The only heat leakage from the susceptor to the cooling chamber is through these baffle openings. The largest diameter of the airfoil determines how small the baffle openings are, so that when the cluster is lowered, the baffle stays in place and does not come into contact with the mold.

Turbine blades using advanced material technology require tightly controlled process parameters if the blades are to have the mechanical and metallurgical properties needed to withstand the high temperatures, high alternating stresses, and the corrosive gases found in a jet engine. In order to produce airfoils with these properties, trial and error has been used to obtain the correct parameters, such as withdrawal rate, furnace temperature, mold thickness, baffle contour, and insulation location. Due to the interlocking variables in the directional solidification, a great amount of time is spent attempting to find a process which will produce any acceptable airfoil, let alone finding the optimum process. The furnace time used to discover the correct process for a new airfoil would be more efficiently used by making production parts. In order to minimize costly trial and error, a computer simulation of the solidification within a complex casting would give the design engineer a look into the casting itself and an optimum process could be determined without using expensive furnace time.

The objective of this work is to: 1) develop a mathematical model of the directional solidification process that is accurate and feasible for large 3D problems

of arbitrary furnace, mold and baffle geometry, 2) verify the code with analytical solutions, and 3) compare model temperature predictions with experimental measurements conducted on instrumented test castings. To implement this modeling technique, a Lawrence Livermore view factor integration code called FACET and a finite element code called TOPAZ3D was modified. The resulting MODFACET/MODTOPAZ codes are able to accurately model the radiation exchange of a directional solidified casting to the components of the furnace, the chill plate, other castings, and even the baffle.

1. LITERATURE REVIEW

There are many finite element codes which are able to model conventional casting processes (e.g. ANSYS, ABAQUS, TOPAZ, MARC). The largest obstacle in simulating the directional solidification process is obtaining the correct radiation view factors during the withdrawal. A view factor is a geometrical quantity which is associated with the amount of radiation that leaves one surface and reaches a second surface [2]. Because the mold is moving in relationship to the furnace, the view factors change over time. Thus, in order to calculate the radiation heat rate in the mold during the casting, the view factors must be corrected over time. View factor calculations are computationally expensive when dealing with a complex shape such as an airfoil and therefore calculating the view factors of each surface for each time step is not economical.

The first simplification researchers have made in the past is to assume that the airfoils are cast in an axisymmetric furnace (See Figure 5) in which only one blade was being cast. Morimoto, Yoshinari and Nyama [3] modeled a single crystal test cylinder in an axisymmetric furnace and skirted the view factor problem by modeling radiation with simple heat transfer coefficients and furnace temperatures. A constant coefficient and temperatures were assumed for the susceptor and the cooling chamber and were changed respectfully, as a function of time and distance from the chill plate. No reference or mention was made of the origins of the heat transfer coefficients used. The casting which was modeled was a simple single crystal cylinder with a helix grain restrictor. The helix was modeled with a straight tube. No attempt was made to model the gap formed by the shrinking metal and the mold wall. Temperature curves from the simulation were compared to experimental results and were in general agreement. Modeling the highly nonlinear enclosure radiation with linear coefficients can only yield general trends into the heat flow of

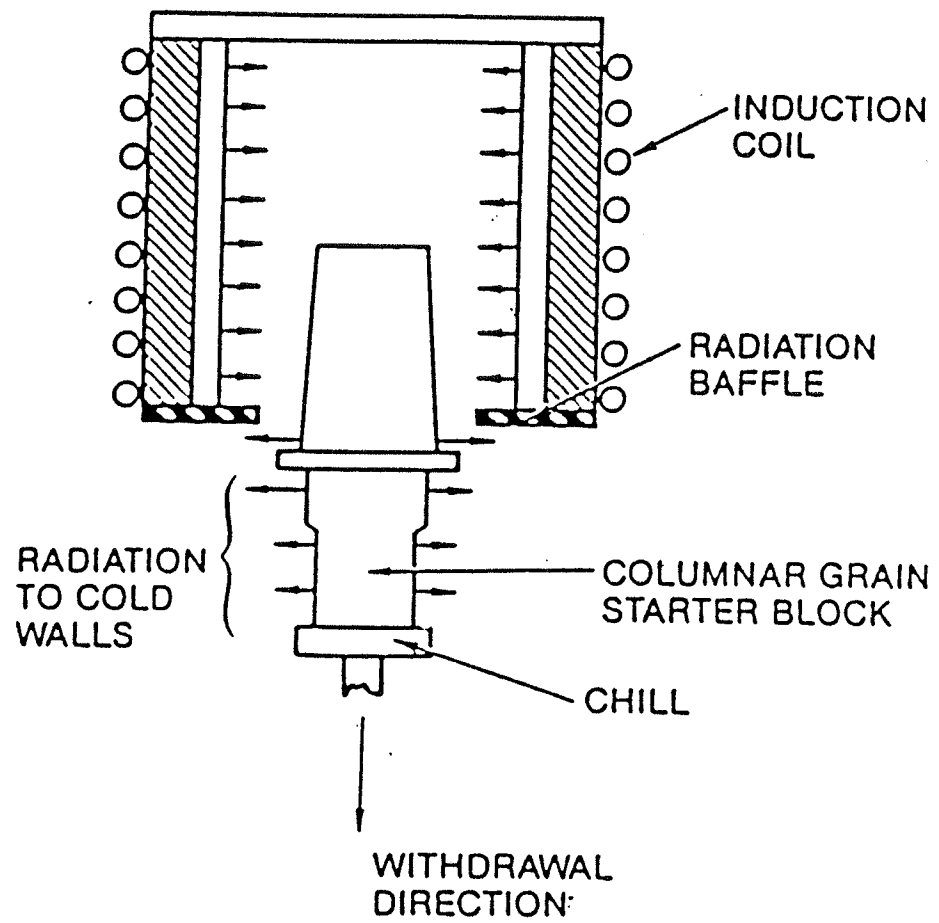


Figure 5. Schematic of a single airfoil being casting in a small axisymmetric furnace.

the casting and are restricted to simple shape castings in axisymmetric furnaces. This method is not very well able to model complex airfoils casting in cluster arrangement.

Early work by Giamei and Erickson [4] involved the modeling of a cylindrical ingot by applying experimental temperature curves as boundary conditions. This method is obviously restricted to simple shape castings which have been fully instrumented and cast. This modeling method requires a vast amount of data to yield accurate results and will not be able to model blades which are still on the drawing board. It also eliminates the chance to see the effects on the process when the casting parameters are changed. Using experimental data as boundary conditions limits the use of the model.

Work by Roches and Chevrier [5] involved the modeling of a 3D sham blade using enclosure radiation. A lone blade and three blades cast in a cluster were modeled using a method that appears to be similar to the "simple wall method" developed in this research. This method assumes a constant vertical diameter furnace (susceptor and cooling chamber) which follows the diameter of the outer baffle and varies the temperature of the furnace mesh to model the movement of the casting against the susceptor and cooling chamber. Using this procedure, the view factors do not change during the process and therefore only need to be calculated once. When compared to experimental results, there were some inaccuracies in the early stages of solidification, but the evolution of the mushy zone and the solidification rate are well simulated. Roches and Chevrier do not use a large baffle in their cluster arrangement. The European turbine blade industry use smaller furnaces than the United States industry and can obtain high thermal gradients without using large baffles. The simple wall method is unable to model large baffles or temperature differences in the susceptor/baffle top and cooling chamber/baffle

bottom. These factors are more important in the United States because of the use of larger contoured baffle sizes. Thus, Roches and Chevrier method will not accurately model blades cast in large clusters.

More recent work by Mador, Duffy, Giamei and Landis [6] involved modeling the directional solidification of 2D cylinders and 3D rectangular bars. The heat flux at the mold surface was modeled by using a temperature-dependent effective convection coefficient. The coefficient was a function of surface temperatures, analytically determined view factors to the baffle and to the hot and cold zones, and the emissivity of the mold surface. The view factors for every surface pair during the withdrawal were calculated and then used in the radiation boundary condition. For the 2D cylinder, there were only three view factor curves to consider: The mold surface to: 1) the hot susceptor, 2) the cooling chamber and 3) the baffle. The separate baffle surfaces were not considered in the model. Radiation was implemented in a MARC user subroutine.

Comparison of predicted and experimental temperature curves show exceptional agreement. It was mentioned in the paper that due to inherent thermocouple inaccuracy, the experimental data may be no more accurate than the predicted results. This is a problem that must be considered when dealing with all experimental results. However, the six digit accuracy of computer simulation cannot be duplicated in a highly controlled research environment, let alone in a production foundry.

The analytically calculated view factor method used in the cylinder and rectangular bar casting cannot be used when modeling the casting of a complex shape airfoil. It is not economical to track what every surface on the mold will see during the withdrawal process when there are hundreds of radiation surfaces. Only

when dealing with simple shape castings in an axisymmetric furnace can the analytical method be an alternative.

The most advanced modeling work to date has been done by Giamei, Mador, Duffy and Morris [7-8] and involves the casting of a blade in a cluster with three other blades. A view factor integration code was written to replace the earlier analytical method used with the MARC package. Because the user subroutine calculates time-dependent view factors during the transient heat flow analysis, the number of radiation view factors that change during the withdrawal must be recalculated at every time step. This will dramatically increase the computational time of the heat flow model. In their model, the mold can exchange radiation with the furnace hot and cold zones, the surface of the radiation baffle, the copper chill plate, itself, and other blades in the cluster. The view factors of the blade do not change between itself, other blades in the cluster, and the chill block. There are no large or deeply contoured baffles to obstruct the blade from other blades. This greatly reduces the number of view factors that must be calculated. The view factors of the blade to the furnace wall are the only surfaces which need recalculating. Since only a small portion of the view factor matrix need to be updated, the problem becomes manageable. Even so, the authors stated that the full cluster simulation took 61.5 CPU hours on a VAX 8600.

In order to reduce the number of view factor calculations further, the surfaces on the clustered blades were grouped into larger planar zones. Each zone is assumed to be isothermal and the average temperature over the zone is used in the radiation boundary condition. There was no explanation given on how large sections of the mold can be considered isothermal when such a high thermal gradient is achieved in the directional solidification process. To assert the accuracy of the view factor analytical method, temperature histories were compared against experimental data

from the casting of a 3D rectangular bar. No verification test was presented for the selective view factor integration method, therefore no conclusion can be made on the accuracy of the large section assumption.

The selective view factor method is an excellent way to model the directional solidification of a columnar grain turbine blade. The required thermal gradient is not as high as a single crystal blade, thus no complex baffles are normally used. Once the view factors change between blade surfaces, such as when an large baffle is used, the selective integration method must calculate every view factor at every time step. This method does not have the ability to decide when a view factor needs to be recalculated so it must calculate them all. This is not very efficient when less than 10 percent of the view factors are affected by the baffle during a time step. The selective integration method is an accurate method for castings which do not large or deep contoured baffles. It is not able to model the directional solidification of single crystal turbine blades.

In summary, no modeling method is currently able to accurately and economically simulate the directional solidification of single crystal airfoils. The technical need for a method which will predict the liquidus/solidus temperature curve and the thermal gradient across a blade would be of great benefit to engineers who have been forced in the past to make decisions on casting parameters based solely on past experience and intuition. The goal of this work is to devise such a method which will ultimately lead to reducing trial-and-error in the foundry, optimizing casting parameters and predicting blade defects.

2. THEORY

In order to fully describe the view factor exchange method of modeling directional solidification, both the view factor integration code FACET and the finite element heat transfer code TOPAZ3D must be introduced to demonstrate how enclosure radiation is handled. A less complex modeling method is also introduced, called the simple wall method, which uses the original FACET/TOPAZ3D code. This method serves as a building block for the more advanced view factor exchange method.

2.1 FACET VIEW FACTOR INTEGRATION

FACET is a computer code which calculates the radiation view factor between three dimensional surfaces with obstructing third surfaces. The view factor integration equation:

$$F_{ij} = \frac{1}{A_i} \int_{A_i} \int_{A_j} \frac{\cos\beta_i \cos\beta_j}{\pi r^2} \quad (1)$$

is used to calculate the view factor, F_{ij} , between a pair of surface elements i and j , or "surface pair". The FACET manual [9] explains the three different algorithms that are used when the surface pair have a common edge, are separate disjoint surfaces or have self or third surface obstruction. Figure 6 illustrates the symbols used in Eq. (1) as surface i radiates to a second surface j . The view factors become a function only of geometry if we assume that the two surfaces are black, isothermal, diffusely emitting and reflecting radiation. A surface is defined by four nodes and the surface definition is in accordance with the right hand rule. For a complete enclosure, FACET calculates the view factors for every surface pair in the given mesh. Before FACET calculates a view factor for a surface pair, it determines whether the surface pair

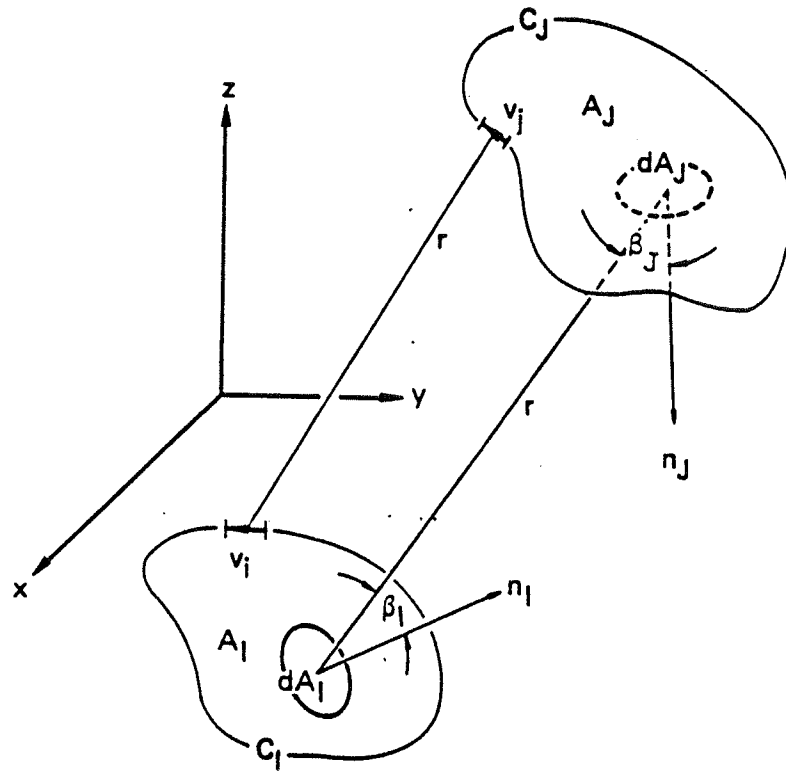


Figure 6. Sketch illustrates the symbols used in integrating the view factor F_{ij} of two 3D surfaces.

calculates a view factor for a surface pair, it determines whether the surface pair can see each other or whether a third surface obstructs their view. Obstruction surfaces are specified as surfaces which may block the view of other surfaces, so that FACET does not have to check every surface for third surface obstruction. If there is partial obstruction of a surface pair, the view factor is calculated using a subsurface of each surface. The smaller divisions of one surface are checked for obstruction of the second surface. Subsequently, the partial obstruction view factors are calculated by specifying the number of divisions for the surfaces in the input file. The increased divisions have better accuracy and much higher computer costs.

When FACET discovers a surface pair can see each other, it calculates the view factor and then goes on to the next surface pair. Using the reciprocity equation:

$$A_i F_{ij} = A_j F_{ji} \quad (2)$$

FACET only has to integrate half of the full $N \times N$ matrix, where N is the total number of surfaces making up the enclosure.

2.2 TOPAZ3D ENCLOSURE RADIATION

There are two ways in which to solve for the heat flux generated by enclosure radiation, the radiosity matrix solver and the iterative radiosity solver. Both methods are outlined in ref. 10. The matrix solver is used when the emissivity is constant, while the iterative solver is used when the emissivity is a function of wavelength. Both routines have been used in the development of the view factor exchange method, but the iterative solver is the fastest and simplest way to solve for the enclosure radiation heat flux with variable view factors.

2.2.1 Radiosity Matrix Solver

The TOPAZ solution procedure for solving enclosure radiation is to guess at the surface temperatures and then calculate the net radiation heat flux for all surfaces using the equation:

$$q_{i,NET} = \epsilon_i \sigma T_i^4 - \alpha_i H_i. \quad (3)$$

The heat flux includes the emitted radiation and the absorbed portion of the irradiation from other surfaces. The irradiation H_i arriving per unit area at surface i from all n surfaces of the enclosure is:

$$H_i = \sum_{j=1}^n F_{ij} B_j \quad (4)$$

where F_{ij} are the view factors between surfaces and B_j is the radiosity from the j th surface calculated by:

$$B_j = \epsilon_j \sigma T_j^4 + \rho_j H_j \quad (5)$$

This equation for B_j includes the radiation emitted by the surface and the reflected portion of the irradiation. Assuming the gray body condition where $\rho = 1 - \epsilon$ and $\alpha = \epsilon$, the radiosity at surface i is:

$$B_i = \epsilon_i \sigma T_i^4 + (1 - \epsilon_i) \sum_{j=1}^n F_{ij} B_j \quad (6)$$

which can be generated for n surfaces and put into the matrix form:

$$\{B\} = [X]^{-1} \{\Omega\} \quad (7)$$

where:

$$X_{ij} = \delta_{ij} - (1 - \epsilon_i) \frac{F_{ij}}{\epsilon_i} \quad (8)$$

and:

$$\Omega_i = \sigma T_i^4. \quad (9)$$

Given a guess at the surface temperatures, the radiosity matrix $\{B\}$ can be solved and then irradiation H_i can be computed using the equation:

$$H_i = \frac{1}{1 - \epsilon_i} (B_i - \epsilon_i \sigma T_i^4). \quad (10)$$

The finite element conduction problem is then solved using a linearized Taylor series expansion of the form:

$$q_{i,NET} = 4 \epsilon_i \sigma T_i^3 T_i - 3 \epsilon_i \sigma T_i^4 - \alpha_i H_i \quad (11)$$

where T is the temperature from the previous iteration.

Once the conduction problem is solved, the temperatures are compared for error. If a specified criterion is not satisfied, the radiosity matrix is computed with improved temperatures and the process iterates until it converges and satisfies the criterion.

2.2.2 Iterative Radiosity Solver

The second TOPAZ solution procedure for solving enclosure radiation is to guess at the surface temperatures and then calculate the net radiation heat flux for all surfaces using the equation:

$$q_{i,NET} = \epsilon_i \sigma T_i^4 - \alpha_i H_i. \quad (3)$$

The heat flux includes the emitted radiation and the absorbed portion of the irradiation from other surfaces. The irradiation H_i arriving per unit area at surface i from all n surfaces of the enclosure is:

$$H_i = \sum_{j=1}^n F_{ij} B_j \quad (4)$$

where F_{ij} are the view factors between surfaces and B_j is the radiosity from the j th surface. Assuming the gray body condition where $\rho = 1 - \epsilon$ and $\alpha = \epsilon$, the radiosity can be calculated from:

$$B_j = \epsilon_j \sigma T_j^4 + (1 - \epsilon_j) H_j \quad (5)$$

The iterative solver assumes the irradiation (H_i) is zero during the first calculation of the radiosity using Eq. 5. It then calculates the irradiation using Eq. 4, using the new radiosity values and recalculates the radiosity again. This iterative pattern is

repeated until the present and past radiosity values converge within a specified value.

The finite element conduction problem is then solved using a linearized Taylor series expansion of the form:

$$q_{i,NET} = 4 \epsilon_i \sigma T_i^3 T_i - 3 \epsilon_i \sigma T_i^4 - \alpha_i H_i \quad (11)$$

where T is the temperature from the previous iteration.

Once the conduction problem is solved, the temperatures are compared for error. If a specified criterion is not satisfied, the radiosity matrix is computed with improved temperatures and the process iterates until it converges and satisfies the criterion.

2.3 SIMPLE WALL METHOD

The simple wall method uses a few basic steps to simulate relative movement of the furnace and blades, which the view factor exchange method builds upon. The method works as follows: 1) It is based on a Lagrangian formulation to model the furnace and baffle, which are moving upward together at the withdrawal velocity, while the airfoil parts remain stationary. 2) The susceptor and cooling chamber are assumed to have the same radius so can be modeled as a continuous wall, made up of many elements. 3) The view factors between each element on the surface of the ceramic mold and the elements that make up the surface of the furnace interior are calculated. 4) A temperature/time function curve is assigned to each furnace wall node according to its vertical height so that as a baffle passes by an element during the withdrawal, the temperature of the element ramps from the susceptor temperature to the cooling chamber temperature.

Since the susceptor and cooling chamber are modeled with a continuous wall around the casting, the view factors do not change during the withdrawal process.

Only the temperature of the wall changes. The simple wall method must simplify the furnace interior by moving the susceptor and cooling chamber wall to the radius of the outer baffle, in this way the gap between the mold and baffle can be modeled. When the furnace wall is moved in, the view factor that was of the baffle top is now taken up by the susceptor and likewise with the baffle bottom and the cooling chamber. Since the mold surfaces are exchanging radiation with the susceptor and cooling chamber instead of the baffle surfaces, the temperatures must be equivalent in order to obtain the correct heat flow.

Figure 7 illustrates the steps used in the simple wall method for modeling directional solidification. It shows the fixed thermal histories assigned to two of the nodes making up the furnace wall.

There are two deficiencies involved in moving the furnace interior to the baffle radius: 1) the baffle top surface is assumed to be at the same temperature as the susceptor, and 2) the baffle bottom surface is assumed to be at the cooling chamber temperature. The one disadvantage of the simple wall method is its inability to model the obstruction of mold surfaces from each other. The interaction of multiple, contoured baffles with the numerous airfoils in a cluster is a three dimensional problem which the simple wall method cannot model.

2.4 VIEW FACTOR EXCHANGE METHOD

All previous directional solidification models have been restricted to either one blade castings or calculating view factors every time step. The view factor exchange method developed in this research works on the basis that as the baffle moves in relationship to the mold, it obstructs some surfaces from each other. If total obstruction is assumed, then the baffle replaces the view of those surfaces to each other with a view of each surface to the top or bottom of the baffle. Since the baffle

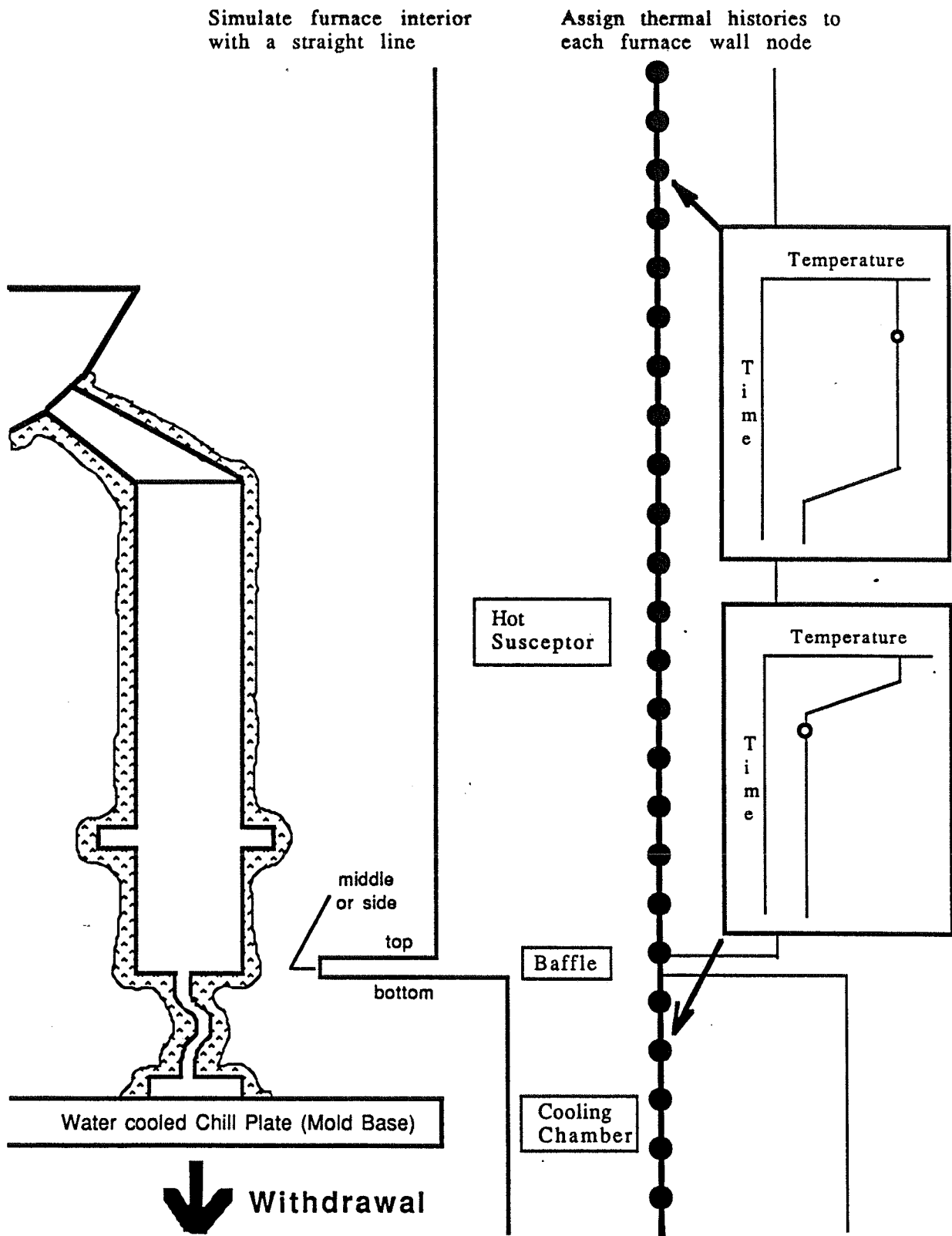


Figure 7. Illustration of steps used in implementing the simple wall method.

does not change shape and only moves vertically, there is a specific height range in which the baffle will obstruct each surface from another surface. This height range or "obstruction range" corresponds to a time range for a given withdrawal rate. During the heat transfer analysis, if the view factor matrix can be adjusted to take into account the baffle obstructing certain surfaces at these times, we will be able to model the physics of the withdrawal problem.

To illustrate one of the principles underlying the view factor exchange method, Figure 8 shows the view of surface i to the furnace wall that is obstructed by the baffle. The dashed lines show the two extreme views surface i can have. Because of the position of the baffle, surface i sees the top of the baffle instead of surfaces 2 through 6 at this time. It would be accurate to say that the view factor of surface i to the baffle top is equal to the sum of the view factors of surface i to surfaces 2 through 6. Figure 9 shows the baffle in a higher position in which it obstructs the view of surface i of surfaces 1 through 4. Surfaces 5 and 6 are revealed to surface i because the baffle has moved up.

Figure 10 illustrates schematically the times and corresponding positions when a baffle will obstruct a surface pair and when it will reveal them. If we assume a very thin baffle which cannot partially obstruct a surface pair, the baffle in Figure 10 will obstruct the surface pair i and j when it lies within the obstruction range which is defined by two intercept heights h_{ij} and h_{ji} . When the baffle is either above or below the obstruction range, the surface pair is unobstructed so its view factor remains unchanged.

The obstruction range is determined for each surface pair by the following procedure: 1) Calculate the line connecting the centroids of the two surfaces, 2) Define the locus of travel of the extreme edges of the baffle with vertical planes, 3) Calculate the intercept points of the line and the planes. The obstruction range is

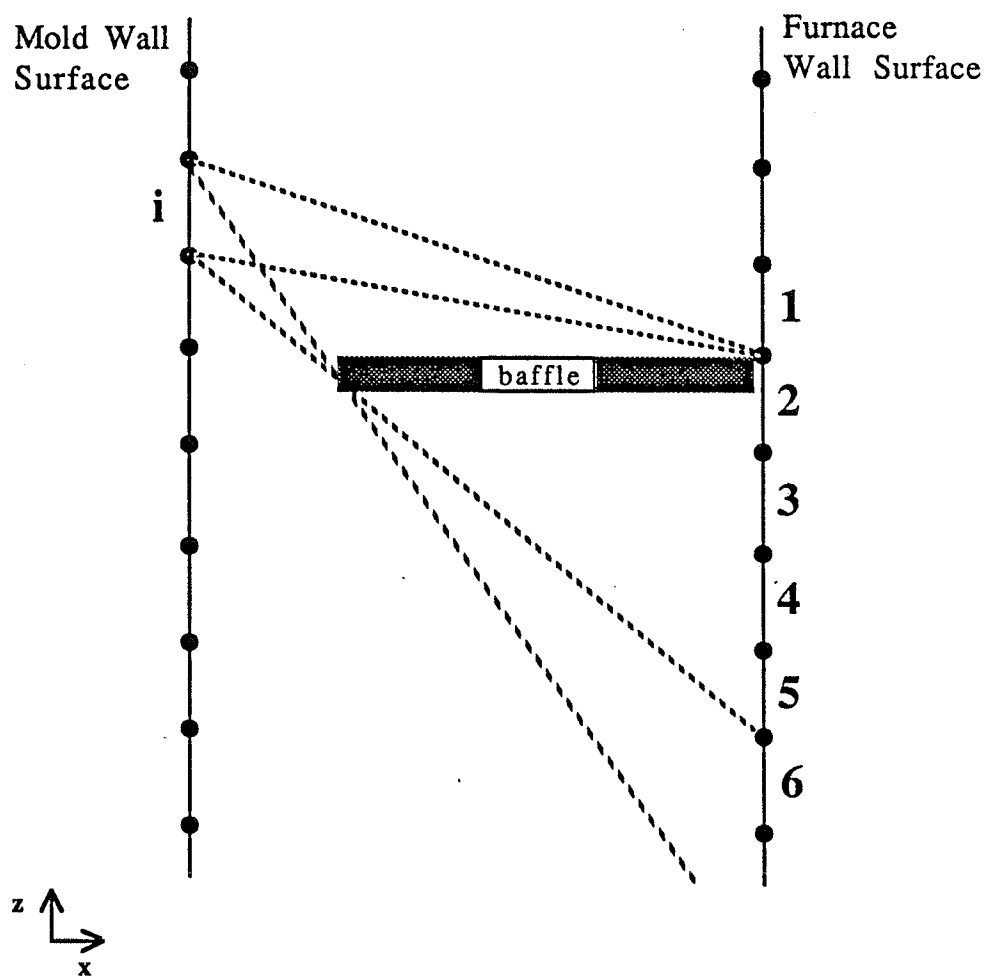


Figure 8. Illustration of the baffle obstructing the view of surface i to surfaces 2 through 6 on the furnace wall

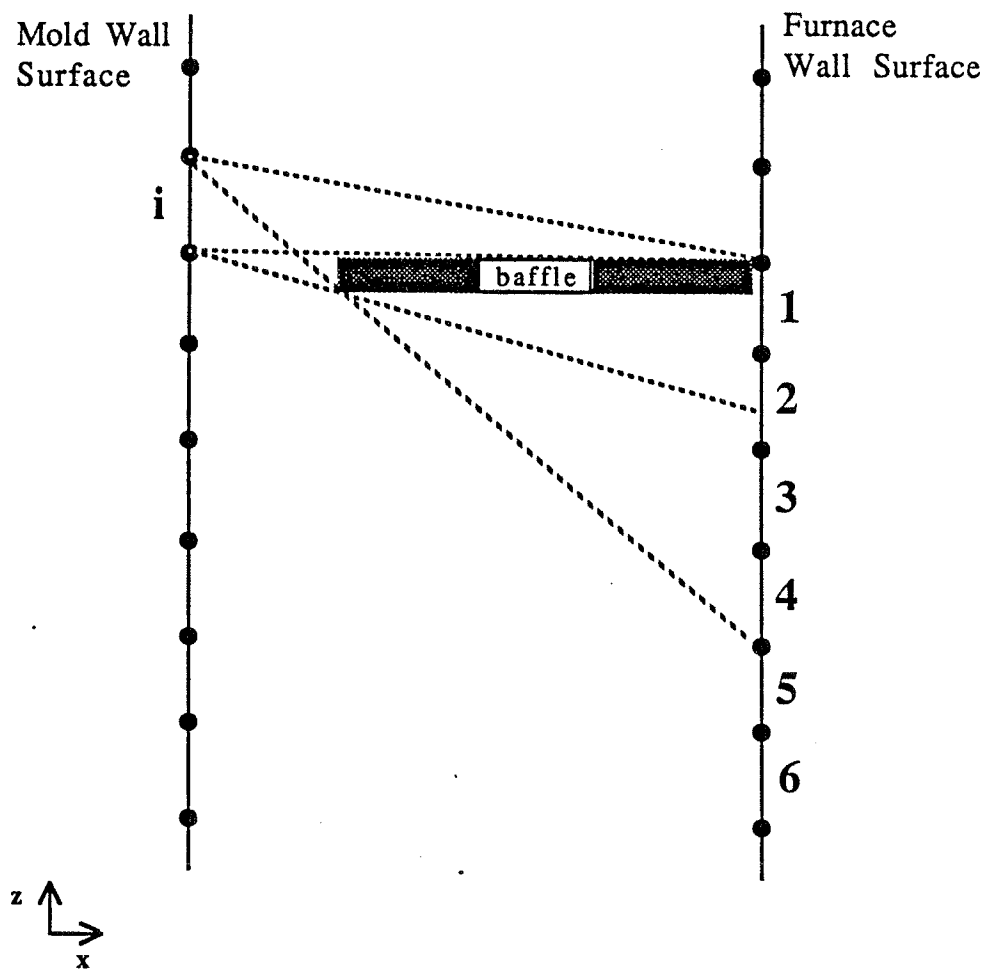


Figure 9. Illustration of the baffle obstructing the view of surface i to surfaces 1 through 4 on the furnace wall and revealing surfaces 5 and 6.

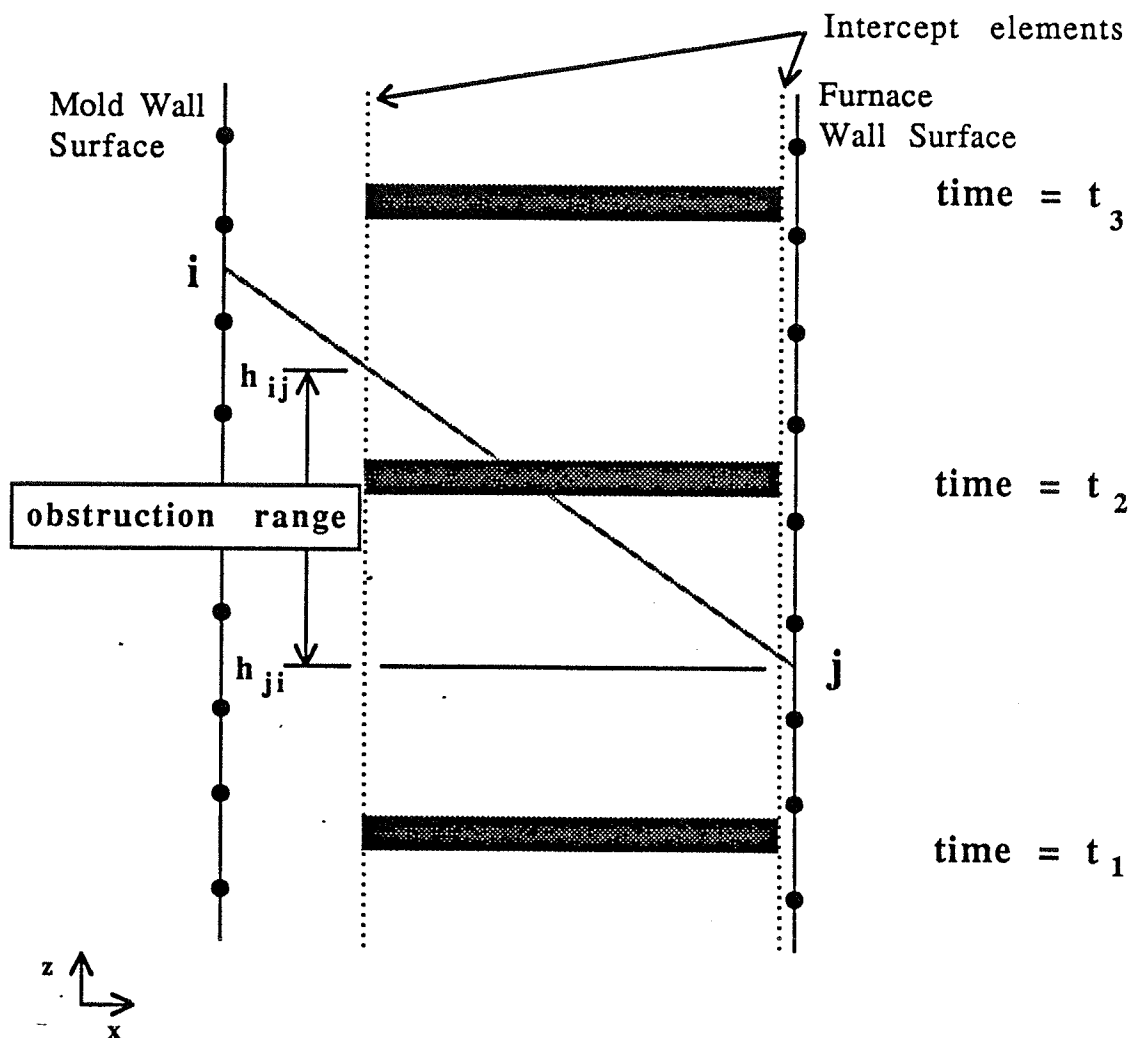


Figure 10. Illustration of how the obstruction range is calculated for a surface pair and the baffle.

defined by the heights of the two intercept points, h_{ij} and h_{ji} . Any time during a simulation when the height of the thin baffle lies within the obstruction range, the baffle is blocking the surface pairs view. Instead of surface i seeing surface j , it sees the top of the baffle. Inversely, instead of surface j seeing surface i , it is seeing the bottom of the baffle.

The obstruction range and view factor for every surface pair and the baffle withdrawal rate provide all the necessary information for the heat transfer model. Before the enclosure radiation heat flux is calculated, the present time and withdrawal rate are used to determine the baffle height. The baffle height during the time step is compared against every surface pair obstruction range in order to determine which view factors must be corrected for the obstruction of the baffle. When the baffle is obstructing a surface pair, the view factor of the surface pair is replaced by identical view factors of each surface to the baffle, and the original view factor is changed to zero. If the baffle is not obstructing a surface pair, no exchange takes place and the original view factor is used for the surfaces. After this height check and exchange has been completed for every surface pair, the view factor matrix is correct for that specific baffle position.

As an example of the view factor matrix manipulation, Figure 11 shows the view of surface i to surface j being blocked by the baffle. In order to correct for the obstructing baffle, the view factor F_{ij} is moved in the view factor matrix to the location corresponding to surface i seeing the baffle top surface. The same procedure is used for surface j and the bottom of the baffle. In order to calculate the radiation heat flux into the baffle, corresponding view factors for the baffle are calculated using Eq. (2). and inserted into the view factor matrix.

One of the great advantages of this method is that heat flow to the baffle is modeled over time. This allows the calculation of the baffle surface temperatures

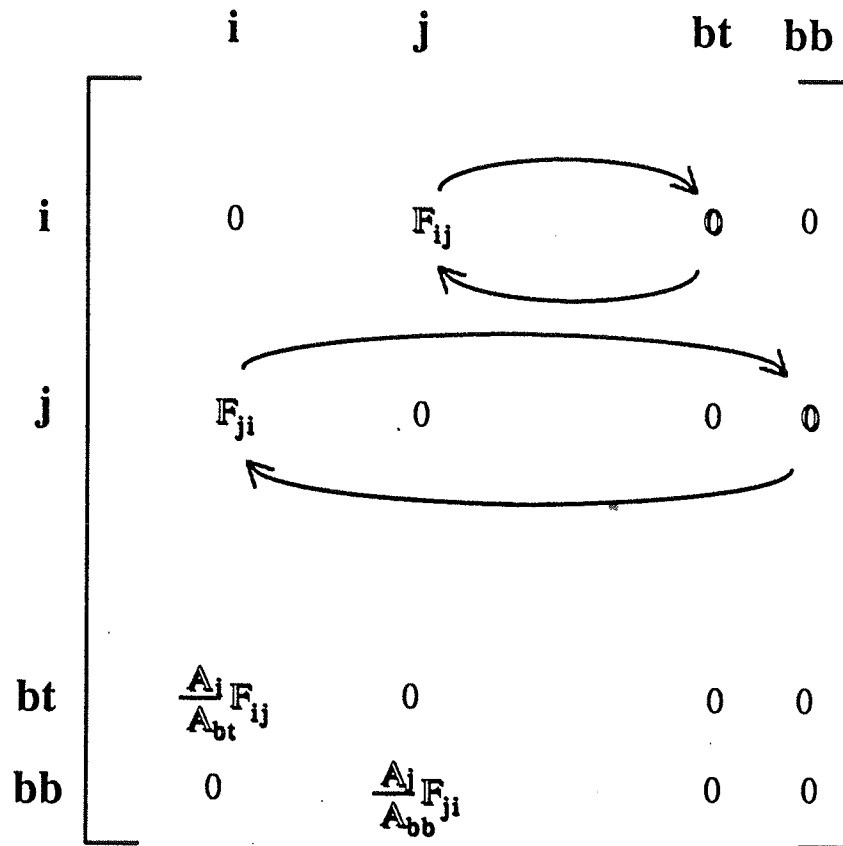
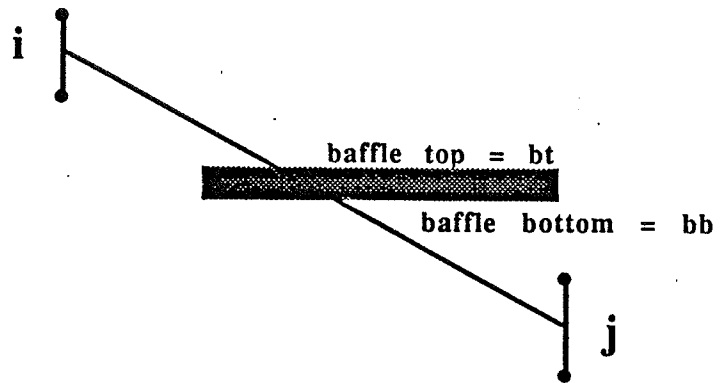


Figure 11. The view factor exchange takes place in heat flow analysis and baffle obstructs and reveals different surfaces over time.

which will eliminate the guess work involved with determining baffle temperatures required in other methods. With the proper boundary conditions on the baffle or temperature histories, the movement and obstruction of the baffle can be accurately modeled. The second great advantage of this method is that the computationally intensive calculation of the complete view factor matrix needs to be done only once.

3. PROCEDURE

3.1 MODIFICATIONS TO FACET

To implement the view factor exchange method described in the previous section, modifications were made to both FACET and TOPAZ. In FACET, the creation of two new element types, the intercept element and the baffle element, was required. Neither of these elements undergo view factor calculations in FACET, since they are not part of the radiation surface enclosure.

3.1.1 Intercept Elements

The intercept element is a four node surface which traces out the vertical path or locus of travel of the edges of the baffles. It is used to find the height range in which the baffle obstructs the view of each pair of radiating surfaces. When FACET finds that an intercept element is obstructing the view of surface i to surface j , it will calculate the height in which the line connecting the two centroids intersects the intercept element. A surface pair is normally obstructed by two intercept elements, so two intercept heights are calculated. The height closest to the surface i will be stored in the matrix location $i-j$ and the second height will be stored in matrix location $j-i$. These two heights correspond to the obstruction range in which a baffle will obstruct the view of those two surfaces from each other as shown in Figure 10.

After this intercept calculation, FACET will calculate the view factor between the two surface elements, just as if the intercept element was not there. This pattern is repeated for every surface pair in the enclosure mesh. At the end of a FACET run, a $N \times N$ matrix of intercept heights when using one baffle, (or two $N \times N$

matrices when using two baffles) will be written out in binary form for input into TOPAZ.

3.1.2 Baffle Surface Elements

The purpose of this modified FACET surface is to generate matrix locations for the baffle surfaces with which to exchange view factors inside of TOPAZ. These modified surfaces will cover an actual baffle mesh. The baffle will be placed at an arbitrary height and will not move and will not be connected with the rest of the casting mesh. It is simply there to provide space in the view factor matrix for later manipulations in TOPAZ.

3.2 MODIFICATIONS TO TOPAZ3D

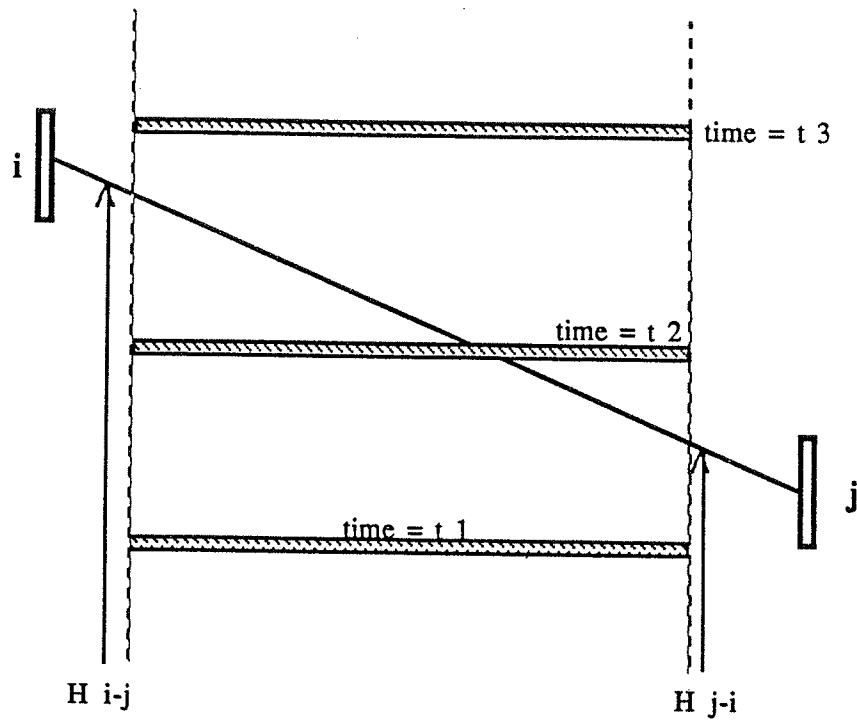
At each time step, just before TOPAZ constructs inverts the $[X]$ found in Eq. (8), the baffle height at that time is compared to the intercept range of each surface pair. If the baffle is not blocking the view of the two surfaces, the original view factor is used in the matrix formulation. If the baffle is within the obstruction range, the view factor F_{ij} is given as the view factor of the baffle surface to each of the blocked surfaces. The original view factor of the surface pair is changed to zero. This allows the radiation boundary condition to change as the baffle blocks the view of different surface pairs. The baffle can be modeled and the changing surface temperatures will be used in the heat flow formulation of the casting. With only one run of FACET and the addition of an obstruction range matrix, TOPAZ can model the dynamic heat flow characteristics of the high gradient, directional solidification of a casting.

The enclosure-radiation-heat-flux-boundary-condition subroutine has been altered so that a modified view-factor matrix is constructed and used in the calculation of the radiosity matrix. A simple algorithm is used to compute the modified view factor matrix. A comparison of the two intercept heights H_{i-j} , H_{j-i} , and

the baffle height takes place to determine whether surface i is actually seeing the top of either baffle, the bottom of either the baffle or surface j . Figure 12a shows the geometric configuration with surface i higher than surface j . At time= t_1 , the baffle height is below the intercept heights so no exchange takes place. At time= t_2 , the baffle height is below intercept height H_{i-j} but higher than intercept H_{j-i} . This means that the surface i is above surface j . When the baffle obstructs their view, surface i will see the top of the baffle and surface j will see the bottom of the baffle. The VF_{i-j} is exchanged with the $VF_{i-\text{baffle top}}$ and VF_{j-i} is exchanged with $VF_{j-\text{baffle bottom}}$. In order to obtain the correct baffle view factors, the reciprocity equation, Eq. (2) is used. The $VF_{\text{baffle top}-i}$ is the VF_{i-j} multiplied by the area ratio $A_i/A_{\text{baffle top}}$, and the view factor of the baffle bottom to surface j is calculated in the same way. These six operations are illustrated in Figure 11.

The second geometric configuration possible is with surface i lower than surface j (See Figure 12b). When the intercept height H_{i-j} is higher than H_{j-i} , it shows that surface i will see the bottom of the baffle and surface j will see the top of the baffle, when the baffle obstructs the surfaces' view.

In all likelihood, the contour of a baffle surface will require it to be made of several surface elements. In order to have a surface radiate to several elements on a baffle surface, a baffle element surface area ratio calculation is used to obtain a uniform view factor and heat flux across the baffle surface. This area ratio is the individual element area divided by the total baffle surface area. Figure 13 shows how the simple surface area ratio will work to determine the individual view factors. After all the surface pair heights are checked, the view factor from surface i to each baffle surface is multiplied by each baffle element surface ratio and placed in the modified view factor matrix. This is how the view factor of the baffle surface is split up into individual elements.



time = t 1

$H_{i-j} > \text{Baffle Height}$
 $H_{j-i} > \text{Baffle Height}$
 no obstruction, use original view factor

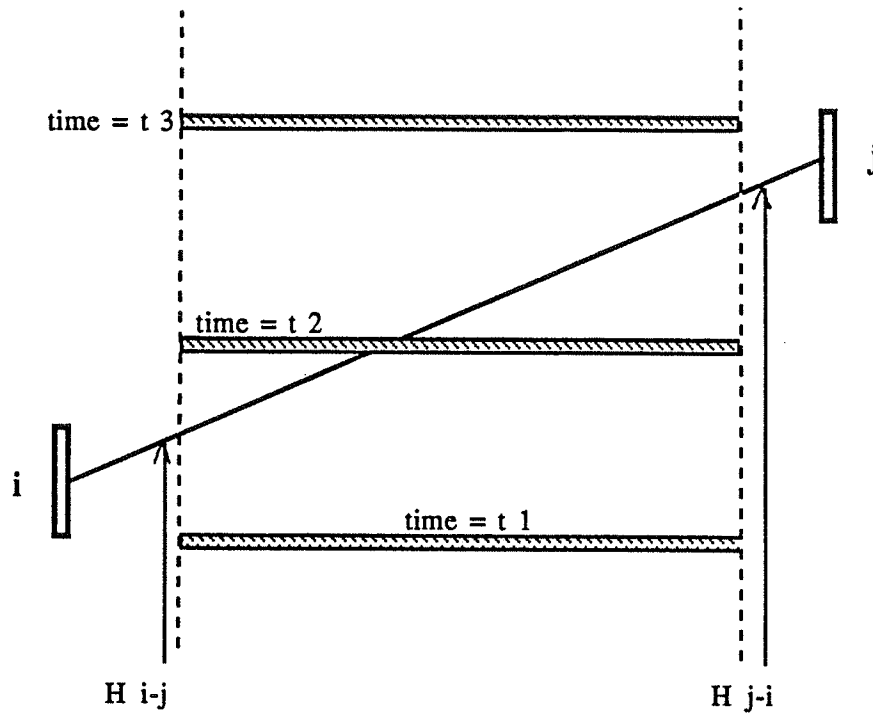
time = t 2

$H_{i-j} < \text{Baffle Height}$
 $H_{j-i} > \text{Baffle Height}$
 $VF_{i-\text{baffle top}} = VF_{i-j}$, $VF_{j-\text{baffle bottom}} = VF_{j-i}$
 $VF_{\text{baffle top}-i} = VF_{j-\text{baffle bottom}}$
 $VF_{\text{baffle bottom}-j} = VF_{i-\text{baffle top}}$
 $VF_{i-j} = 0$, $VF_{j-i} = 0$

time = t 3

$H_{i-j} < \text{Baffle Height}$
 $H_{j-i} < \text{Baffle Height}$
 no obstruction, use original view factor

Figure 12a. View factor exchange logic when surface i is above surface j.



time = t 1

$H_{i-j} > \text{Baffle Height}$
 $H_{j-i} > \text{Baffle Height}$
 no obstruction, use original view factor

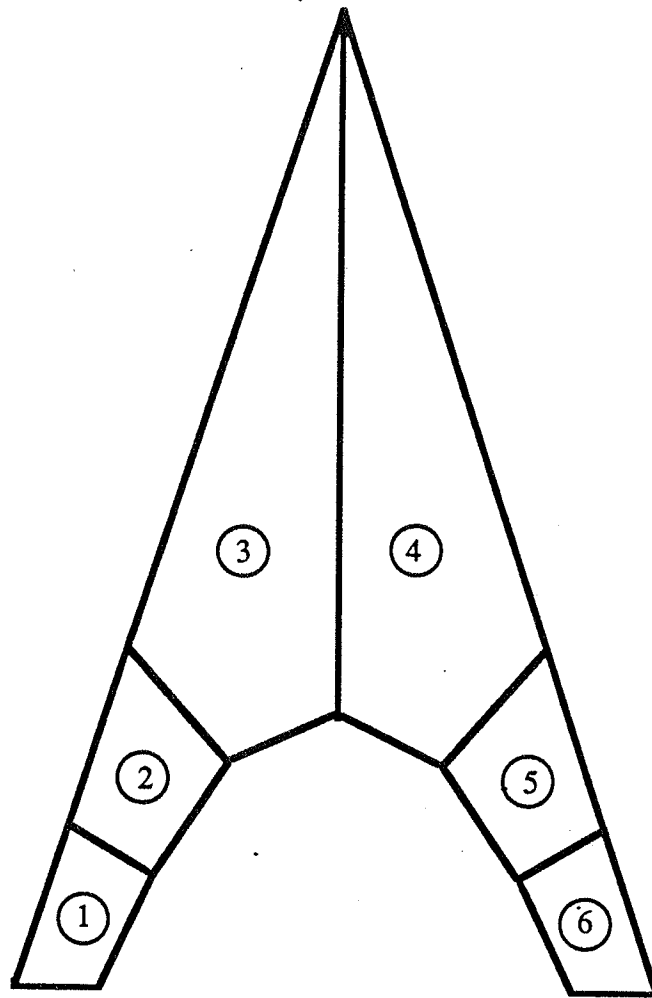
time = t 2

$H_{i-j} > \text{Baffle Height}$
 $H_{j-i} < \text{Baffle Height}$
 $VF_{i-\text{baffle bottom}} = VF_{i-j}$, $VF_{j-\text{baffle top}} = VF_{j-i}$
 $VF_{\text{baffle bottom}-i} = VF_{j-\text{baffle top}}$
 $VF_{\text{baffle top}-j} = VF_{i-\text{baffle bottom}}$
 $VF_{i-j} = 0$, $VF_{j-i} = 0$

time = t 3

$H_{i-j} < \text{Baffle Height}$
 $H_{j-i} < \text{Baffle Height}$
 no obstruction, use original view factor

Figure 12b. View factor exchange logic when surface i is below surface j.



$$VF_{i-1} = (A_{total}/A_1) VF_{i-total \text{ baffle top}}$$

$$VF_{i-2} = (A_{total}/A_2) VF_{i-total \text{ baffle top}}$$

$$VF_{i-6} = (A_{total}/A_6) VF_{i-total \text{ baffle top}}$$

Figure 13. Calculations used to obtain a uniform view factor and heat flow over a multi-element baffle surface.

The sum of all the view factors for an element or row sum, is normally equal to one. However, the baffle cannot partially obstruct a surface pair, depending on the refinement of the surface mesh, the row sum of the baffle surface may be larger or smaller than one. Therefore, a check of the row sum is made for each baffle and then used to increase or decrease each view factor so that the row sum does equal 1. The row sum error is shown in the printout file in order to indicate the need for mesh refinement.

Giving the baffle appropriate thickness and material properties allows it to behave as if surface i is radiating to it and take part in the simulation. By exchanging heat with surfaces radiation to it, the baffle will develop a vertical temperature gradient and simulate the actual graphite board. One limiting approximation in the baffle temperature calculation is no gradient will develop across the surface of the baffle due to differences in radiation. Alternatively, the baffle could be given a temperature history, if such information was known, in the same manner as the furnace wall temperature is specified as a function of withdrawal speed and time.

3.3 SIMULATION PROCEDURE

The procedure to run a directional solidification simulation requires the generation of an eight node brick element mesh of the casting, mold and possibly the chill plate and runners. An enclosure of four node surface elements around the casting is also needed. There are several mesh generators available to help with creating the input deck into FACET and TOPAZ: the generator in FACET/TOPAZ [9,11], INGRID [12] and the Investment Casting Simulation Software (Supertab/ICSS) [13], made by Structural Dynamics Research Corporation.

3.3.1 Simple Wall Method

Modeling directional solidification with the simple wall method requires the four node element enclosure constructed around the casting be the same radius as the enclosing baffle. The baffle can be contoured, but cannot obstruct the view of the mold surface from any other blade, (if a cluster arrangement is being modeled) or of itself. The FACET input deck needs the nodal data, surface data, and also the obstruction surface data. Obstruction surfaces are elements which may obstruct other surface pairs. The furnace walls define the enclosure around the mold and cannot obstruct any surfaces, so are not listed as obstruction surfaces.

The mesh refinement required for the furnace wall depends on the size of the mold mesh and the size of the furnace. The furnace wall elements should be less than or equal to the thickness of the baffle. Because the furnace wall will be as close to the mold as the baffle edge would be, the mesh must be as thin as the baffle in order to duplicate the temperature ramp.

The number of divisions used in the FACET model is dependent on the mesh refinement, personal preference and past experience. The row sum of each surface is shown in the FACET printout file, and all the values should be very close to unity. Accuracy of the row sums increase with increasing number of divisions, but so does computation cost. To date, there is no data available to correlate the row sum error and heat flux error for the directional solidification process.

The TOPAZ input deck includes the time step information, nodal data, element data, and boundary conditions. The surface data for the mold and furnace wall are input on the enclosure radiation data card. A heading for surface participation in conduction part of the problem and curve number for emissivity are also included on this card. All the surface elements which define the mold, participate in the conduction part of the problem and should be given an appropriate emissivity. All

the surface elements which define the furnace wall do not participate, and Lawrence Livermore version of TOPAZ automatically gives these surfaces an emissivity of 0.9999.

Each row of furnace nodes with the same vertical height should also be given a temperature/time function curve which corresponds to the travel of the baffle up the furnace wall. The temperature curve can be a simple ramp that starts at the susceptor temperature and when the baffle reaches the nodes height, ramps to the cooling chamber temperature. The ramp can be the time it takes to have the thickness of the baffle pass the node.

To illustrate the steps needed for a simulation using the simple wall method, Figure 14 shows a flow chart of the overall process. In this model, Supertab/ICSS is used as the mesh generator of FACET and TOPAZ. The input deck for FACET contains the nodal data, surface data and obstruction surface data. At the end of the FACET run, the view factor matrix is written to a file for TOPAZ to read. The input deck into TOPAZ contains the model mesh, plus the furnace wall node temperature functions and the correct enclosure radiation input deck. At the end of the heat flow analysis, TOPAZ writes out the temperature output file for specified times in which the post-processor Supertab/ICSS is used to display temperature contours, history curves or nodal heat flows. This information can be used by the design engineer to locate premature solidification in parts of the airfoil, a non-planar solidification front, or areas where defects are likely to occur, who can then change casting parameters to correct or minimize the problem areas.

3.3.2 View Factor Exchange Method

The model procedure using the view factor exchange method differs from the simple wall method in only a few ways. The furnace enclosure again needs the same

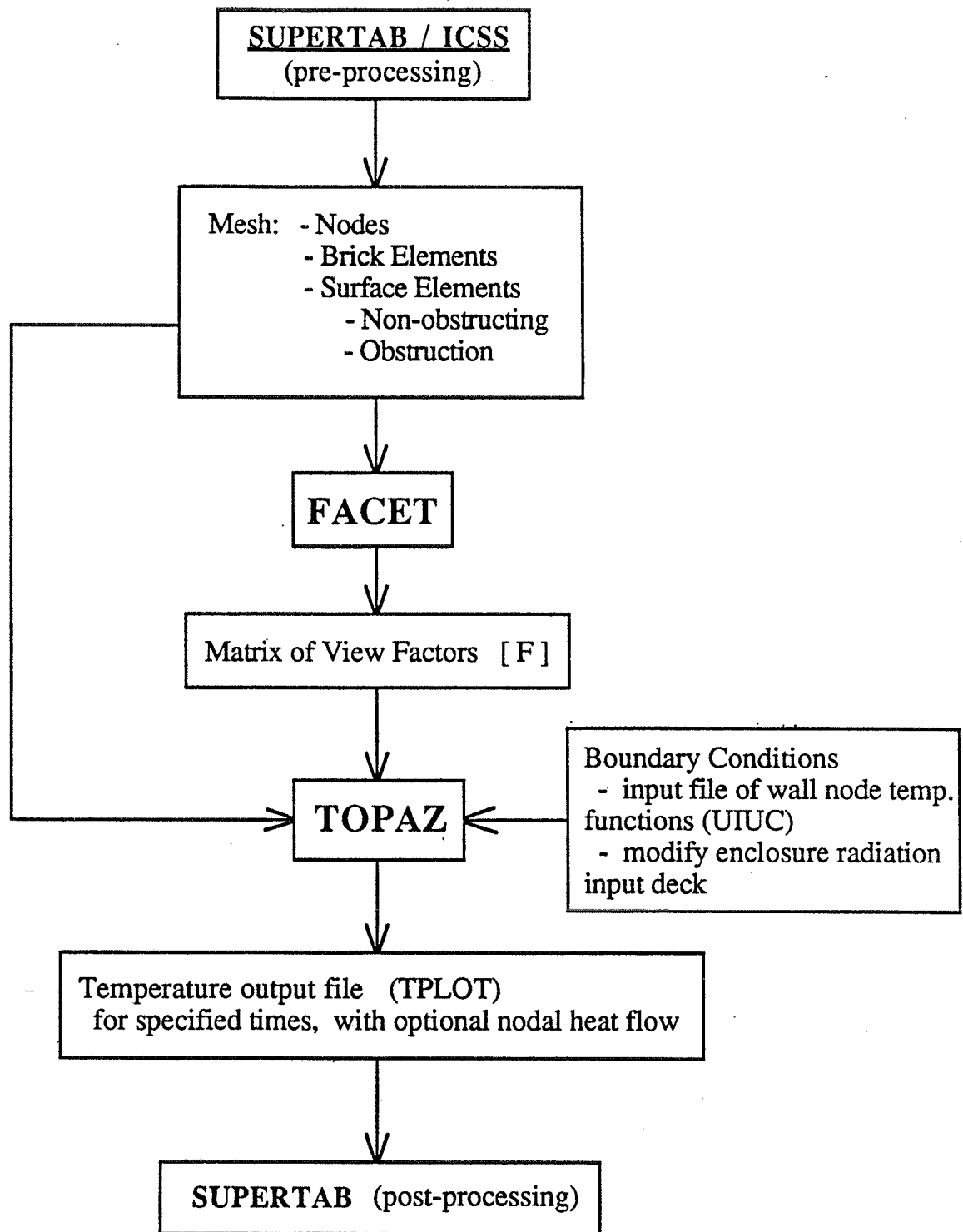


Figure 14. Flowchart of complete directional solidification simulation using the simple wall method.

radius as the susceptor/cooling chamber wall. Eight node brick elements should be used to mesh the baffle(s) used in the process, and they should not be connected to any other elements. Radiation surfaces must be defined on the top and bottom surfaces of all the baffles. The only other change in the input file is the addition of the intercept surfaces. These elements should extend vertically and follow the contour of the baffle edge and thereby enclose each baffle as it travels past the mold wall. To complete the enclosure of the baffle, a layer of intercept elements should lay horizontal at the initial and final heights of the baffle.

The creation of two new elements in FACET has required the addition of new quantities in the input deck [9]. Figure 15a describes card 2 of the MODFACET input deck. The number of #1 and #2 intercept and baffle surfaces need to be included in the input file along with a choice between nodal formats. The Lawrence Livermore nodal format and the format by ICSS are illustrated in Figure 15b. Figure 15c is a copy of the surface data deck for FACET with the addition that the modified surfaces must be input last. This is so the MODTOPAZ does not check for an obstruction range for the modified elements and will not calculate the heat flux for intercept surfaces. The surface number of each of the new elements is read in with the same format as the obstruction surface data. Figure 15d describes the input format for the #1 and #2 intercept elements. The #1 intercept elements define the locus of travel of the #1 baffle and likewise with the #2 intercept elements. Figure 15e describes the input format for the top and bottom surfaces for the #1 baffle and Figure 15f, the format for the #2 baffle surfaces.

The input deck into TOPAZ has also been modified slightly. As shown in Figure 16a, card 2 has the additional input values of the number of FACET intercept surfaces, the number of baffle surfaces for both baffles [11]. These values are checked against

MODFACET INPUT FILE DESCRIPTION

CONTROL CARDS

<u>Columns</u>	<u>Card 2</u> <u>Quantity</u>	<u>Format</u>
1-5	Geometry type (NDIM) EQ.1: axisymmetric EQ.2: 2D planar EQ.3: 3D	I5
6-10	Number of materials (NUMMAT)	I5
11-15	Number of nodal points (NUMNP)	I5
16-20	Number of surfaces (NUMEL)	I5
21-25	Number of surface subdivisions (NDIV) (Default = 5)	I5
26-30	Number of obstructing surfaces (NBLK)	I5
31-35	Number of times to use 2D plane for axisymmetric 180 degree rotation (NROT) (Default = 13)	I5
36-40	Data check flag (ICHECK) EQ.0: normal execution EQ.1: data check only	I5
41-45	Number of #1 baffle surfaces (NIBS)	I5
46-50	Number of #2 baffle surfaces (NOBS)	I5
51-55	Number of #1 intercept surfaces (NINSI)	I5
56-60	Number of #2 intercept surfaces (NINSO)	I5
61-65	Debug printout (IBUG) EQ.0: debug off EQ.1: debug information printed	I5
66-70	ICSS nodal input format (ISDRC) EQ.0: Lawrence Livermore format EQ.1: ICSS nodal format	I5

Figure 15a. MODFACET input deck for card 2.

NODAL POINT DATA

ISDRC = 0

<u>Columns</u>	<u>Quantity</u>	<u>Format</u>
1-5	Node point number	I5
6-10	Skip	5X
11-20	x or r coordinate	E10.0
21-30	y or z coordinate	E10.0
31-40	z coordinate (for 3D only)	E10.0
41-45	Generation increment (INC)	I5

NODAL POINT DATA

ISDRC = 1

<u>Columns</u>	<u>Quantity</u>	<u>Format</u>
1-5	Node point number	I5
6-18	x or r coordinate	E13.5
19-31	y or z coordinate	E13.5
32-44	z coordinate (for 3D only)	E13.5

Figure 15b. MODFACET input deck for nodal point data

SURFACE DATA

<u>Columns</u>	<u>Quantity</u>	<u>Format</u>
1-5	Surface number	I5
6-10	Node N ₁	I5
11-15	Node N ₂	I5
16-20	Node N ₃	I5
21-25	Node N ₄	I5
26-30	Surface material number	I5
31-35	Number of surfaces to be generated following this one	I5
36-40	Generation increment (INC)	I5

The baffle and intercept surfaces must be the last surfaces generated. All normal surfaces must be defined first, then the baffle surfaces and the intercept surfaces are defined last.

Figure 15c. MODFACET input deck for surface data.

#1 INTERCEPT SURFACE DATA

<u>Columns</u>	<u>Quantity</u>	<u>Format</u>
1-5	Surface number (KINTI)	I5
6-10	Number of surfaces to be generated following this one	I5
11-15	Generation increment	I5

#2 INTERCEPT SURFACE DATA

<u>Columns</u>	<u>Quantity</u>	<u>Format</u>
1-5	Surface number (KINTO)	I5
6-10	Number of surfaces to be generated following this one	I5
11-15	Generation increment	I5

Figure 15d. MODFACET input deck for intercept surface data.

#1 BAFFLE TOP SURFACE DATA

<u>Columns</u>	<u>Quantity</u>	<u>Format</u>
1-5	Surface number (KTOPI)	I5
6-10	Number of surfaces to be generated following this one	I5
11-15	Generation increment	I5

#1 BAFFLE BOTTOM SURFACE DATA

<u>Columns</u>	<u>Quantity</u>	<u>Format</u>
1-5	Surface number (KBOTI)	I5
6-10	Number of surfaces to be generated following this one	I5
11-15	Generation increment	I5

Figure 15e. MODFACET input deck for #1 baffle surface data.

#2 BAFFLE TOP SURFACE DATA

<u>Columns</u>	<u>Quantity</u>	<u>Format</u>
1-5	Surface number (KTOPO)	I5
6-10	Number of surfaces to be generated following this one	I5
11-15	Generation increment	I5

#2 BAFFLE BOTTOM SURFACE DATA

<u>Columns</u>	<u>Quantity</u>	<u>Format</u>
1-5	Surface number (KBOTO)	I5
6-10	Number of surfaces to be generated following this one	I5
11-15	Generation increment	I5

Figure 15f. MODFACET input deck for #2 baffle surface data.

MODTOPAZ INPUT FILE DESCRIPTION

<u>Columns</u>	<u>Card 2</u>	<u>Format</u>
	<u>Quantity</u>	
1-5	Number of elements with internal heat generation (NHGEN)	I5
6-10	Number of nodes at which nonzero initial temperatures are specified (NIT)	I5
11-15	Number of nodes at which temperature boundary conditions are specified (NTBC)	I5
16-20	Number of flux boundary condition surfaces (NFBC)	I5
21-25	Number of convection boundary condition surfaces (NCBC)	I5
26-30	Number of radiation boundary condition surfaces (NRBC)	I5
31-35	Number of enclosure radiation surfaces (NRSEG)	I5
36-40	Number of radiation bands (NBAND)	I5
41-45	Number of emissivity vs. wavelength curves (NECURV)	I5
46-50	Radiation calculation type (IRTYP) EQ.1: view factors EQ.2: exchange factors	I5
51-55	Number of special internal boundary elements (NIBC)	I5
56-60	Number of FACET intercept surfaces (NINS)	I5
61-65	Number of #1 baffle surfaces (NIBS)	I5
66-70	Number of #2 baffle surfaces (NOBS)	I5

Figure 16a. MODTOPAZ input deck for card 2.

the surface number output by FACET in order to make sure the correct intercept matrix is read in.

In order to reduce the computer time during a simulation with small time steps, Figure 16b shows the addition of varying the number of times the view factor matrix is recalculated. Another addition to the input deck is the enclosure radiation data card shown in Figure 16c. An initial withdrawal rate and distance is added to the input deck, plus a final withdrawal rate and an initial baffle gap height. The baffle gap is the vertical distance from the Z axis to the initial withdrawal height of the baffle. A extra card has been added to input the cooling chamber temperature and the emissivity curve numbers for the "no participation in conduction" surfaces that model the cooling chamber and the susceptor. The specified cooling chamber temperature is a value between the cooling chamber temperature and the susceptor temperature. Because the temperature are ramped to model the side of the baffle, any temperature below the specified cooling chamber temperature is given the cooling chamber emissivity. Any surface with a temperature above the specified temperature is given an emissivity for the susceptor wall.

The same procedure outlined in the simple wall method for defining enclosure radiation surfaces and furnace node temperature/time function curves is used for the view factor exchange method. Each horizontal row of furnace nodes should be given a temperature/time curve to model the withdrawal process.

The steps to implement a simulation of the directional solidification of an airfoil are very straight forward and shown in Figure 17. To simulate directional solidification using the view factor exchange method, the intercept and baffle elements must be manually input into the FACET input deck created by Supertab/ICSS. At the end of the MODFACET run, the view factor matrix and the intercept height matrix are written to files for MODTOPAZ to read. Additional MODTOPAZ input changes

<u>Columns</u>	<u>Card 5</u> <u>Quantity</u>	<u>Format</u>
1-5	Type of problem EQ.0: linear problem EQ.1: nonlinear problem	I5
Define the following variables for a nonlinear problem:		
6-10	Number of time steps between conductance matrix reformatations EQ.0: default set to 1	I5
11-15	Number of time steps between equilibrium iterations EQ.0: default set to 1	I5
16-20	Maximum number of conductance matrix reformatations EQ.0: default set to 10	I5
21-25	Maximum number of equilibrium iterations permitted per conductance matrix reformation EQ.0: default set to 10	I5
26-35	Convergence tolerance for equilibrium iterations EQ.0: default set to 0.0001	E10.0
36-45	Relaxation parameter EQ.0: default set to 1.0	E10.0
46-50	Number of time steps between radiosity matrix reformatations EQ.0: default set to 1	I5

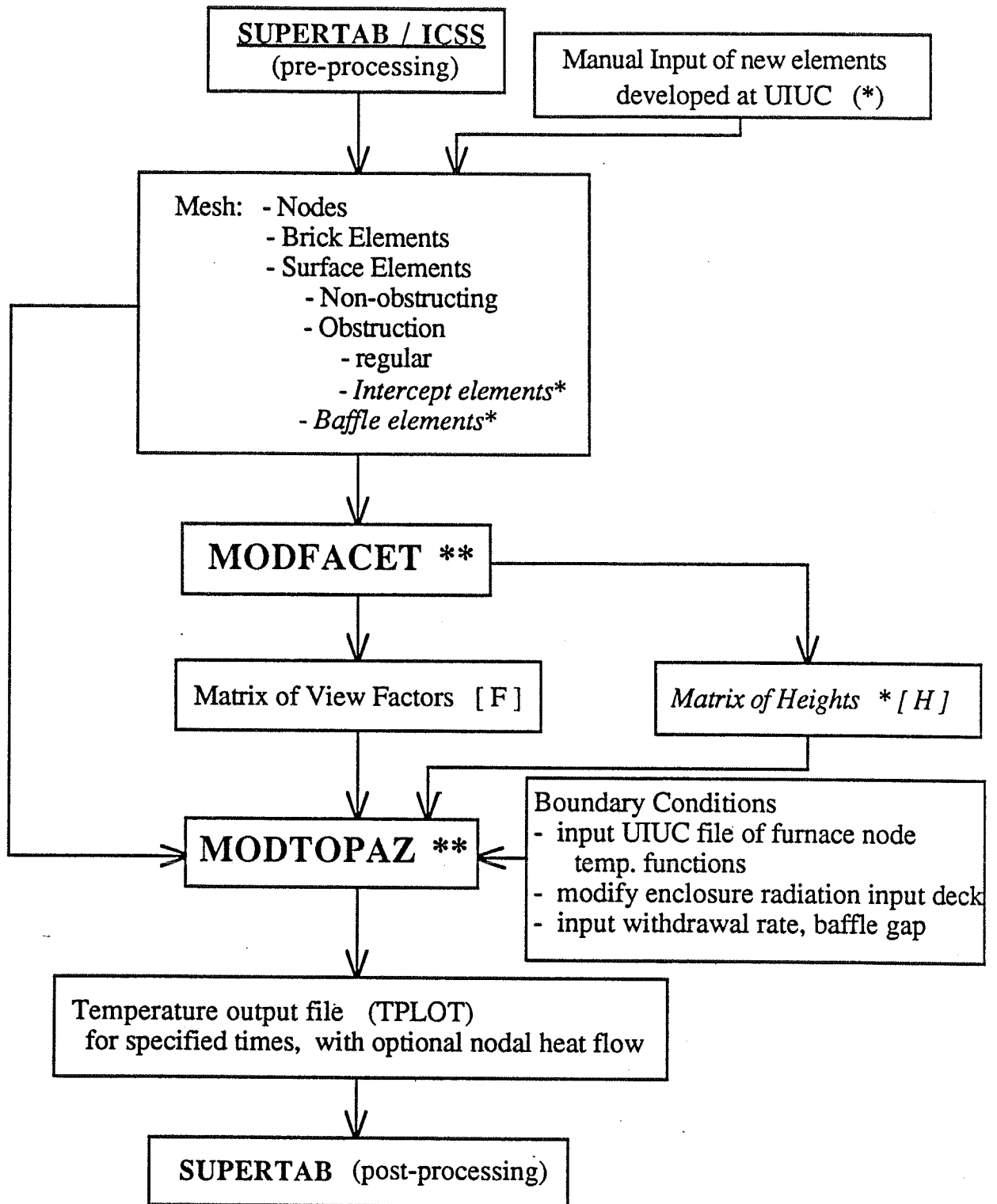
Figure 16b. MODTOPAZ input deck for card 5.

5.13 Enclosure Radiation Data Cards

<u>Columns</u>	<u>Card 1</u>	<u>Format</u>
	<u>Quantity</u>	
1-10	Stefan-Boltzmann constant (SIGMA)	E10.0
11-20	Radiosity convergence tolerance (TOLB) (default = 1.E-04)	E10.0
21-25	Maximum number of radiosity iterations (ITMAXB) (default = 100)	I5
26-35	Directional solidification withdrawal rate #1 (WITHD1)	E10.0
36-45	Distance traveled at withdrawal rate #1 (DIST1)	E10.0
46-55	Directional solidification withdrawal rate #2 (WITHD2)	E10.0
56-65	Initial baffle gap above origin (GAP)	E10.0

<u>Columns</u>	<u>Card 2</u>	<u>Format</u>
	<u>Quantity</u>	
1-10	Cooling chamber surface temperature (TCOLD)	E10.0
11-15	Emissivity curve number for cooling chamber surfaces (NECOLD) (default = 0.9999)	I5
16-20	Emissivity curve number for susceptor surfaces (NEHOT) (default = 0.9999)	I5

Figure 16c. MODTOPAZ input deck for enclosure radiation data card 1.



** Lawrence Livermore programs modified at UIUC

Figure 17. Flowchart of complete directional solidification simulation using the view factor exchange method.

are the withdrawal rates, distance and baffle gap. At the end of the heat flow analysis, Supertab/ICSS can be used to post process and analyze the data.

4. VERIFICATION SIMULATIONS

The purpose of this section is to determine the accuracy of the simple wall method and the view factor exchange method implemented into FACET/TOPAZ. An actual experimental casting geometry, shown in Figure 18, was used as the basis for the boundary conditions for a test case in which the accuracy of the two methods could be investigated. The view factors of a chosen element on the mold surface to the furnace wall surfaces were calculated for a complete range of baffle positions using an analytical formula. The corresponding heat flux to this element was then calculated analytically, assuming appropriate temperatures for all the surfaces. The same problem was then solved using FACET and TOPAZ3D, implementing both the simple wall method and the view factor exchange method. In running TOPAZ3D, the nodes comprising the furnace component surface were fixed to specified temperatures and the nodes of the casting mold were given a specified temperature history which was taken from experimental casting results shown in Figure 19. The view factors and heat flux calculated by the two methods are compared with the exact analytical calculations. Emphasis is placed on the accuracy of the heat flux calculations since they will directly affect the temperature results of a genuine casting simulation. The resulting heat flux predictions are not physically accurate, since the actual susceptor, baffle and cooling chamber temperatures are not known. These results are therefore used for comparison purposes only.

4.1 BAFFLE ANALYSIS

In order to get some idea for the temperature distribution on a typical baffle, a steady state 2D simulation using ANSYS was completed using the configuration and boundary conditions shown in Figure 20. Simple heat transfer coefficients were

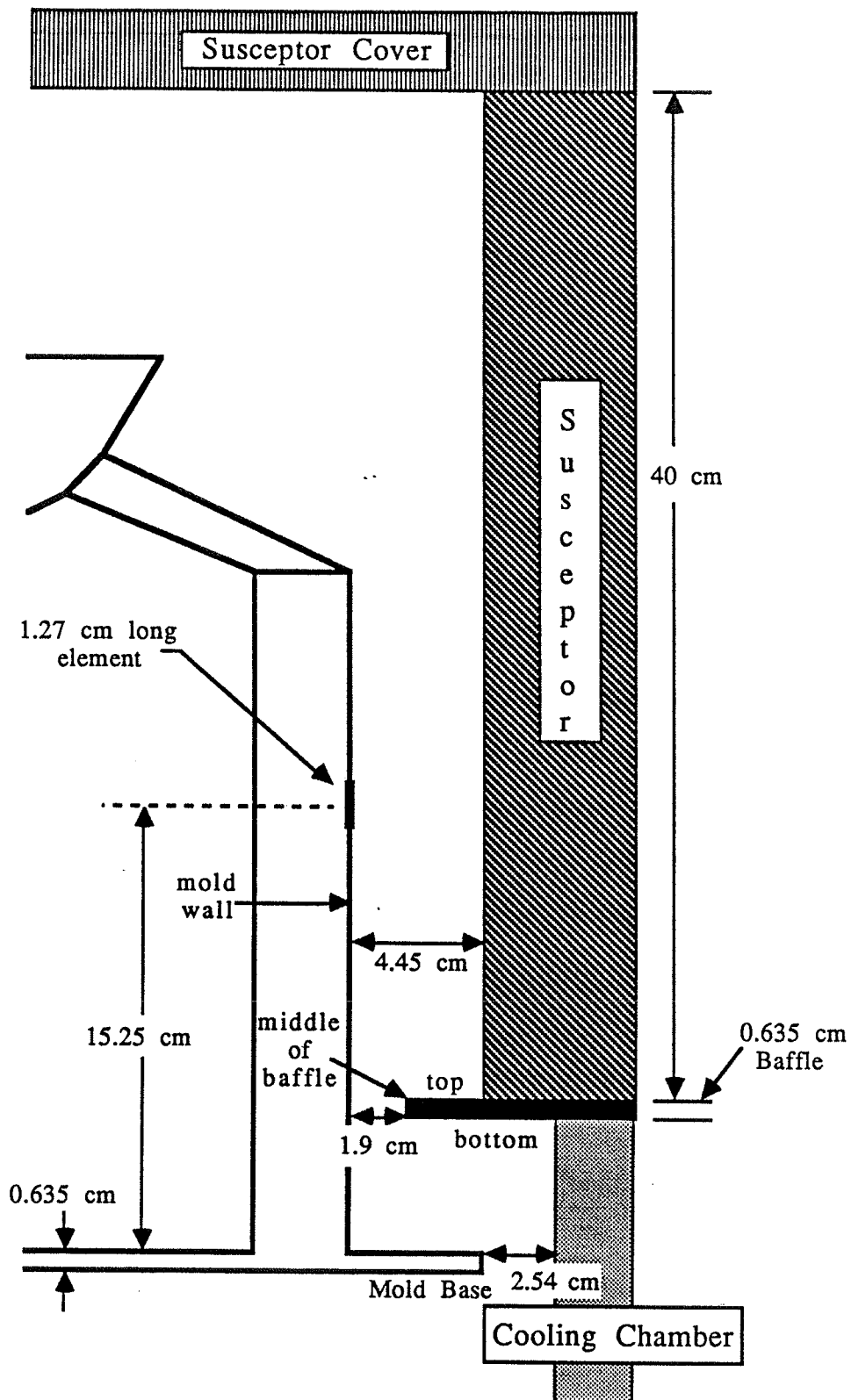


Figure 18. Schematic of mold and furnace geometry used in verification simulations.

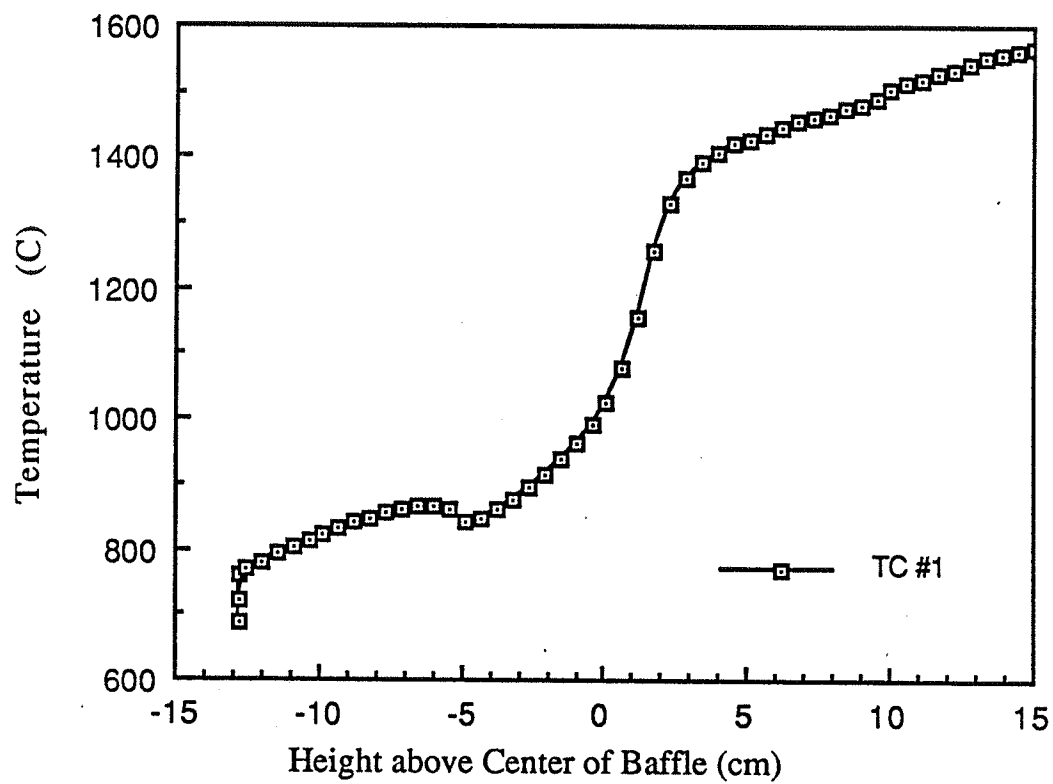


Figure 19. Temperature history of thermocouple #1 from PCC Airfoils, Inc., SMP foundry casting AA-5054.

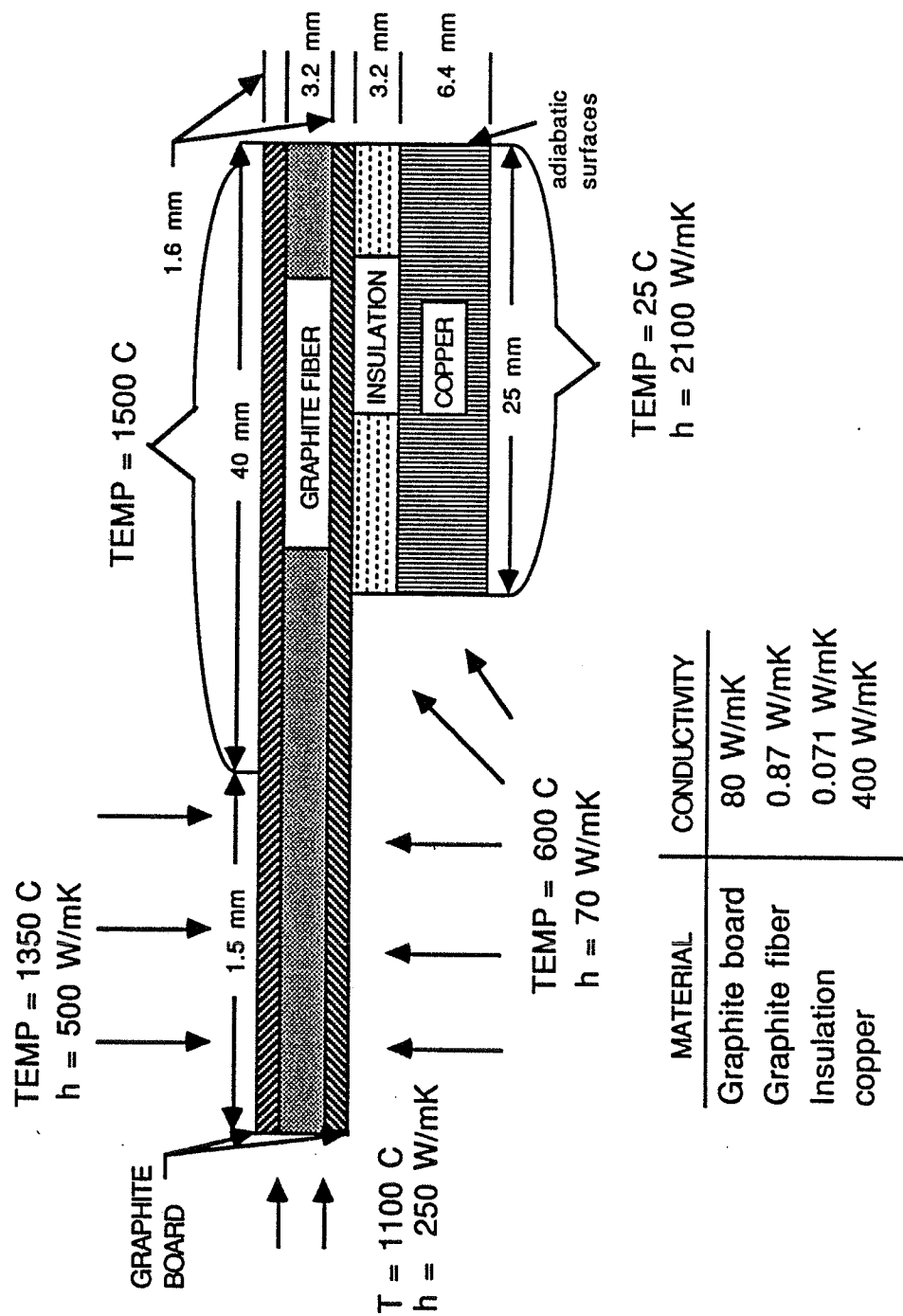


Figure 20. Model boundary conditions used in baffle analysis.

calculated by estimating the temperature of the baffle surfaces and the average temperature of the environment each baffle surface would exchange radiation with. The results shown in Figure 21 reveal that most of the thermal gradient between the susceptor and cooling chamber is in the insulation material. The baffle top averages about 150 C cooler than the susceptor temperature and the baffle bottom is 1100 C hotter than the cooling chamber. These results cause some doubts about the accuracy of the simple wall method which assumes the baffle top surface is at the susceptor temperature and the bottom baffle surface is at the cooling chamber temperature. The magnitude of the errors resulting from this will be revealed later in this investigation.

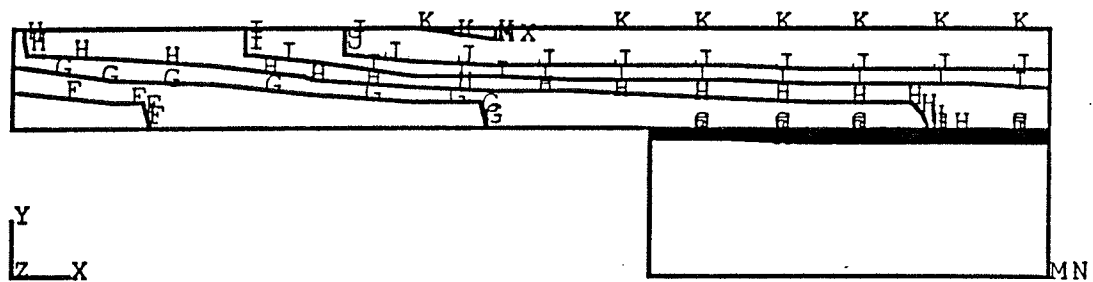
4.2 2D ANALYTICAL MODEL

A computer program was written which calculates the view factor of a surface on the mold wall as the mold is withdrawn from the susceptor. This surface is 1.27 cm long and located 15.25 cm above the mold base. The code uses the two dimensional equations in Figure 22 which were taken from reference 2. The analytically calculated view factors are shown in Figure 23. The +15 cm position is at the very beginning of the casting process. At the 0 cm mark, the casting has been withdrawn 15 cm and the surface is even with the center of the baffle. At the -15 cm mark, the surface element is below the baffle. The graph shows how dominant the susceptor and the cooling chamber view factors are through the majority of the withdrawal process. Only when the surface is within 5 cm of the baffle does the view of the baffle obtain a value over 0.1 and the baffle only reaches a maximum of 0.2 throughout the withdrawal. The graph also shows that the susceptor cover and the mold base are too far away to be seen by the mold surface.

The radiation heat flux is calculated using the equation:

Baffle Model Results
Average Surface Temperatures

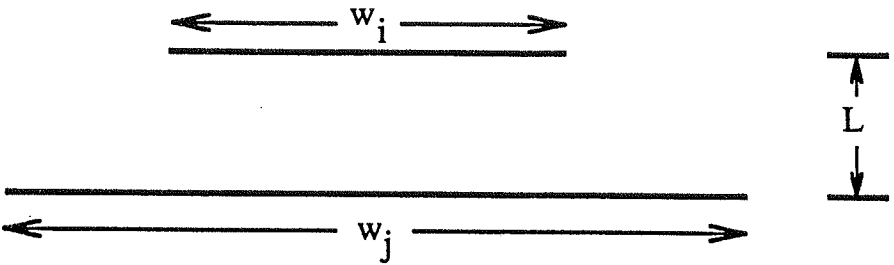
T susceptor = 1565 C (2850 F)
 T baffle top = 1400 C (2550 F)
 T baffle side = 1250 C (2300 F)
 T baffle bottom = 1150 C (2100 F)
 T cooling chamber = 16 C (60 F)



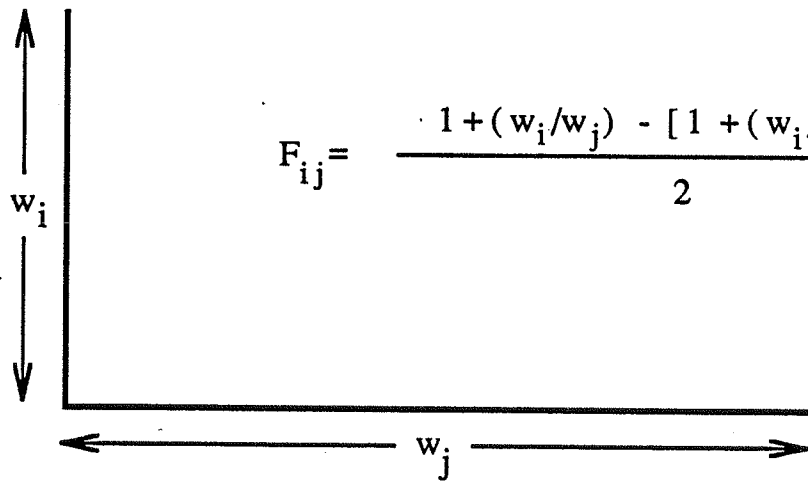
A = 1000 Kelvin	B = 1050
C = 1100	D = 1150
E = 1200	F = 1250
G = 1300	H = 1350
I = 1400	J = 1450
K = 1500	

1 TURBINE BAFFLE ASSEMBLY

Figure 21. Baffle model results show temperature distribution using in improved varifiication simulations.



$$F_{ij} = \frac{[(W_i + W_j)^2 + 4]^{1/2} - [(W_i - W_j)^2 + 4]^{1/2}}{2W_i} \quad \text{where} \quad \begin{aligned} W_i &= w_i / L \\ W_j &= w_j / L \end{aligned}$$



$$F_{ij} = \frac{1 + (w_i/w_j) - [1 + (w_i/w_j)^2]^{1/2}}{2}$$

Figure 22. 2D analytical view factor equations used in verification model. [2]

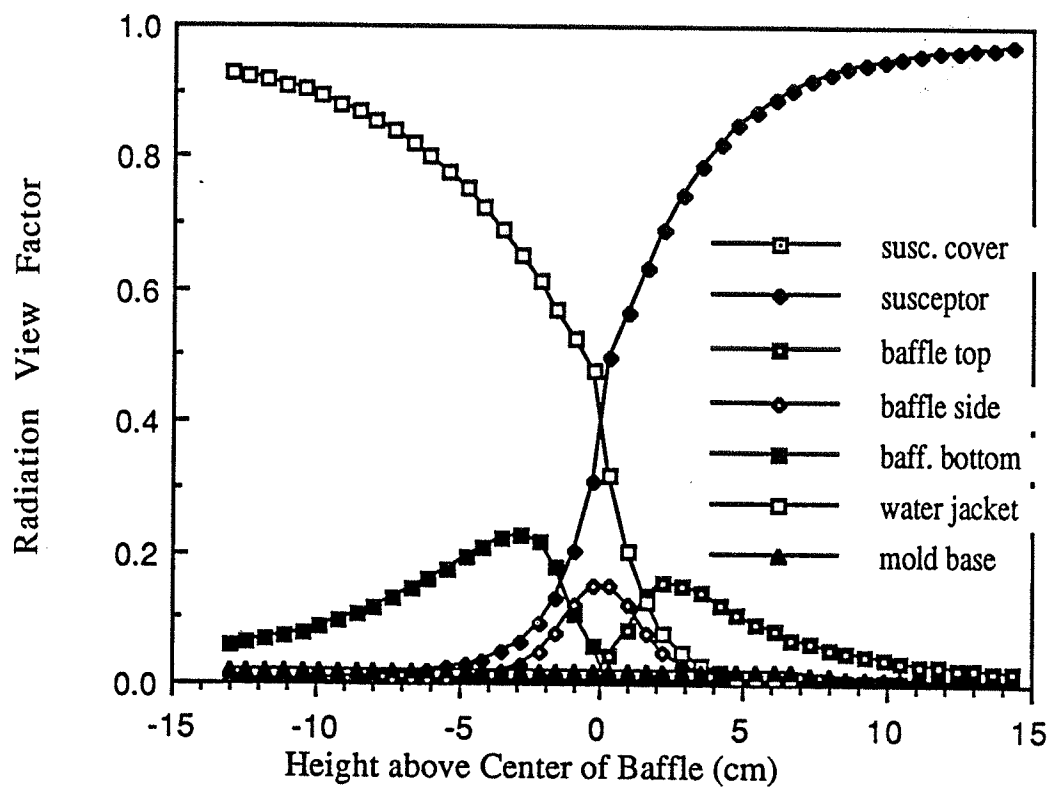


Figure 23. View factor curves of selected mold element to furnace components during the withdrawal process.

$$q'' = VF_{i-j} \epsilon \sigma (T_i^4 - T_j^4). \quad (12)$$

The heat flux into this mold surface element was calculated for a range of furnace positions corresponding to a typical withdrawal cycle. The result is plotted as a function of height above the baffle in Figure 24. The constant temperatures used for the furnace component surfaces are shown in the bottom left of the graph. These temperatures idealize the top and bottom of the baffle as a perfect insulator. The heat flux curve shows heat flowing into the mold surface while it is above the baffle, (negative numbers) and flowing out while the surface is below the baffle. The heat flux calculation was repeated in Figure 25 using improved, more realistic temperatures taken from the baffle analysis. Table 1 shows the temperatures used in the first and second verification models. By changing the temperatures the heat flux curve has flattened out from having a peak heat flux in the hot zone of -20 W/cm^2 to a value of only -14 W/cm^2 . Maximum heat flux leaving the mold surface element in the cooling chamber decreases from approximately 9 W/cm^2 to 6 W/cm^2 .

4.3 ANALYTICAL SENSITIVITY STUDY

One of the main advantages of using models of casting processes is that the casting parameters can be easily altered and their effects analyzed. A simple sensitivity study was conducted to investigate the relative importance of each furnace surface on the heat flux using an analytical method. This was done by varying the temperature of an individual furnace component and comparing the resulting heat flux curves. Figure 26 shows the heat flux into the specified mold element when the temperature of the susceptor changes from 1450 C to 1680 C . The plot clearly shows that the temperature of the susceptor has a dramatic effect on the heat flux into the casting. This is no surprise, since the power to the susceptor induction coils is the primary means of controlling the cooling curves in a

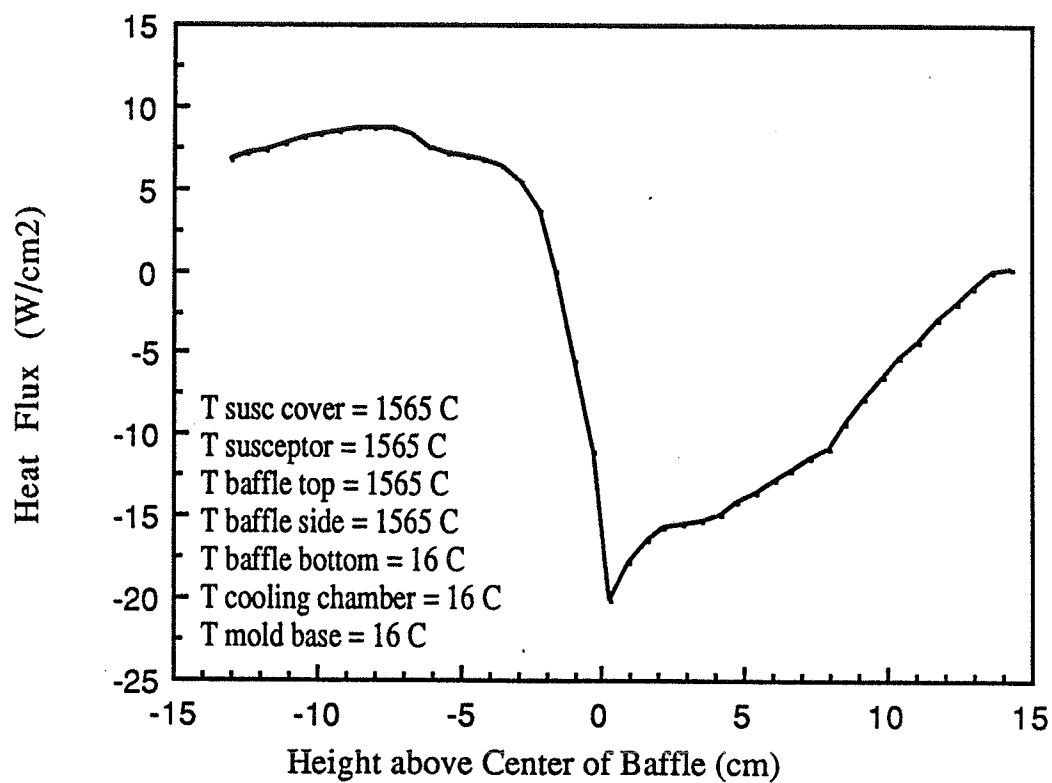


Figure 24. Analytical heat flux curve of mold element using original baffle surface temperatures.

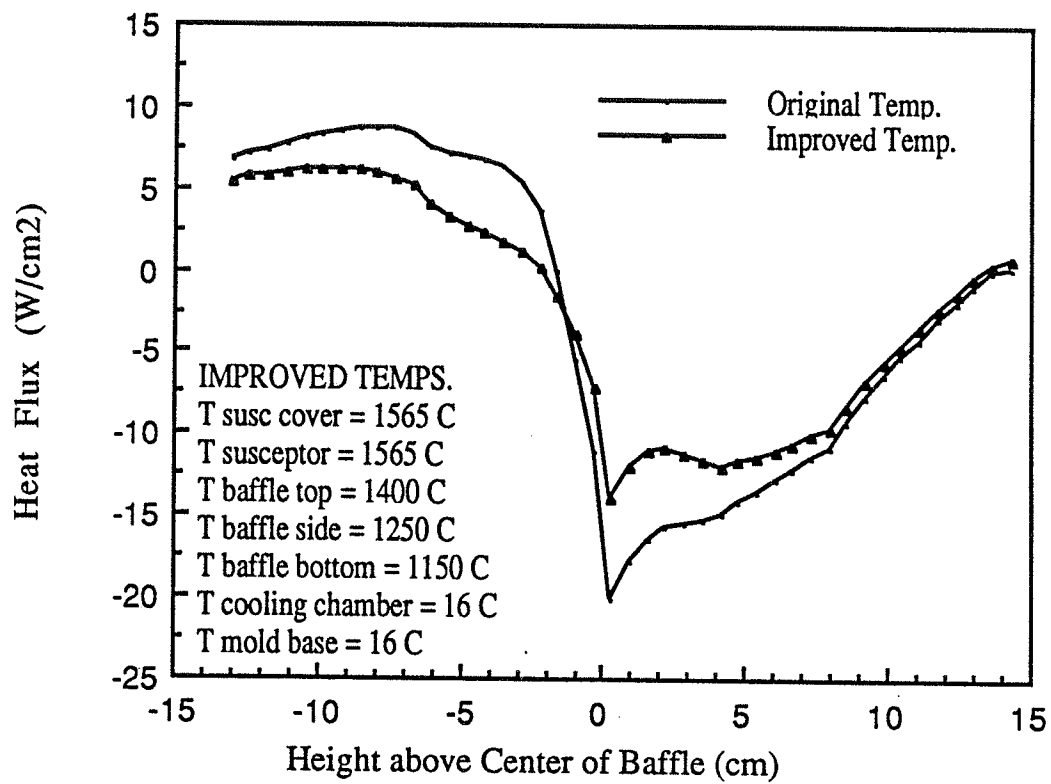


Figure 25. Comparison of analytical heat flux curve using original and improved baffle surface temperatures.

FURNACE COMPONENTS	MODEL #1 ORIGINAL TEMPS.	MODEL #2 IMPROVED TEMPS.
Suceptor cover	1565 C (2850 F)	1565 C (2850 F)
Susceptor	1565 C (2850 F)	1565 C (2850 F)
Baffle top	1565 C (2850 F)	1400 C (2550 F)
Baffle side	1565 C (2850 F)	1250 C (2300 F)
Baffle bottom	16 C (60 F)	1150 C (2100 F)
Cooling chamber	16 C (60 F)	16 C (60 F)
Mold base	16 C (60 F)	16 C (60 F)

TABLE 1. Furnace component temperatures used in the two verification models.

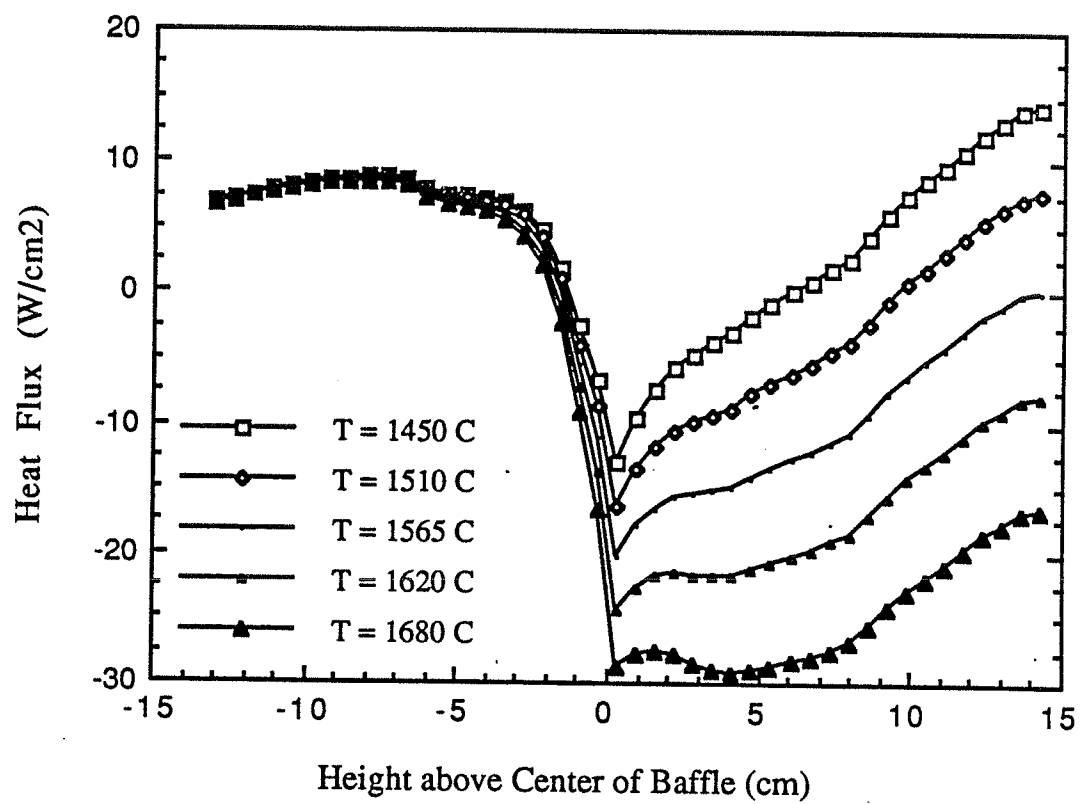


Figure 26. Analytical heat flux curves with varying susceptor surface temperature.

production foundry. Figure 27 through 29 show the localized effect the individual baffle surfaces have on the heat flux. The baffle top surface effects the heat flux curve from 7 cm to 1 cm above the baffle. The baffle side surface effects the heat flux curve from 3 cm to -3 cm from the center of the baffle. Varying the temperature of the baffle bottom surface causes the heat flux curve to change when the mold surface is -2 cm to -10 cm from the baffle center. It can be concluded from the three graphs that all the baffle surfaces have an effect on the heat flux into the mold surface. If the baffle top surface is assumed to be at the susceptor temperature of 1565 C and it is actually at 1400 C, the heat flux curve will have an error of 25 % when the mold element is 3.5 cm above the baffle center. If the surface temperature happened to be 1230 C, a 50 % error in the heat flux would occur at that height. An error of this size just above the baffle will have a great effect on the accuracy and usefulness of the model, because the liquidus/solidus front is usually at that height and this is the region of most importance in defect formation.

Figure 30 shows the effect on heat flux of varying the cooling chamber temperature. The heat flux into the mold element is surprisingly insensitive to temperature changes of the cooling chamber and is not appreciably affected until the chamber reaches 500 C. While the cooling chamber is water cooled and never reaches the boiling point, an ash layer commonly forms over the chamber wall and could result in a higher then expected temperature because of a possible emissivity change. Use of computer modeling would be a useful tool to investigate the effects of the ash layer on the casting process.

4.4 SIMPLE WALL MODEL

The same problem solved analytically was simulated with the simple wall method, using the original Lawrence Livermore FACET/TOPAZ3D code. The susceptor

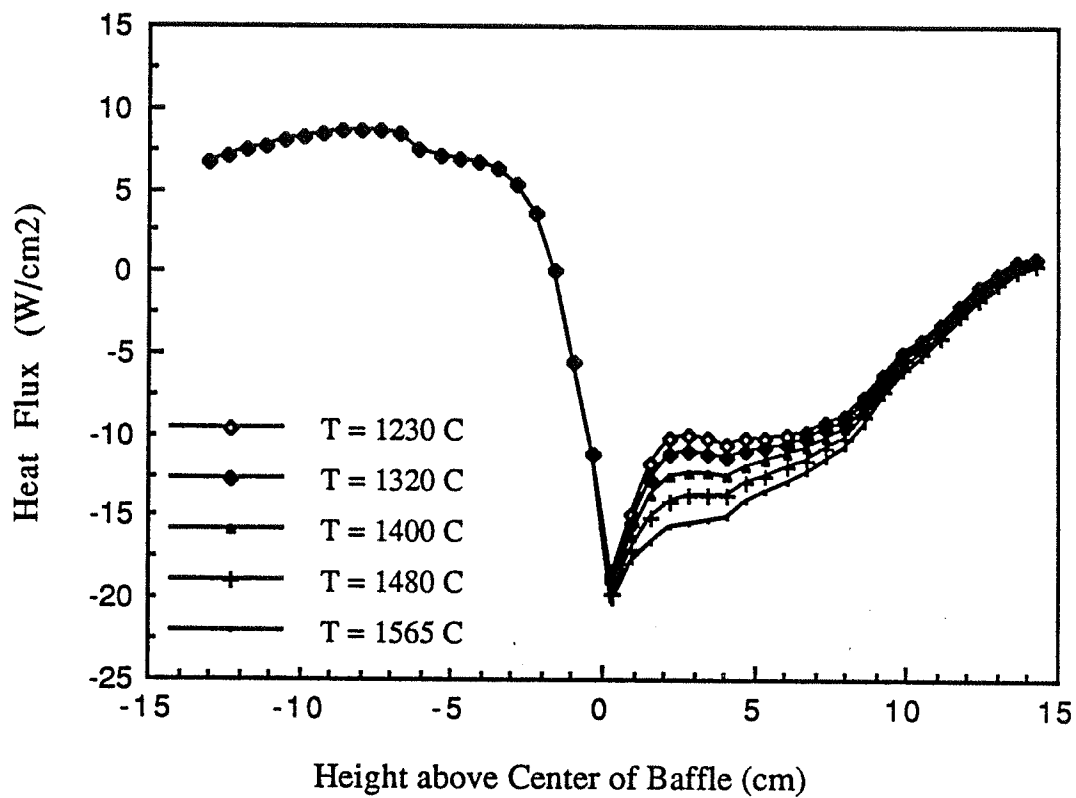


Figure 27. Analytical heat flux curves with varying baffle top surface temperature.

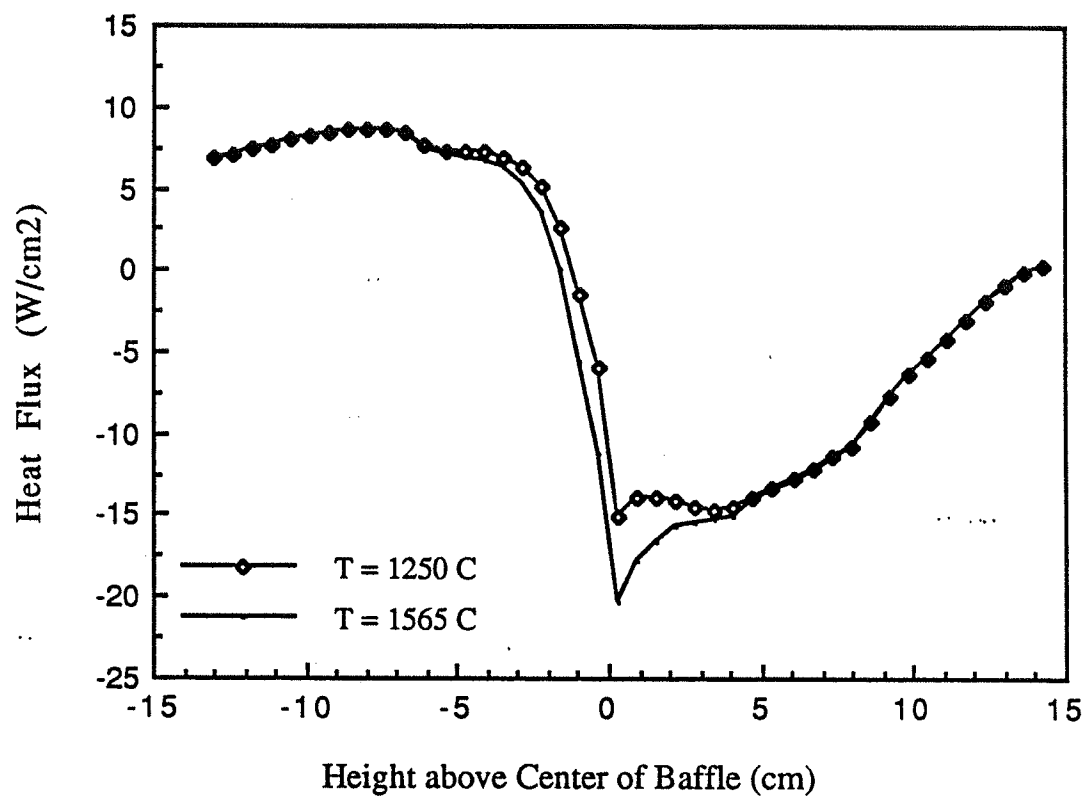


Figure 28. Analytical heat flux curves with varying baffle side surface temperature.

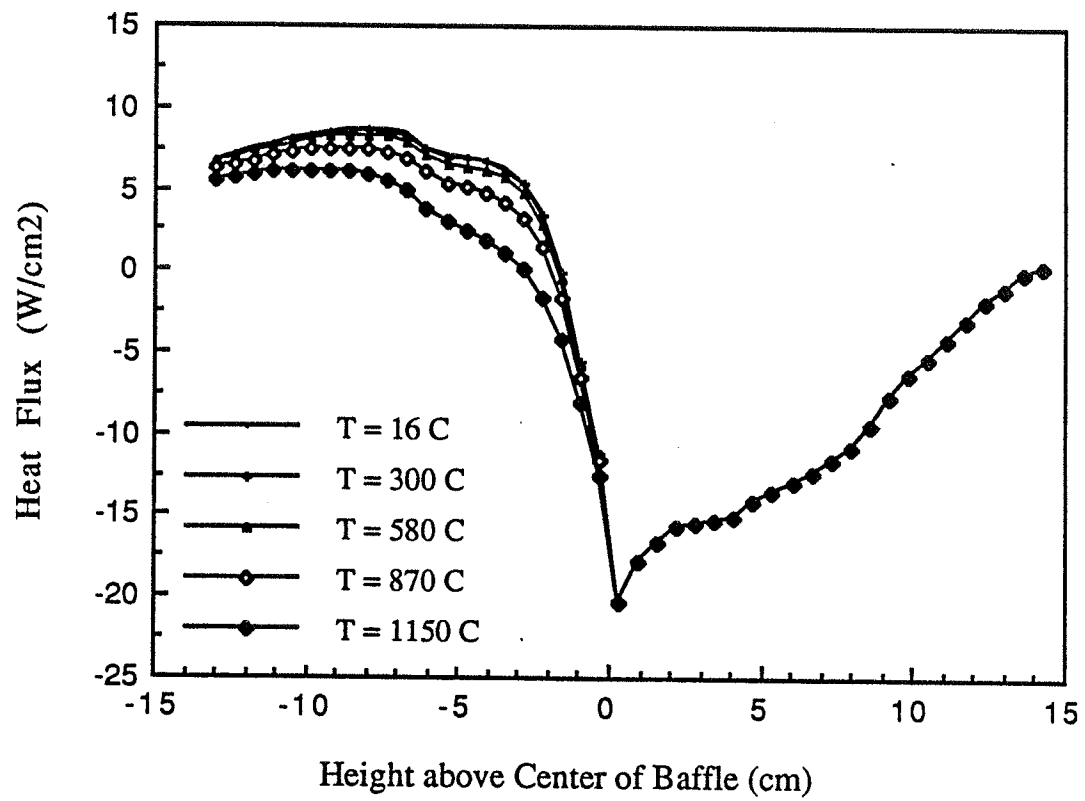


Figure 29. Analytical heat flux curves with varying baffle bottom surface temperature.

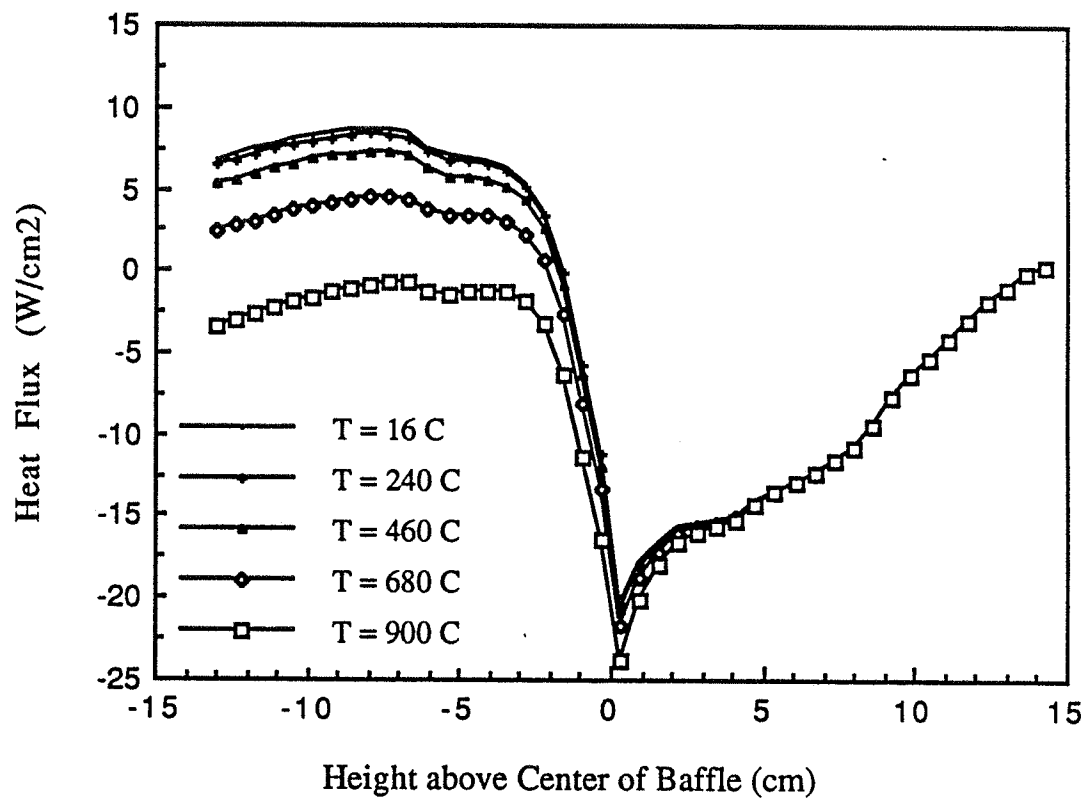


Figure 30. Analytical heat flux curves with varying cooling chamber surface temperature.

and cooling chamber wall was placed 4.45 cm away from the mold wall and the mold base was reduced to a length of 4.45 cm in order to create the enclosure. All other dimensions are the same as in Figure 18. The surface element mesh size for the furnace wall was 0.16 cm high, while the susceptor cover and mold base elements were approximately 0.635 cm.

Figure 31 shows a heat flux comparison between the analytical results and the simple wall method using the ideal, original temperature assignments. The susceptor and baffle top have the same temperature of 1565 C and the cooling chamber and baffle bottom are at 16 C. With these temperatures, the simple wall method should give an exact solution and comes very close to one. The simple wall heat flux curve shows a 1.5 cm offset to the right of the analytical solution. A problem with the temperature/time boundary conditions in TOPAZ3D is believed to have caused this slight offset in the heat flux curve. Problems with FACET calculating 3D view factors for a 2D problem were overcome by manipulating TOPAZ3D so that it can accept 2D view factors.

Figure 32 compares the analytical and simple wall method heat flux curves, using the improved baffle temperatures. These results demonstrate the limitations of the simple wall method. While the analytical curve changes significantly with the temperature of the baffle top at 1400 C and the baffle bottom at 1150 C, the simple wall method is unable to account for these changes and remains the same. The result is a maximum percent error of over 100% over-prediction of heat flux at the critical time when the mold surface element is just above the center of the baffle. As the baffle area increases, the importance of the baffle surface temperature in the heat flux to the mold increases. It is common to have a baffle as large as 20 cm in diameter. Thus, the accuracy of the simple wall method to predict heat flux exchange with a large baffle is expected to be much worse. These results show that the baffle

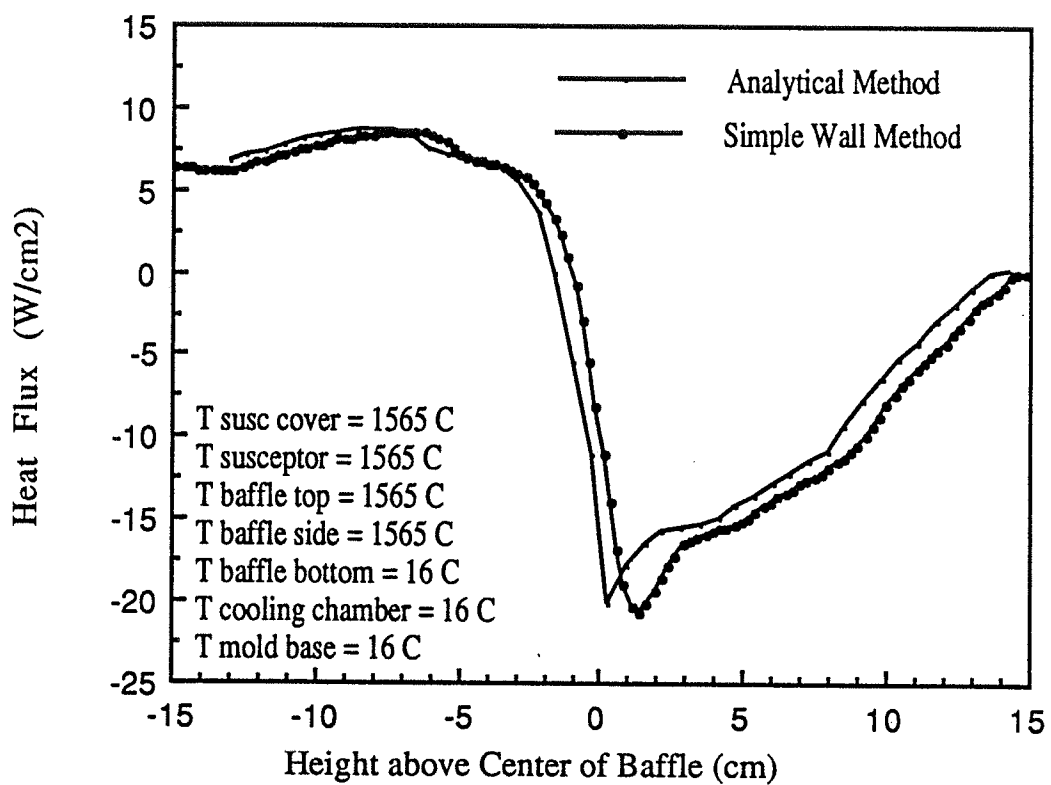


Figure 31. Comparison of heat flux curve using analytical and simple wall method with original baffle surface temperatures.

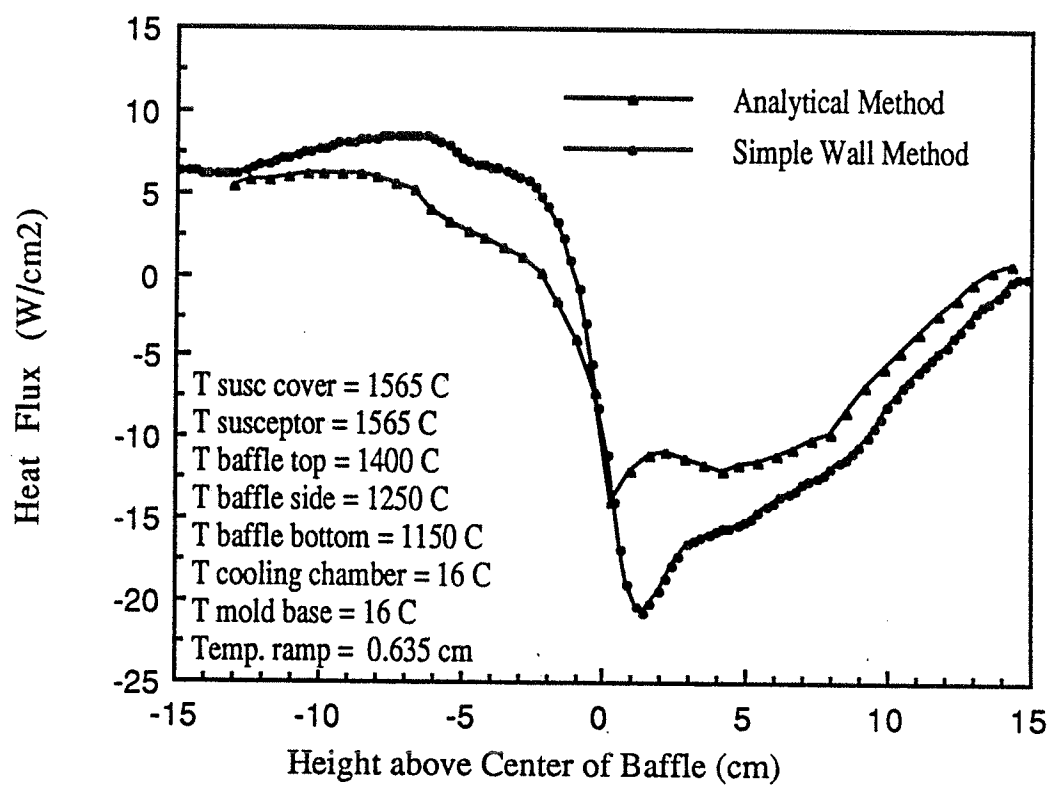


Figure 32. Comparison of heat flux using analytical and simple wall method with improved baffle surface temperatures.

temperature(s) play an important part in the heat flow analysis of the directional solidification of turbine blades and must be modeled correctly in order to obtain accurate results.

4.5 VIEW FACTOR EXCHANGE MODEL

A comparison of the heat flux using the view factor exchange method with the analytical results in Figure 33 and 34 shows the accuracy and flexibility of this new method. The same mesh and temperature/time boundary conditions were used in the exchange model as were used in the simple wall simulation. The simulation for Figure 33 uses the original temperature assignments, with the baffle top surface held constant at 1565 C and the baffle bottom at 16 C. The curve shows excellent agreement with the analytical results, even better than that obtained using the simple wall method. The 2 W/cm² gap between the -2 through -5 cm heights is caused by having the thin baffle at the top of the 0.635 cm temperature ramp along the furnace wall. As the baffle moves up the wall, one or two elements below the thin baffle are at a warm temperature while they should be at the cooling chamber temperature. Adding the baffle thickness to the obstruction range would model a thick baffle in the exchange logic and is being investigated.

The heat flux curves in Figure 34 use the improved, more realistic baffle temperatures. There is good agreement between the view factor exchange curve and the analytical results. The heat flux generated by the view factor exchange method is generally 2 to 3 W/cm² lower than the analytical results. The slight increase in heat flux into the mold surface can also be attributed to the thin baffle assumption used in the view factor exchange. As the baffle becomes level with the mold surface, fewer furnace elements become obstructed by the baffle and the temperature ramp along the furnace wall becomes more important. The mold surface has no view of the

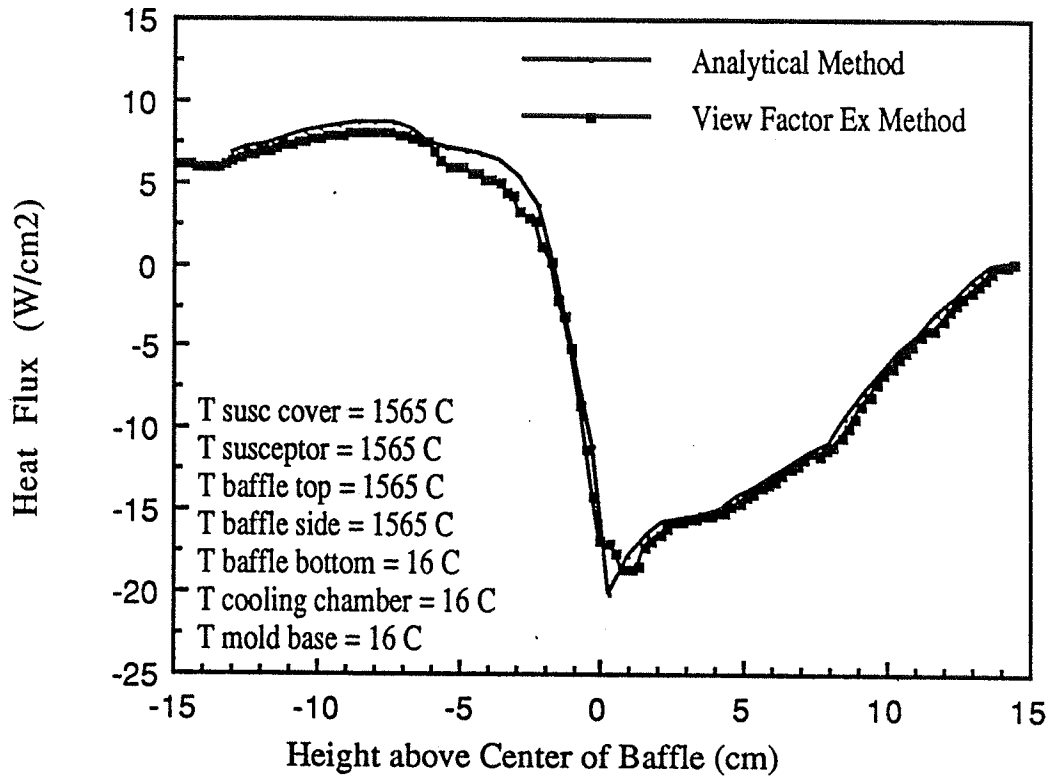


Figure 33. Comparison of heat flux curve using analytical and view factor exchange methods with original baffle surface temperatures.

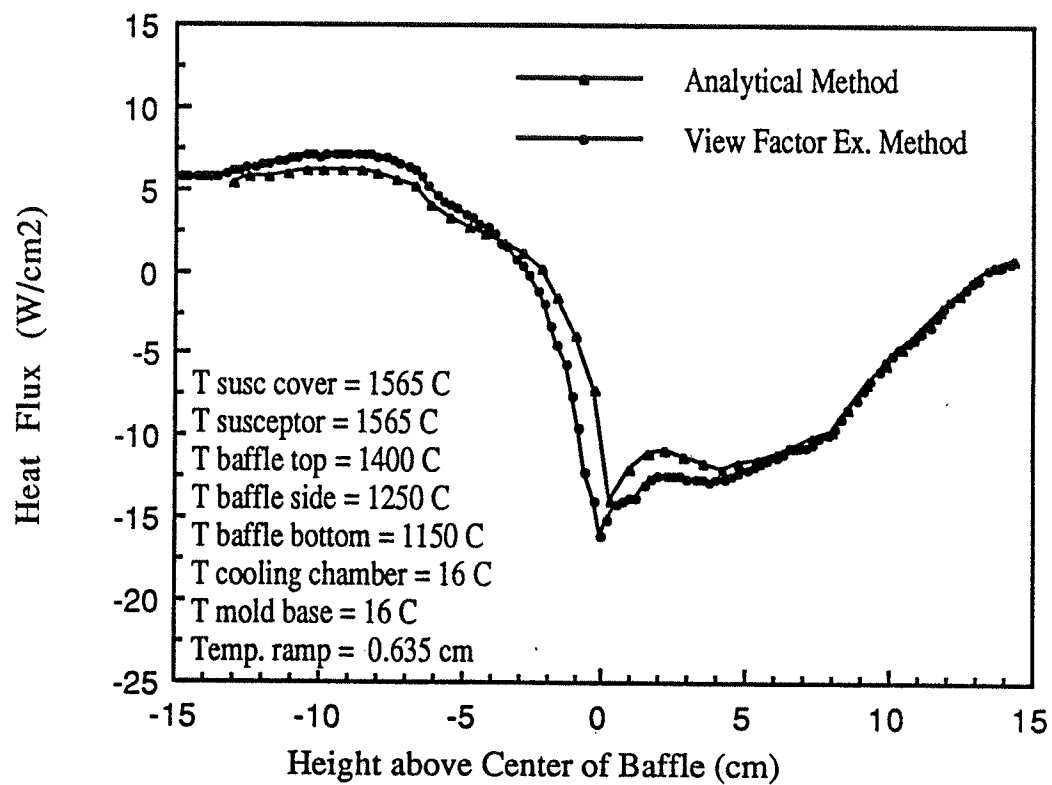


Figure 34. Comparison of heat flux curve using analytical and view factor exchange methods with improved baffle surface temperatures.

baffle at all when it is level with the thin baffle and the furnace wall is too far away to model the side of the baffle with temperature ramping. The results using the view factor exchange method are significantly better than those with the simple wall method and the accuracy is quite reasonable. When combined with the other advantages of this method, it provides an optimal way to model the directional solidification process.

5. EXPERIMENTAL CASTING SIMULATIONS

To demonstrate the capability of the model to simulate a production foundry for casting single crystal airfoils, three casting simulations were performed to predict temperature development in previously instrumented experimental castings. In this previous experiment, a cluster of 15 cylindrical castings was poured and cast. The instrumented test cylinder was cast at PCC Airfoils, Inc. at the SMP foundry and comparisons will be made against that data. Thermocouples were located in one of the castings as shown in Figure 35. Thermocouple number 6 was placed 0.3 cm inside the ceramic mold, approximately 15.25 cm above the bottom of the chill block. Thermocouple number 8 was placed 0.32 cm inside the casting surface, at the same height as thermocouple number 6. The 3.8 cm diameter cylinder casting is approximately 15.25 cm high, with a 7.6 cm (3") chill block/helix grain selector assembly, for a total of 22.9 cm (9"). The ceramic mold is a uniform 0.635 cm thickness around the entire casting. From the leading edge of the ceramic mold, the first baffle had 1.9 cm (0.75") clearance and the susceptor was 4.5 cm (1.75") away. The inner edge of the ceramic mold had approximately 1.27 cm (0.5") of clearance. The first baffle had a constant diameter while the second baffle was contoured to keep 1.27 cm clearance around 120 degrees of the casting.

The boundary conditions used in the simulations were chosen to match experimental conditions and are given in Table 2. The pour temperature was chosen as the susceptor temperature of 1565 C, and the input water temperature was chosen as the cooling chamber surface temperature of 20 C. A temperature ramp of 0.635 cm from the susceptor to the cooling chamber temperature was used to model the baffle thickness. A convection coefficient of 0.2 W/cm²K with a water temperature of 20 C

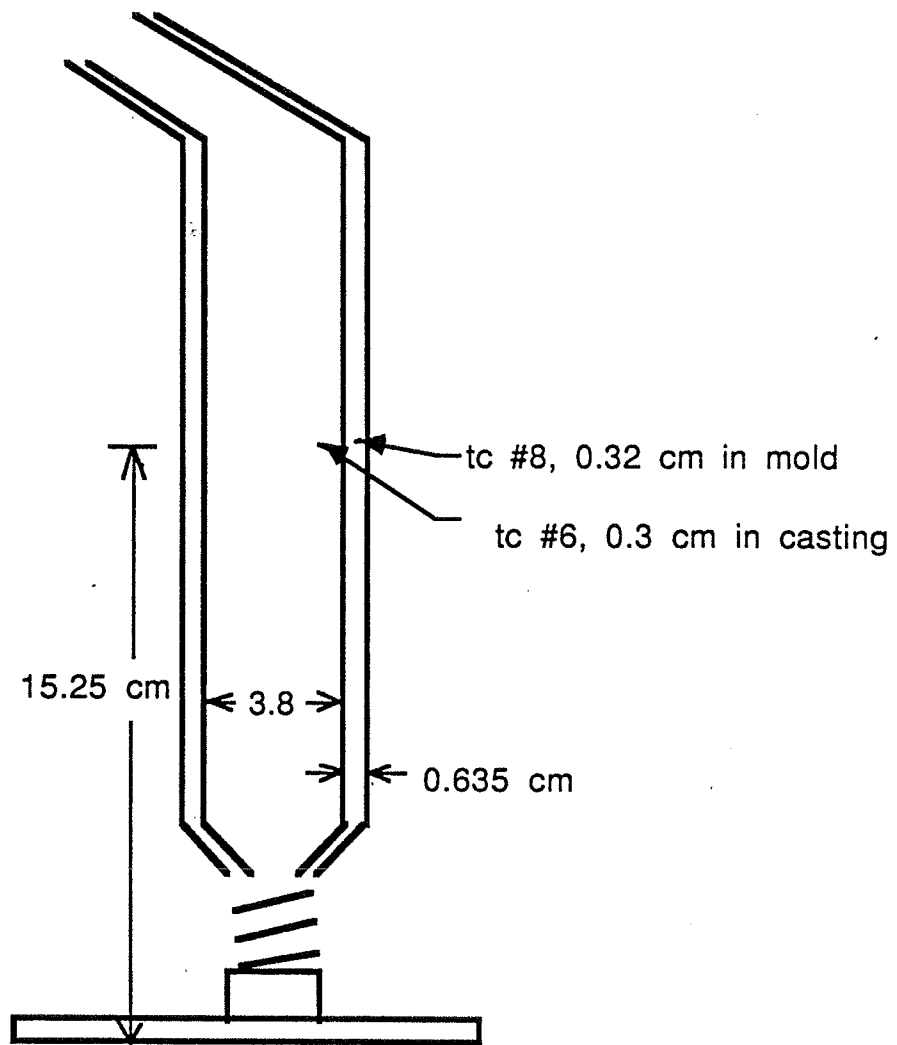


Figure 35. Thermocouple location on experimental casting from cluster A-5056 of PCC Airfoils, Inc. SMP foundry.

	Axi-symmetric Model	Furnace Slice Model	Furnace Slice w/feeders Model
Susceptor Temp	1565 C (2850 F)	1565 C (2850 F)	1565 C (2850 F)
Susceptor Emissivity	1.0	1.0	1.0
Cooling Chamber Temp	20 C (70 F)	20 C (70 F)	20 C (70 F)
Cooling Chamber Emissivity	1.0 - 0.5	1.0	0.5
Chill Plate Cooling Water Temp	20 C (70 F)	20 C (70 F)	20 C (70 F)
Convection Coefficient	0.2 W/cm2-K	0.2 W/cm2-K	0.2 W/cm2-K
Mold Emissivity	0.7	0.7	0.7
Baffle Emissivity	-----	-----	0.5
Chill Plate Emissivity	-----	-----	0.5

Table 2. Boundary conditions used in experimental simulations

was applied to the bottom of the 1.9 cm thick chill plate. Figure 36 shows the casting parameters and material properties of the experimental casting.

5.1 AXI-SYMMETRIC MODEL

For the first heat flow analysis of the directional solidification process, an experimental, single crystal test cylinder was modeled using one element thick slice through the casting. Figure 37 shows the finite element mesh used with the simple wall method. Figure 38 is a blown-up view from left to right of the superalloy casting, the 1.27 cm ceramic mold, the mold enclosure radiation surfaces, the 0.5 cm (0.2") high furnace surface elements, and on the bottom of the figure is the copper chill plate. The susceptor surface has been moved in 2.5 cm from the actual dimensions so that the susceptor and cooling chamber are 1.9 cm from the mold surface.

A comparison of the model results and experimental data is shown in Figures 39 and 40. The predicted versus the measured temperature at the same point is 50 C hotter before it reaches the baffle height. It is 150 C hotter during the sharp temperature drop and cools much faster than the experimental casting. The model does a slightly better job of predicting the thermocouple temperature before it reaches the baffle, but cools much faster than the experimental results. The sharper temperature gradient in the model is caused by the the axi-symmetric assumption. The actual casting was not surrounded on all sides by a susceptor/cooling chamber, but one of a 14 other castings. There was also a second baffle, runners, pour cup and a exposed chill plate in which the casting exchange heat with. This illustrates the important role all these surfaces play in the heat flux to the casting.

Figure 41 and 42 show temperature contours within the metal and mold during withdrawal. Noteworthy features are the 1) increase in the thermal gradient as the

Experimental casting A-5056

Nickel based superalloy

Liquidus = 1430 C (2600 F)

Solidus = 1380 C (2520 F)

Latent Heat = 220 J/g

Pour temperature = 1566 C (2850 F)

Initial withdrawal rate = 0.0042333 cm/sec (6 "/hr)

Distance traveled at initial withdrawal rate = 5.0 cm (2")

Final withdrawal rate = 0.0056444 cm/sec (8"/hr)

Total withdrawal distance = 28 cm (11")

Material	Density (g/cm ³)	Conductivity (W/cm K)	Specific Heat (J/g K)
Nickel Alloy	8.6	0.28	0.57
Ceramic Mold	2.5	0.02	1.2
Graphite Baffle	2.2	0.06	0.7
Copper Chill Plate	8.9	4.0	0.4

Figure 36. Casting parameters and material properties used in simulations

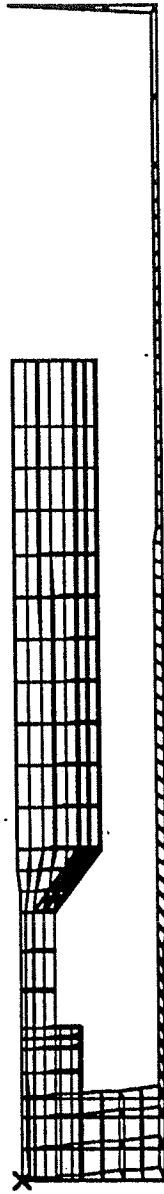


Figure 37. Finite element mesh of axis-symmetric casting using simple wall method.

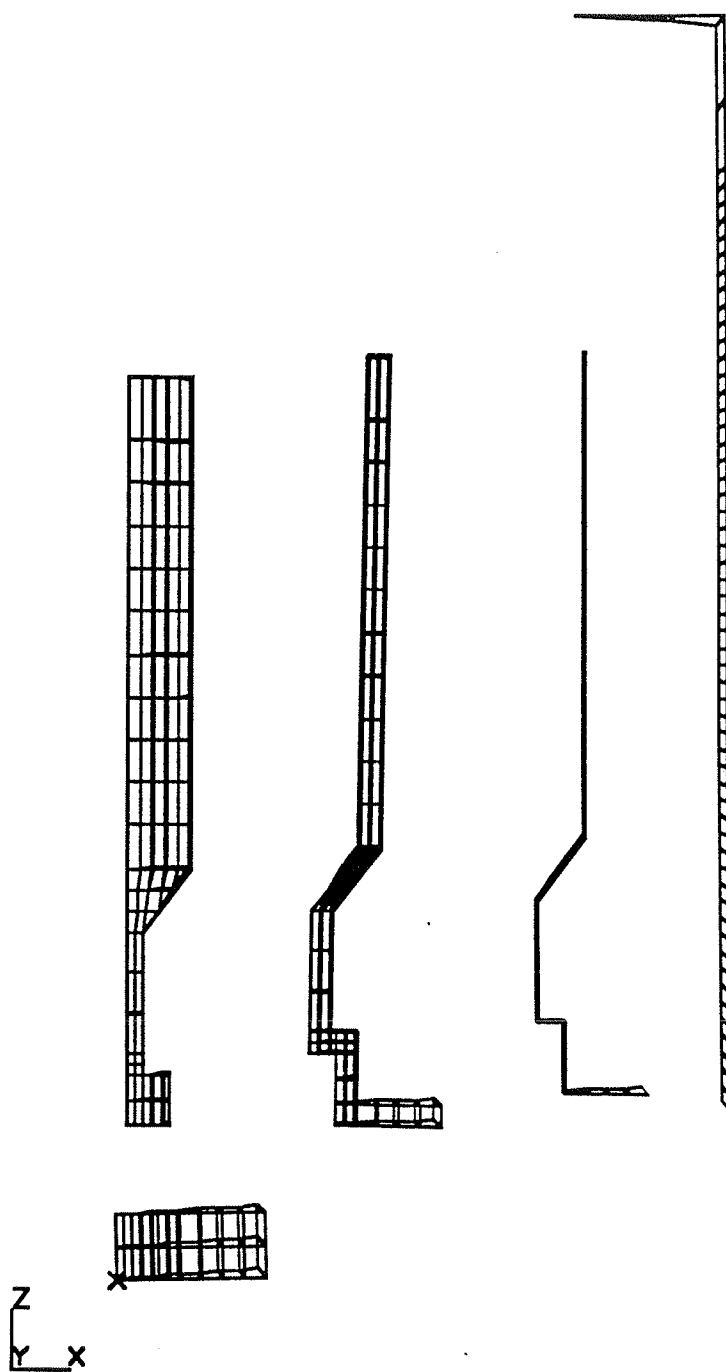


Figure 38. Exposed view of casting, mold, mold surface, furnace surface and chill plate.

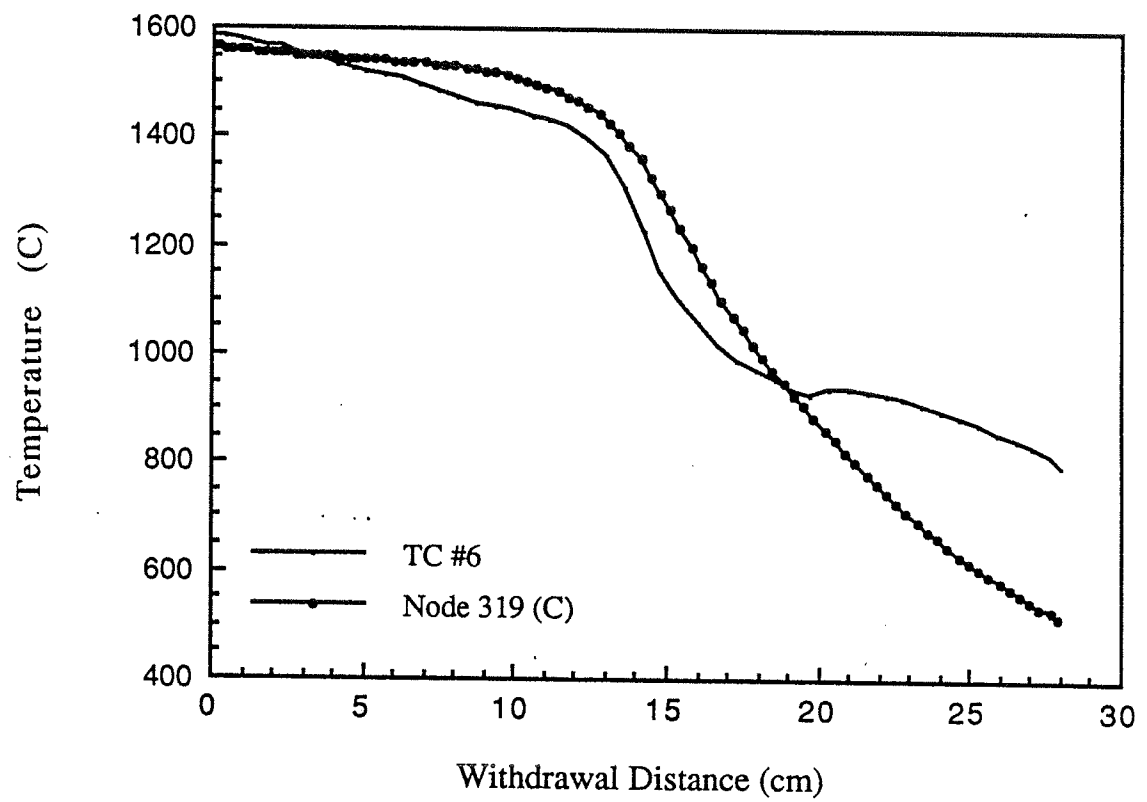


Figure 39. Experimental (TC #6) and predicted (node 319) temperature results using the simple wall method.

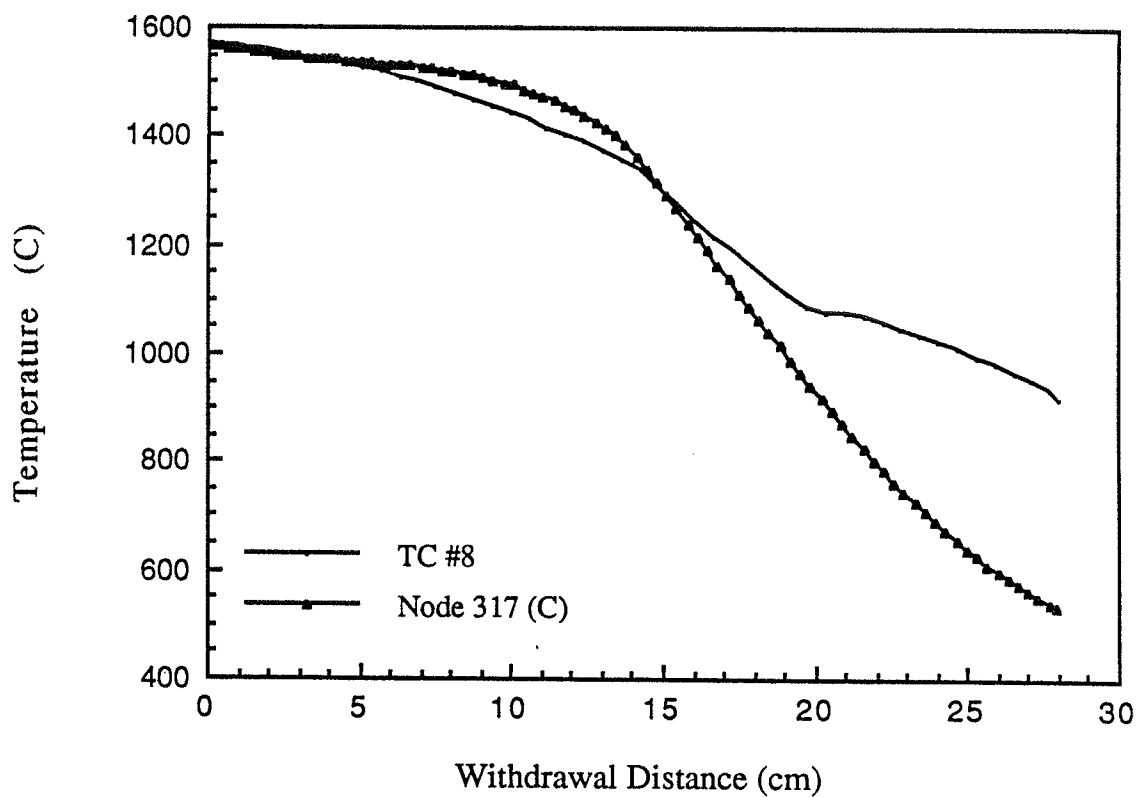
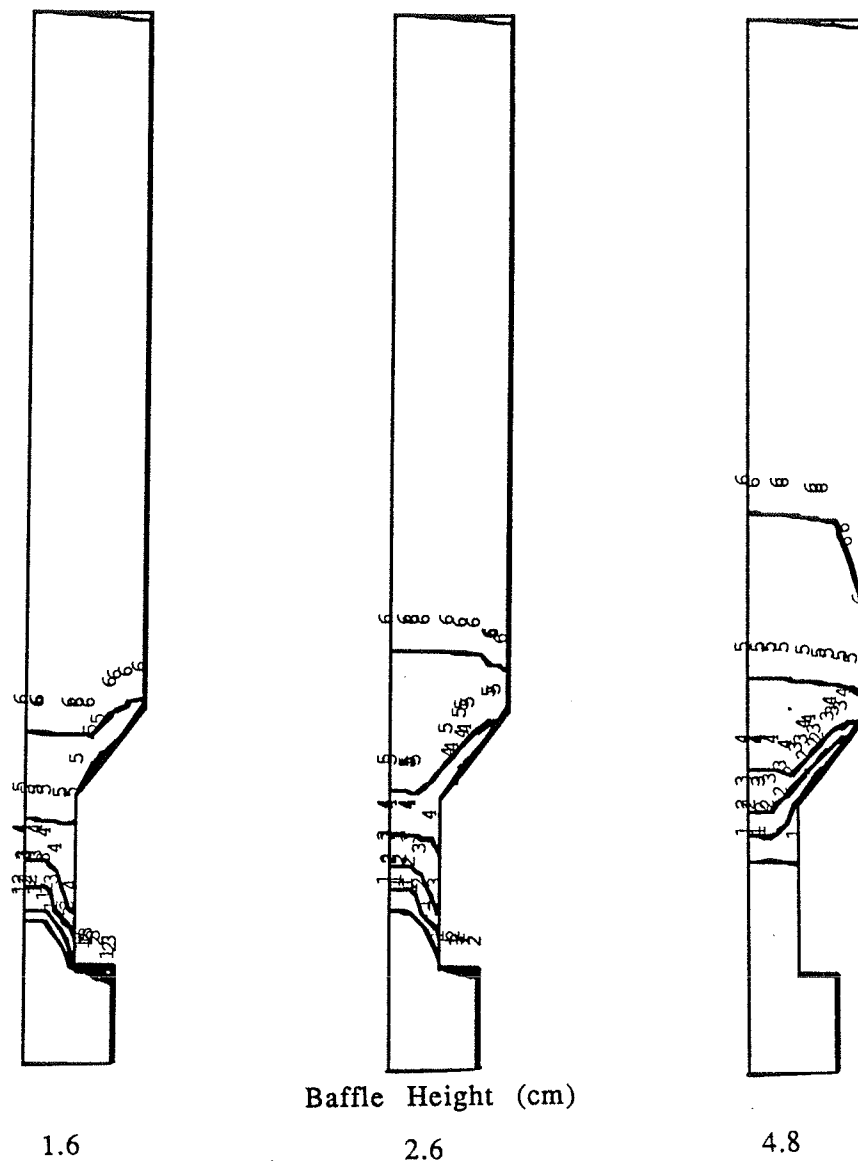


Figure 40. Experimental (TC #8) and predicted (node 317) temperature results using the simple wall method.



Temperature Scale

1 - 1280 C (2330 F)	2 - 1330 C (2420 F)
3 - 1380 C (2510 F)	4 - 1430 C (2600 F)
5 - 1480 C (2690 F)	6 - 1530 C (2780 F)

• Figure 41. Temperature contours at withdrawal heights 1.6, 2.6 and 4.8 cm using the simple wall method.

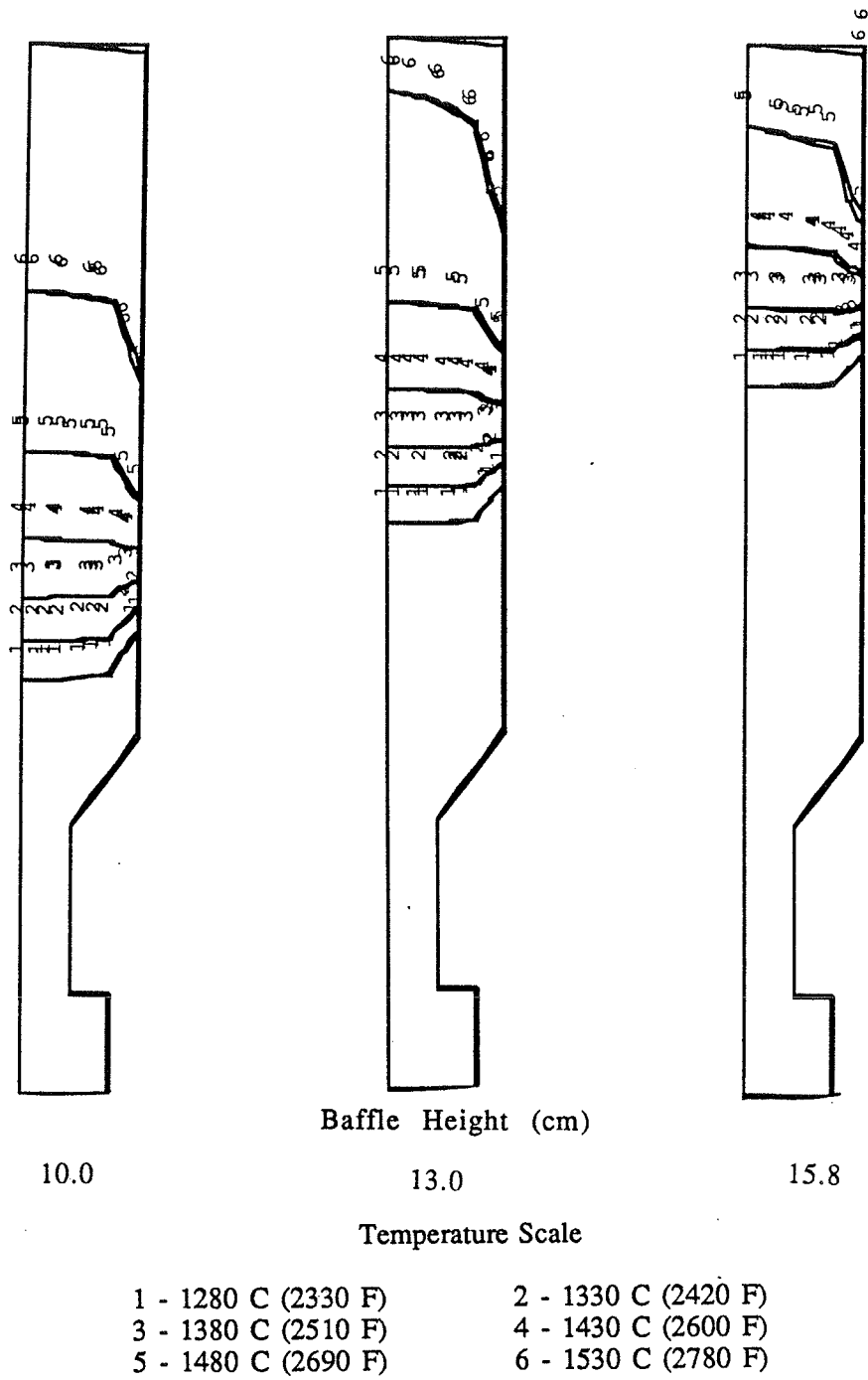


Figure 42. Temperature contours at withdrawal heights 10.0, 13.0 and 15.8 cm using the simple wall method.

liquidus/solidus (curves 4 and 3) travel from the small diameter of the grain selector to the larger diameter cylinder, and 2) the liquidus/solidus appear to be planar throughout the simulated withdrawal process.

Figure 43 shows the mesh used in repeating the above simulation using the view factor exchange method. The susceptor and cooling chamber surface are modeled at the actual distance (4.5 cm) away from the mold surface and the mold base has been extended out to its actual distance. Figure 44 shows an exploded view of the casting, mold, mold surface, graphite baffle, intercept and baffle surfaces, furnace surfaces, and the chill plate. The same boundary conditions used in the first simulation were duplicated here. Figures 45 and 46 show the temperature history comparison. The two curves vary only slightly from the model using the simple wall method. Thus, improved treatment of the small baffle, with a length of only 2.5 cm, did little to effect the heat flux. These results suggest that with only one small baffle present, the temperature variations of the top and bottom outer baffle surfaces are not a factor in the heat flux to the mold and that the simple wall method will be as accurate as the view factor exchange. More models must be run to see how a larger baffle or an upward facing mold ledge increases the error with the baffle surface temperature assumption.

The effects of changing the emissivity of the cooling chamber surface are shown in Figures 47 and 48, where the emissivity was changed from 1.0 to a more realistic value of 0.5. The temperature curves deviate somewhat from the previous simulation once the nodes reach the baffle where they run up to 100 C hotter until the end of withdrawal. Such a gradual deviation below the baffle and below the solidification range may not be considered important, but when the 3D aspects of the casting are taken into consideration as well as the method by which the mold

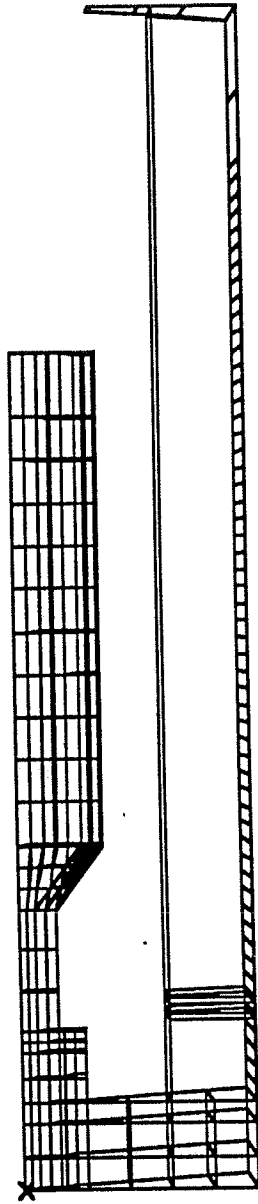


Figure 43. Finite element mesh of axis-symmetric casting using view factor exchange method.

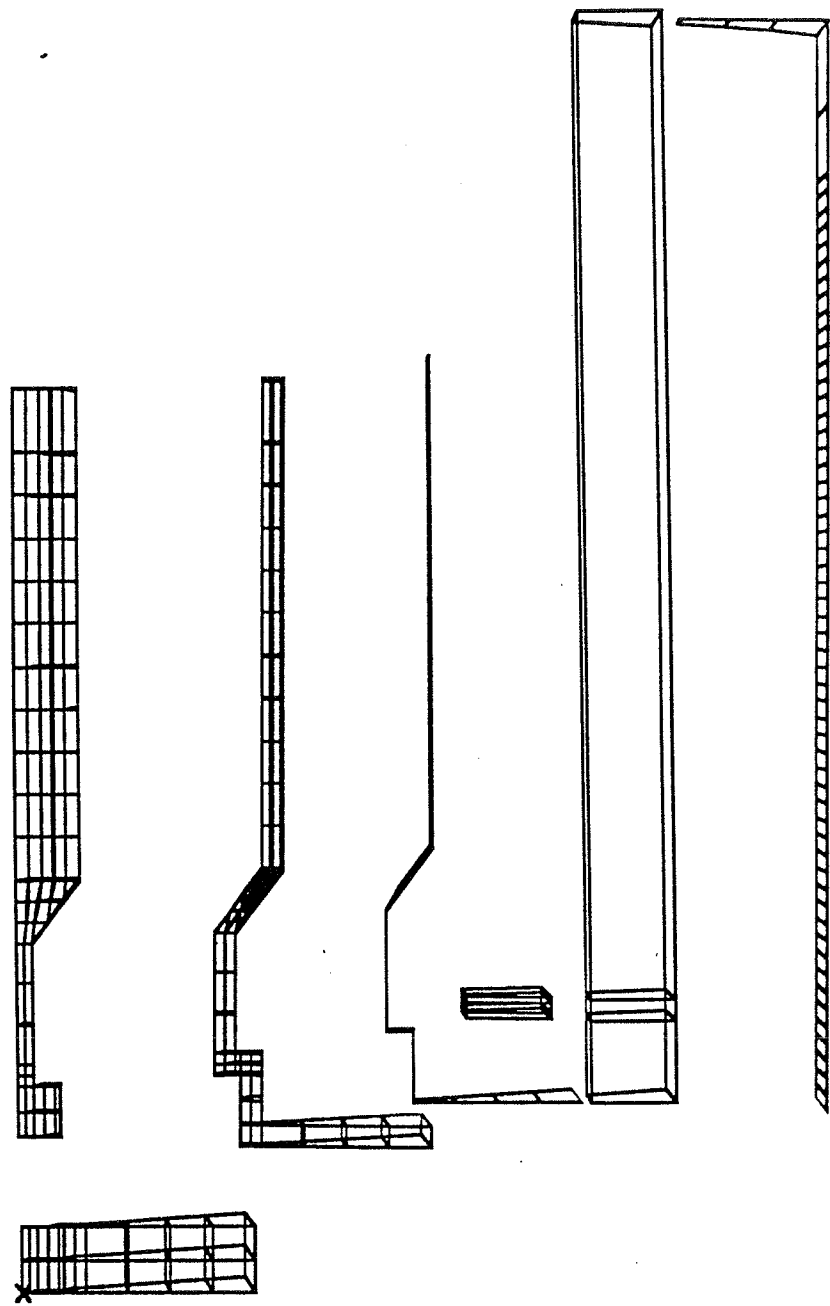


Figure 44. Exposed view of casting, mold, mold surface, baffle, intercept and baffle surfaces, furnace surface and chill plate.

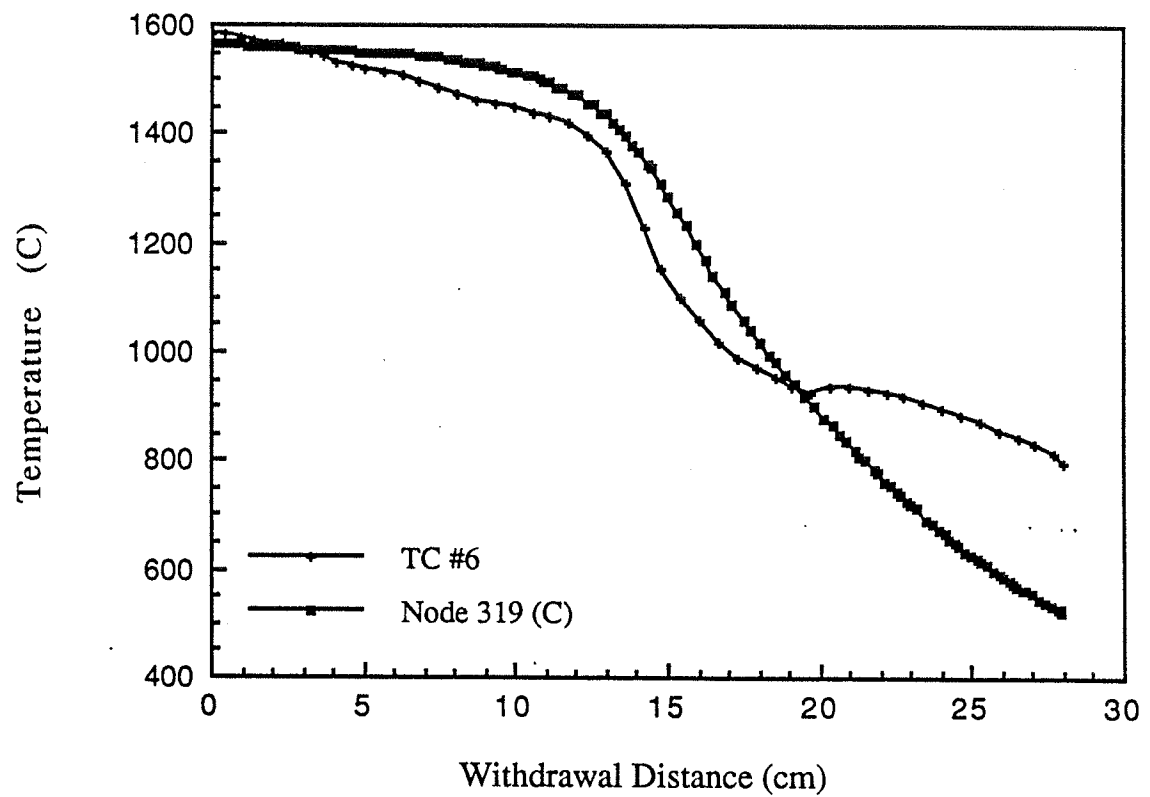


Figure 45. Experimental (TC #6) and predicted (node 319) temperature results using the view factor exchange method.

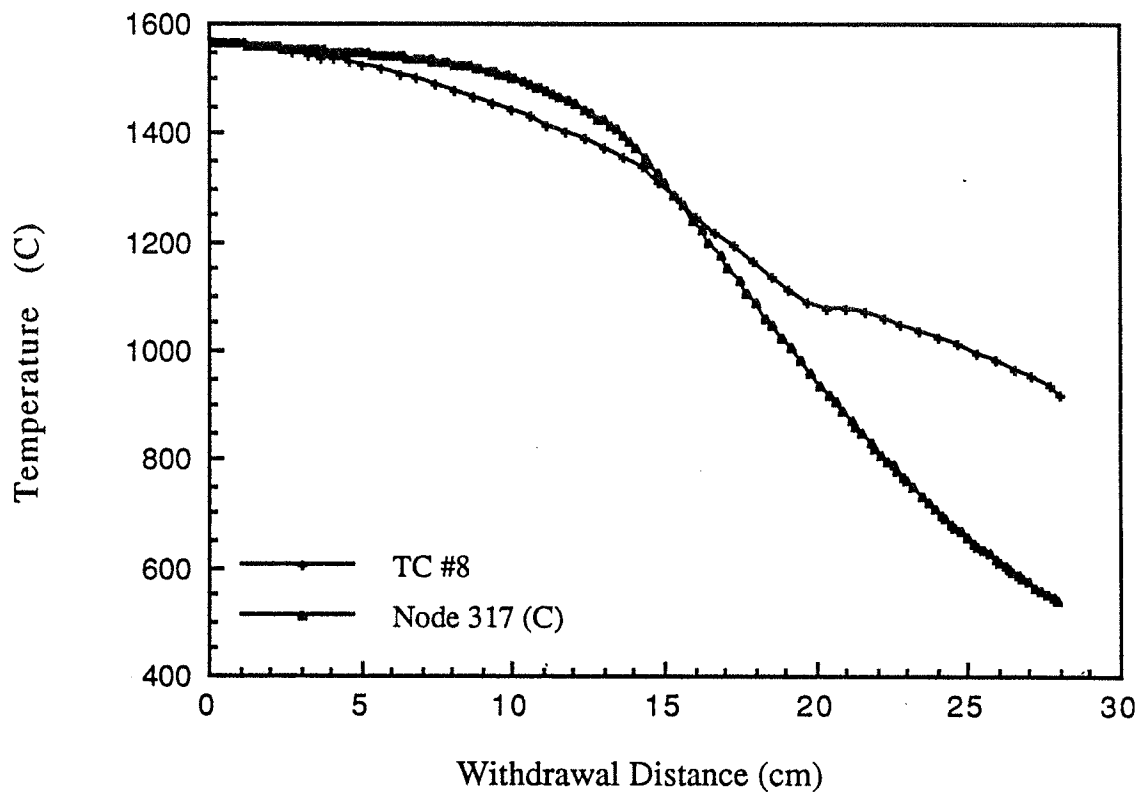


Figure 46. Experimental (TC #8) and predicted (node 317) temperature results using the view factor exchange method.

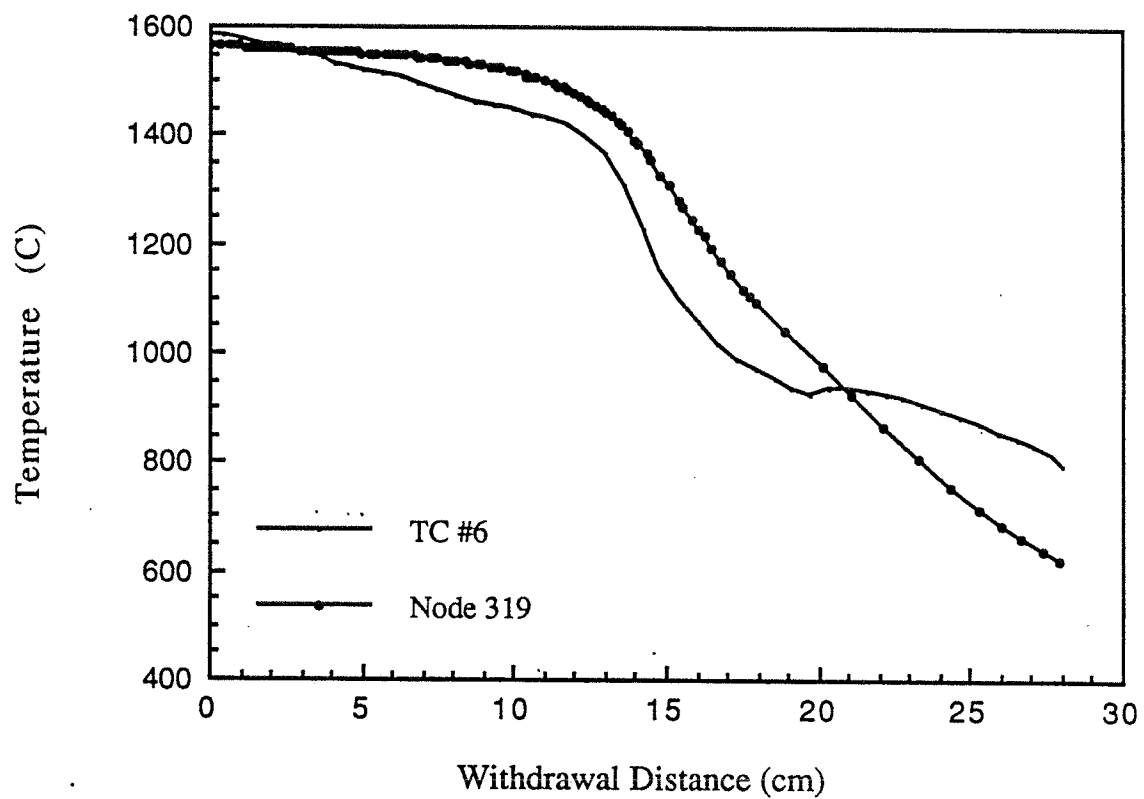


Figure 47. Experimental (TC #6) and predicted (node 319) temperature results using a cooling chamber emissivity of 0.5.

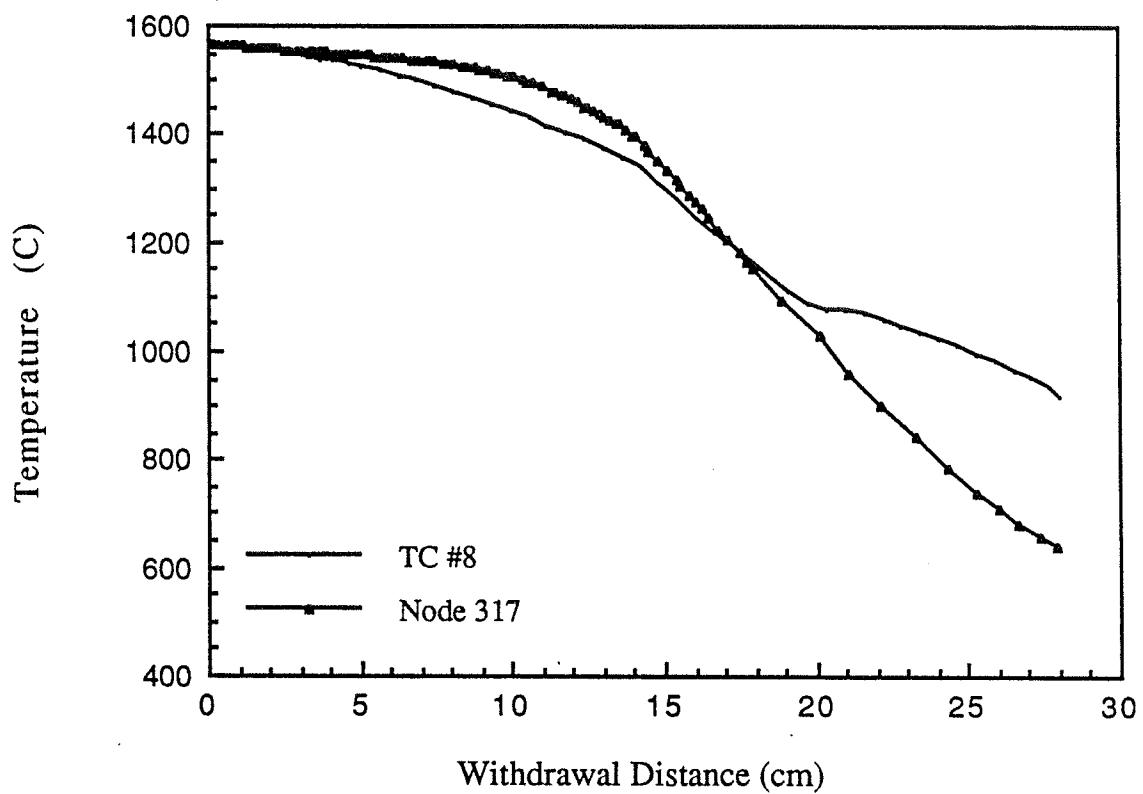


Figure 48. Experimental (TC #8) and predicted (node 317) temperature results using a cooling chamber emissivity of 0.5.

surfaces above the baffle have a view of surfaces below the baffle, the emissivity of the cooling chamber can be a factor in determining the casting quality.

5.2 FURNACE SLICE MODEL

Illustrated in Figure 49 is a 2D slice through the cluster of cylindrical castings. The 23 cm radius furnace wall to the right was modeled with a baffle while the 20 cm radius wall to the left is modeled using the simple wall method. In the center of the cluster is a 24 cm diameter baffle with intercept surfaces reaching a height of 20 cm from the mold base. This is the height at which the second baffle hits the bottom of the pour cup and falls. In the simulation, when the second baffle reaches this height, it is made to disappear and not exchange radiation with the rest of the surfaces. The emissivity of the mold was a constant 0.7 and the furnace wall was kept at 1.0.

There were a total of 2004 nodes, 726 elements and 300 radiation surfaces in this model. The completion time was 5250 seconds with a 20 second time step and the total cpu time on a VAX workstation for the heat flow analysis was 25 hours. The view factors and intercept height matrices for the two baffles are double precision. The view factors were calculated using 2D surfaces while the intercept height matrices were calculated using 3D surfaces.

Figures 50 and 51 give the temperature history comparisons from this model. The predictions are still running 50 C hotter than the experimental results above the baffle, but now the trend is consistent with curves below the baffle running hotter as well. With the addition of the larger baffle and the opposing mold surfaces, the model is predicting the same general sloping curves as the experimental data. Thus the time and temperature gradients are much closer than before.

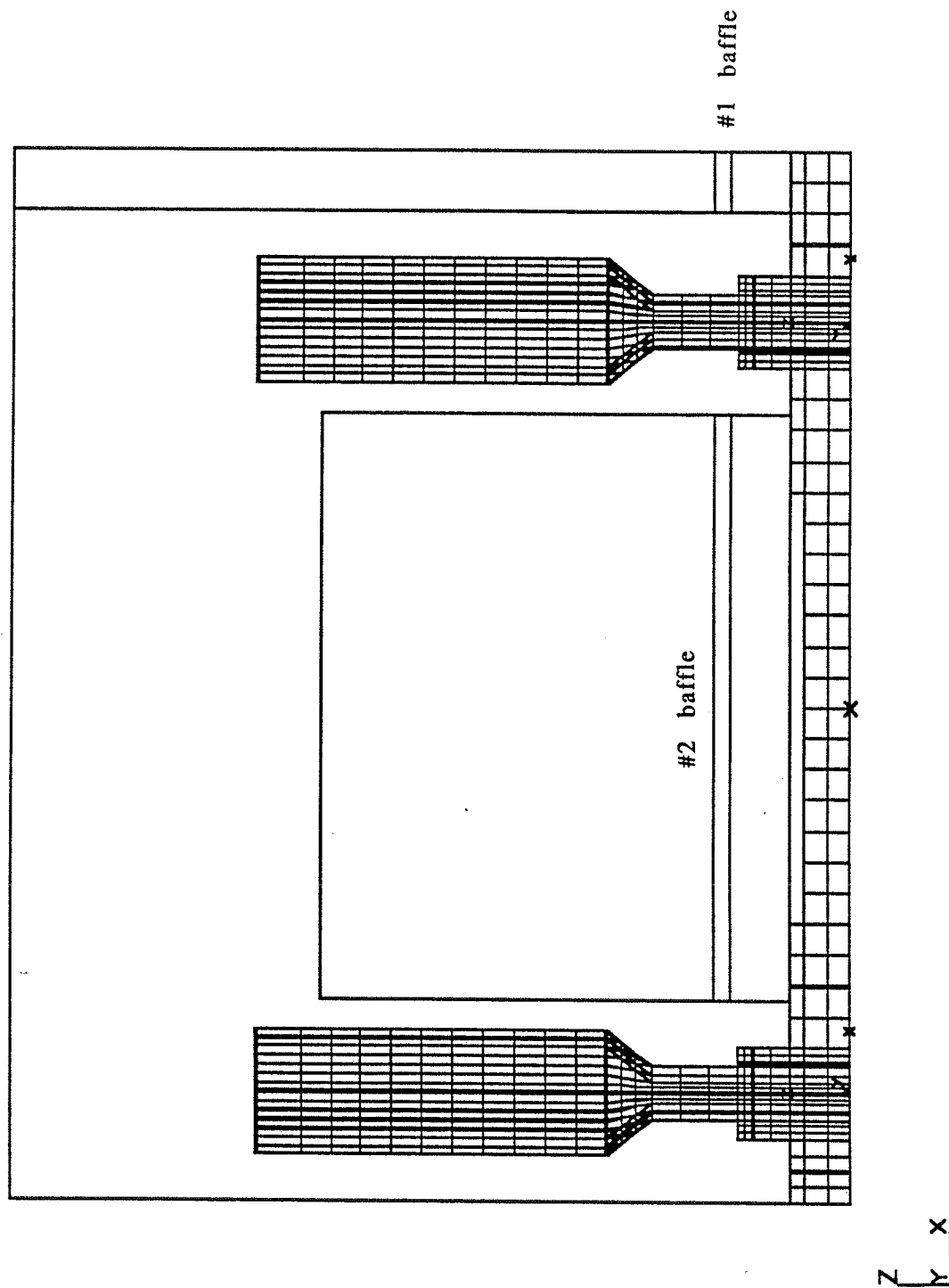


Figure 49. Finite element mesh of 2D slice through casting furnace and cluster.

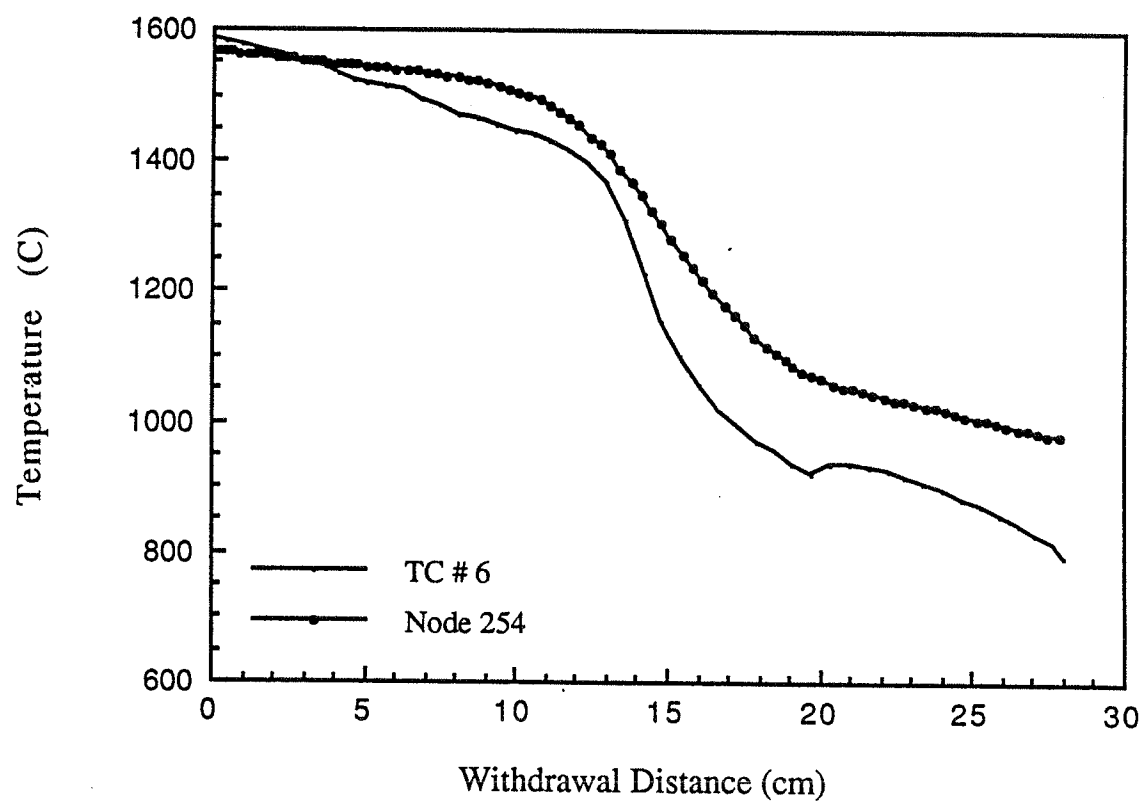


Figure 50. Experimental (TC #6) and predicted (node 254) temperature results from furnace slice model.

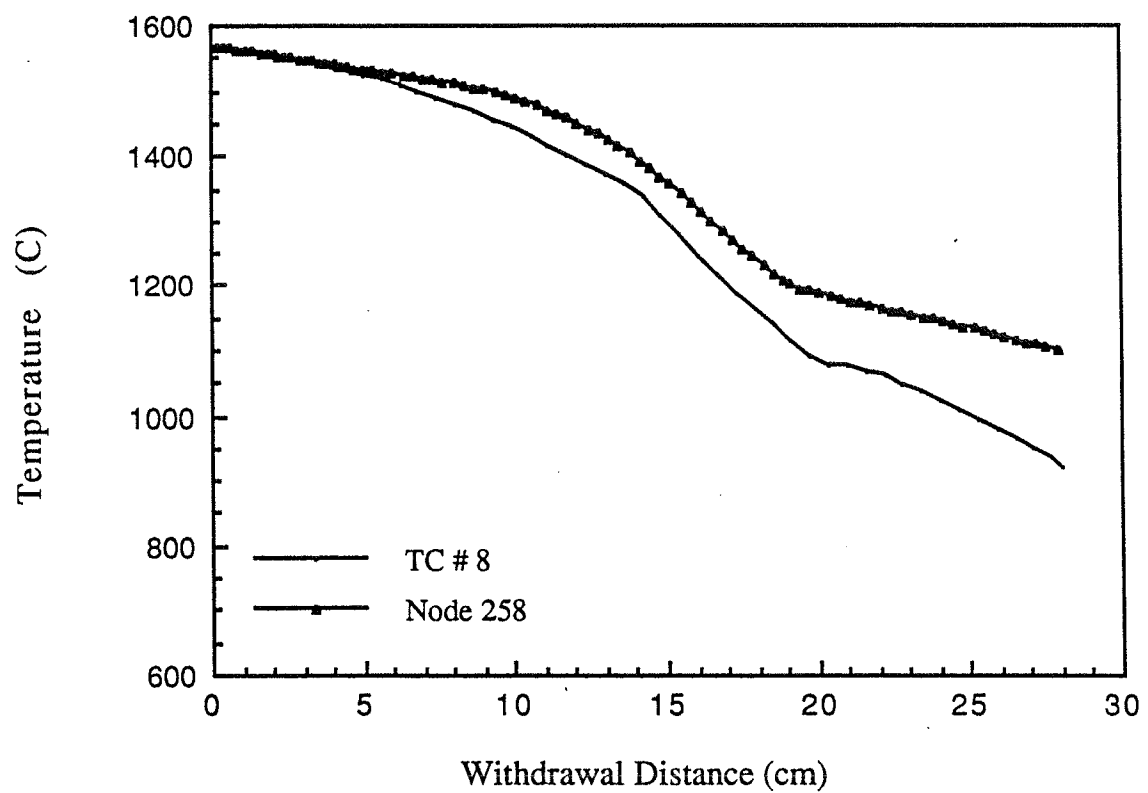


Figure 51. Experimental (TC #8) and predicted (node 258) temperature results from furnace slice model.

The temperature histories of the surfaces of the two baffles are shown in Figures 52 and 53. The temperature gradient across the small first baffle increases during the withdrawal, with the top surface being 50 C hotter at the 10 cm mark and 75 C after 20 cm of withdrawal. The previous two models showed that the temperature difference between the top baffle surface and the susceptor does not effect the casting temperature distribution. After 25 cm of withdrawal, most of the casting has solidified and the baffle surface is only 75 C cooler than the susceptor. The analytical comparison in Figure 27 shows that an 85 C cooler baffle top makes only a slight difference in the heat flux. For a cluster with a small outer baffle, the simple wall method may be the best modeling technique. Although the accuracy will decrease as the baffle size increase and the importance of contoured baffles has not been addressed.

The temperature history of the large second baffle given in Figure 53, shows the baffle runs slightly hotter then the outer baffle and has a higher temperature gradient of 75 C at the 10 cm mark and almost 150 C difference at 19 cm. This is surprising since the interior of the cluster is usually cooler than surfaces with unobstructed views of the susceptor. The hotter temperatures can be attributed to the open top of the 2D cluster. A pour cup and runner obstruct some of the view of the second baffle with the susceptor cover and the susceptor. Addition of these structures would probably cool the baffle, although a 3D casting has gaps between the castings which would cause the baffle to run hot.

Several reasons can be suggested for the consistently high temperatures found in this simulation. All of these correspond to deficiencies in the modelling assumptions are not inherent to the view factor exchange method. Thus, better assumptions could be incorporated into future simulations.

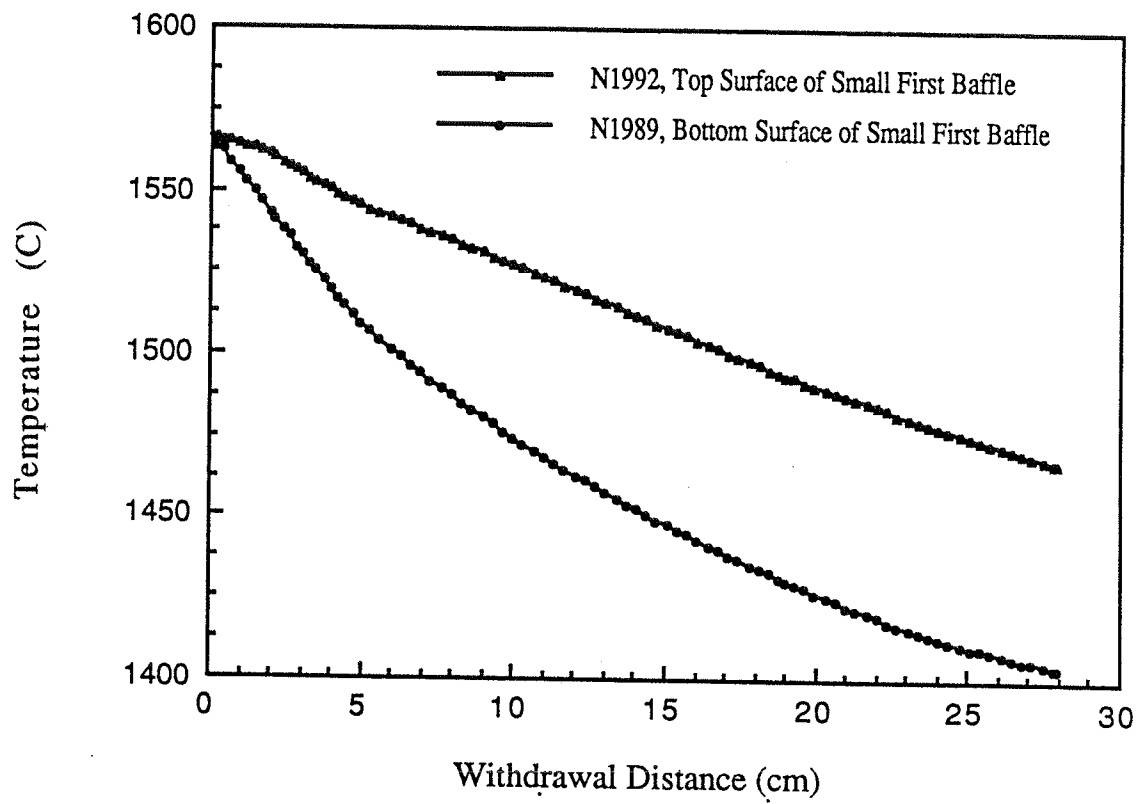


Figure 52. Predicted temperature history of top and bottom surface of small first baffle.

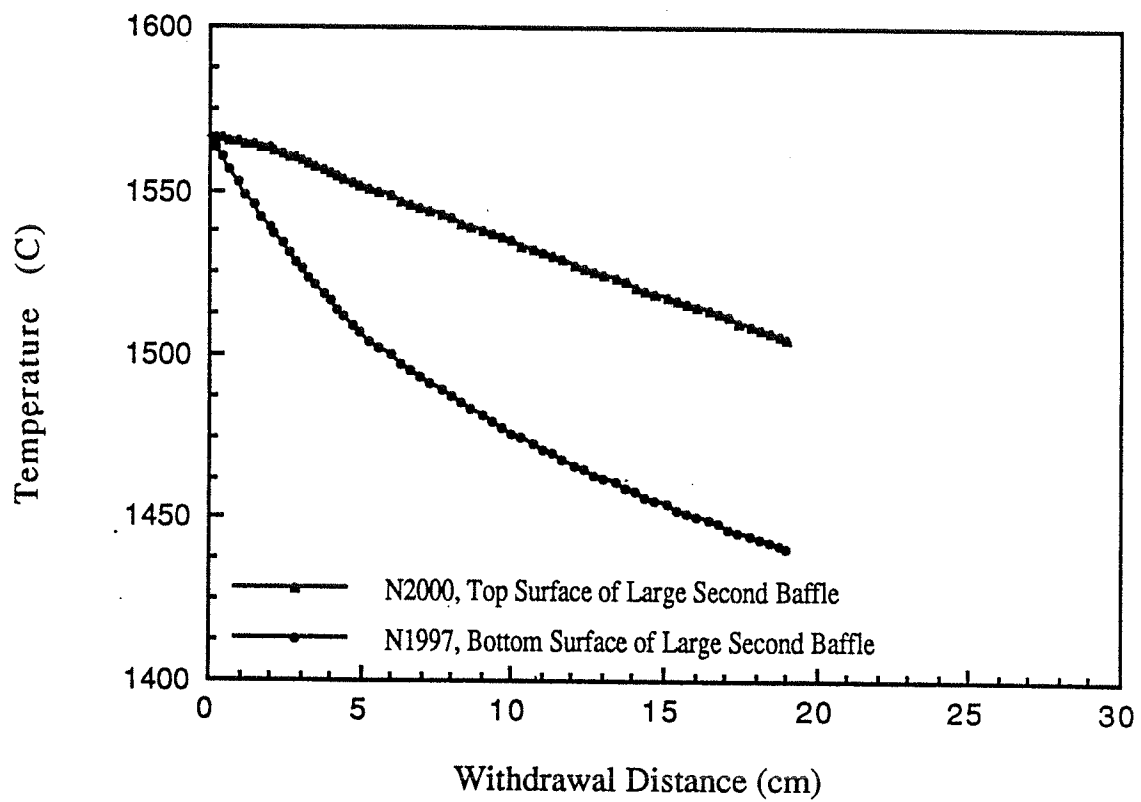
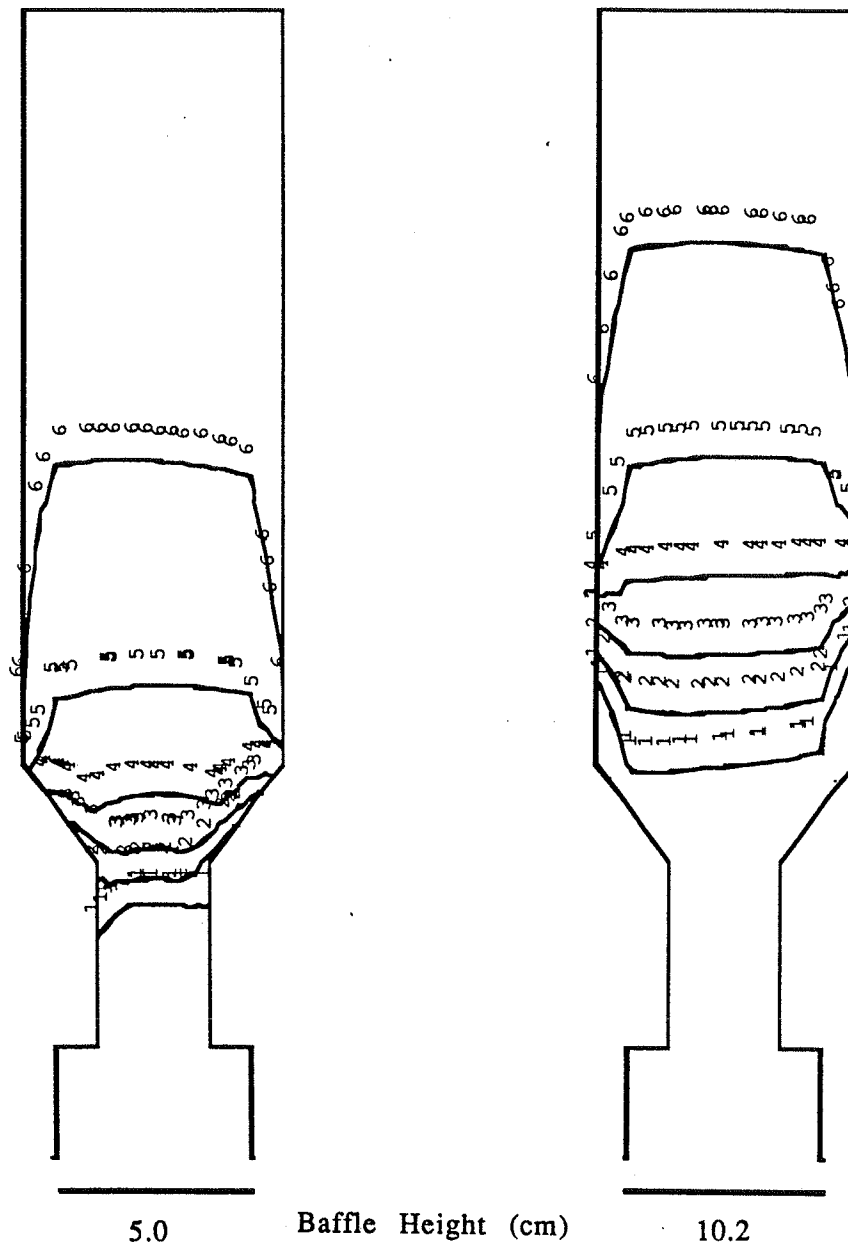


Figure 53. Predicted temperature history of top and bottom surface of large second baffle.

Figures 54 and 55 show the temperature contours in the right side casting during the withdrawal. The mold surface facing the susceptor is 50 C hotter than the back mold surface. This trend is commonly noticed in the foundry and is due to the limited view that the inner mold surfaces have of the hot susceptor. Indeed, the magnitude of the observed temperature difference is of the same order. The prediction of this effect using the view factor exchange model shows encouraging progress over the previous demonstrations. However, a 50 C temperature difference still exists between the predicted and experimental results. The principle problem is the 2D nature of the simulation which prevents heat loss from the "sides" of the actual cylinders. The sides of the mold are not blocked by the baffles and can see the cold mold base and cooling chamber long before the front or back. Addition of this view would definitely have a cooling effect on the over all casting.

Instead of starting at a uniform temperature, a further refinement would be the modeling of the 10 minute hold period before the withdrawal begins. If this procedure was modeled, the casting and baffle would start to cool and develop a temperature distribution at the beginning of withdrawal. With the current radiation surface mesh size, there is no instability due to the thin baffle assumption. The temperature difference across the baffles shows that the view factor method is able to let the baffles undergo a simultaneous heat flow analysis.

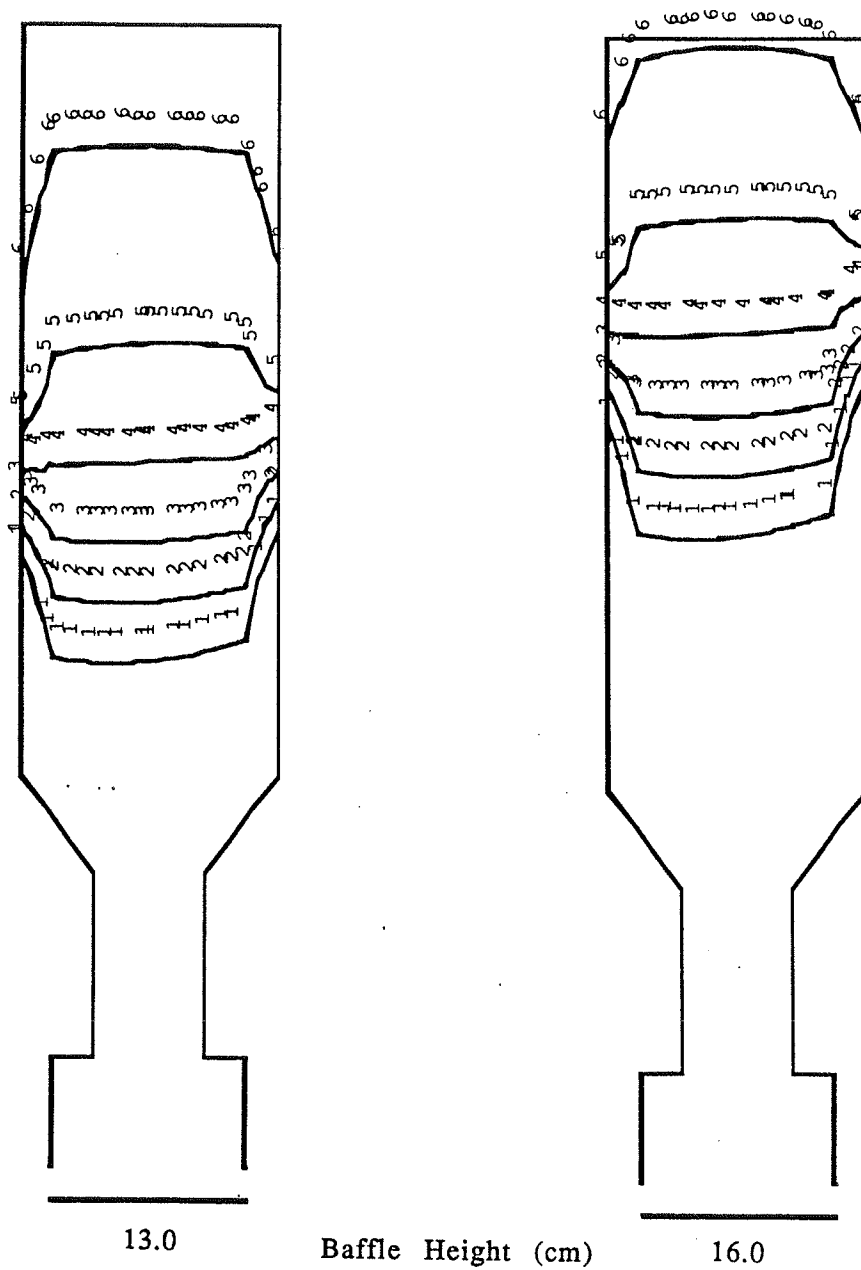
Another variable that has not been modeled is the actual temperature of the susceptor and susceptor cover. In the present model, these surfaces were assumed to be at a constant 1565 C. No cover or susceptor thermocouple was recorded in the experimental casting, so the actual temperature history of the susceptor is not known. From the 2D analytical model, the susceptor cover temperature was shown to have a negligible effect on the front surface of a planar mold. However, the runner, pour cup and both baffles face directly up to the susceptor cover. Thus, the mold



Temperature Scale

- | | |
|---------------------|---------------------|
| 1 - 1280 C (2330 F) | 2 - 1330 C (2420 F) |
| 3 - 1380 C (2510 F) | 4 - 1430 C (2600 F) |
| 5 - 1480 C (2690 F) | 6 - 1530 C (2780 F) |

Figure 54. Temperature contours at withdrawal heights 5.0 and 10.2 cm from the furnace slice model.



Temperature Scale

1 - 1280 C (2330 F)	2 - 1330 C (2420 F)
3 - 1380 C (2510 F)	4 - 1430 C (2600 F)
5 - 1480 C (2690 F)	6 - 1530 C (2780 F)

Figure 55. Temperature contours at withdrawal heights 13.0 and 16.0 cm from the furnace slice model.

could be affected indirectly from the susceptor cover temperature being below the susceptor temperature.

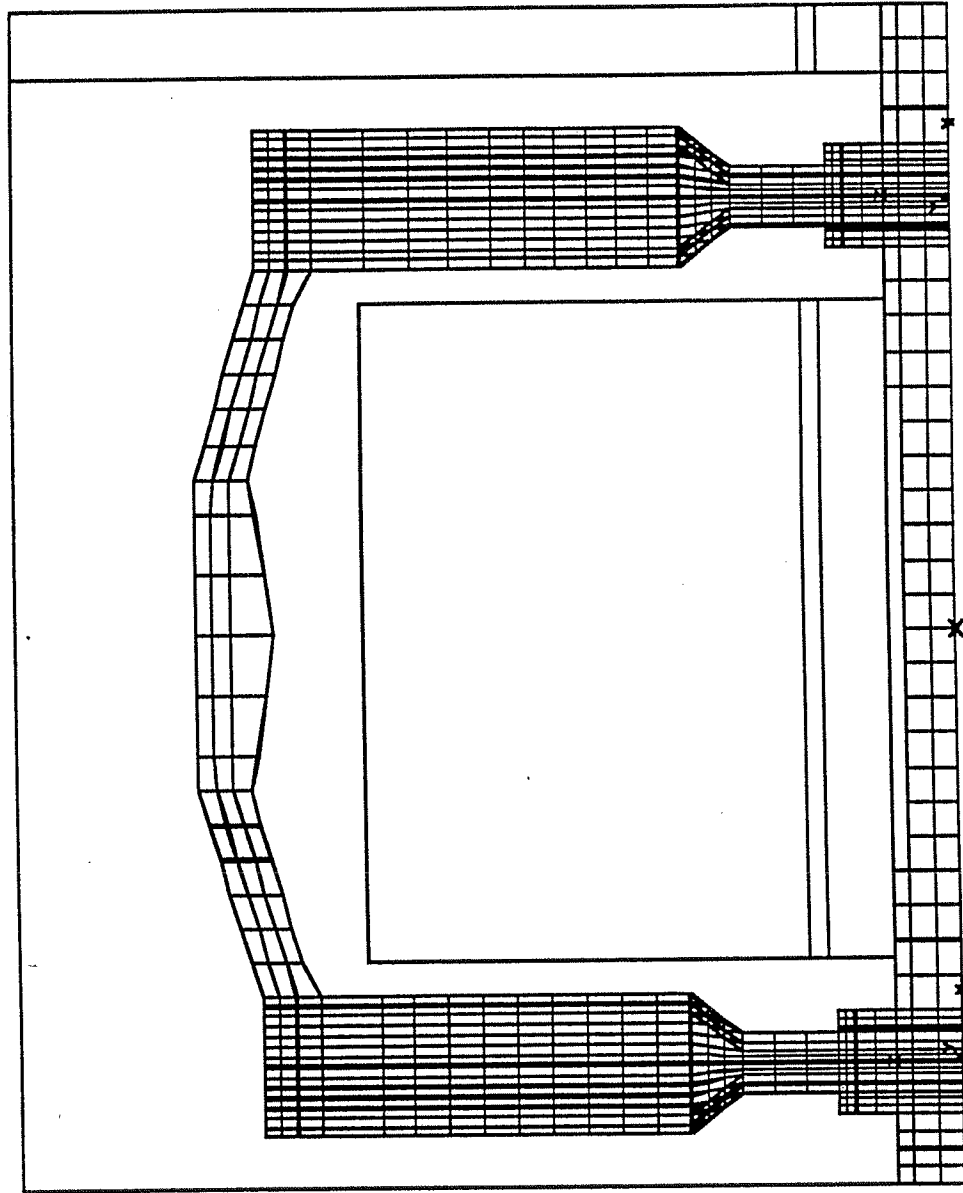
5.3 FURNACE SLICE MODEL WITH FEEDING SYSTEM

The third simulation involves previous furnace slice model with the addition of a runner and pour cup. Figure 56 is the mesh used in the simulation and Figure 57 shows the complex surfaces involved in the enclosure radiation. The experimental casting had an over estimation of the metal that was needed, so Figure 58 illustrates the metal filling the runners and the bottom portion of the pour cup.

There were a total of 2272 nodes, 836 elements and 338 radiation surfaces in this model. The completion time was 5250 seconds with a 60 second time step and the total cpu time on a VAX workstation for the heat flow analysis was 12 hours.

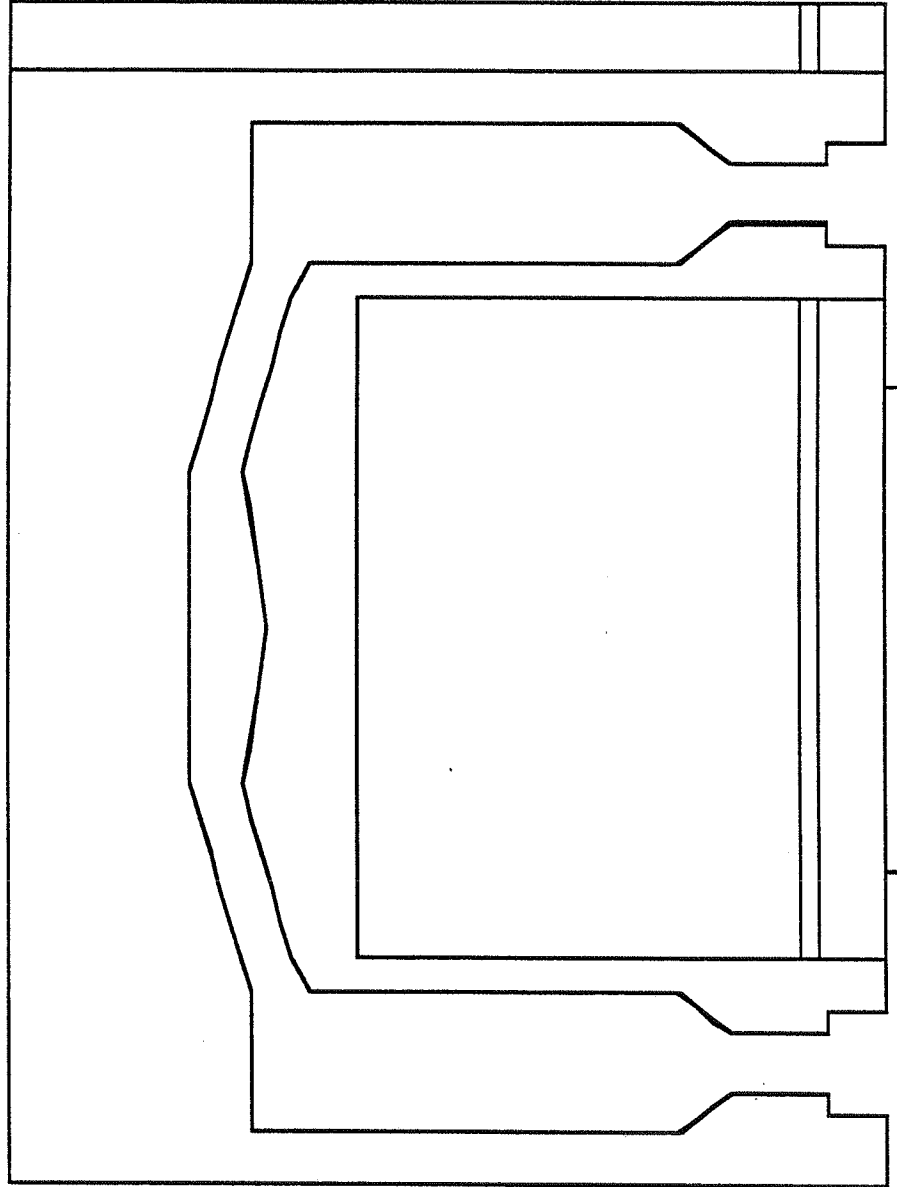
Extremely good correlation exists between the predicted and experimental data. Figure 59 and Figure 60 shows that the addition of the feeding system and a more realistic cooling chamber emissivity of 0.5 measurably improved the correlation. The predictions for the mold thermocouple is still running 50 C hotter, but the 0.32 cm metal location is running cooler. With all the emissivity and temperature assumptions used in the models, the accuracy of this 2D model is very promising.

Figure 61 is the temperature distribution throughout the cluster slice after 11.0 cm of withdrawal. The contours verify that there is very little difference between the simple wall method used on the left hand furnace wall, and the modeling of a small #1baffle. Another point is that the feeders do act as a shield to the interior of the cluster and the inner surfaces are actually 200 C cooler than the susceptor. The impact of this temperature difference is shown in the contours in Figures 62 through 65. The inner half of the mold is over 200 C cooler than the front of the mold. The thermal gradient is not as high as the previous model and the solidification front has



X
Y
Z

Figure 56. Finite element mesh used in furnace slice with feeding system model.



x

Figure 57. Radiation surfaces, baffle surfaces and intercept surfaces for model.

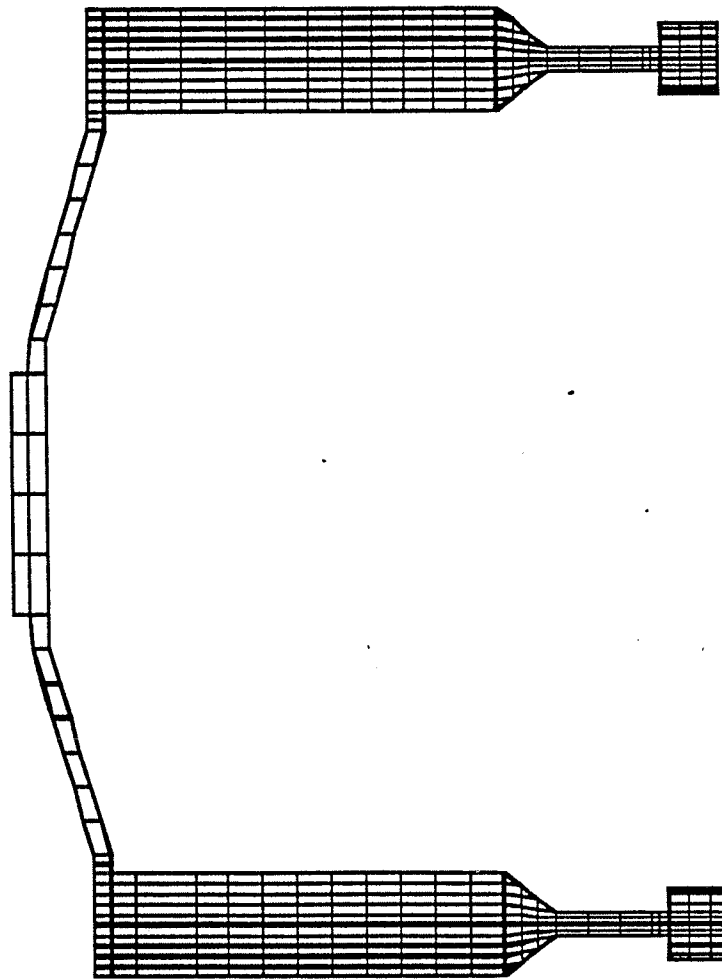
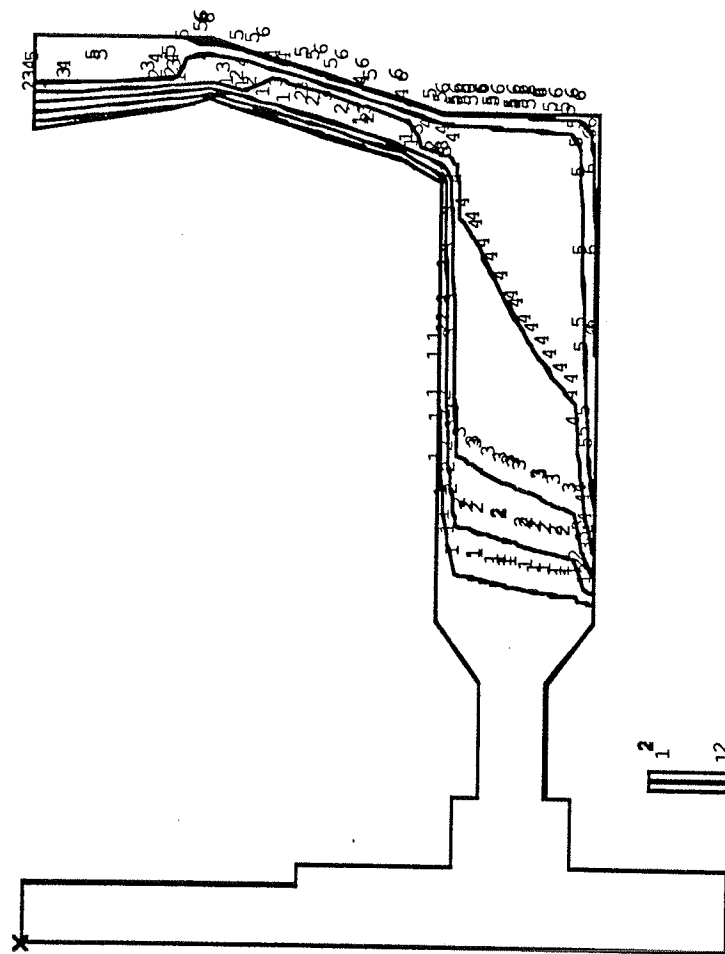


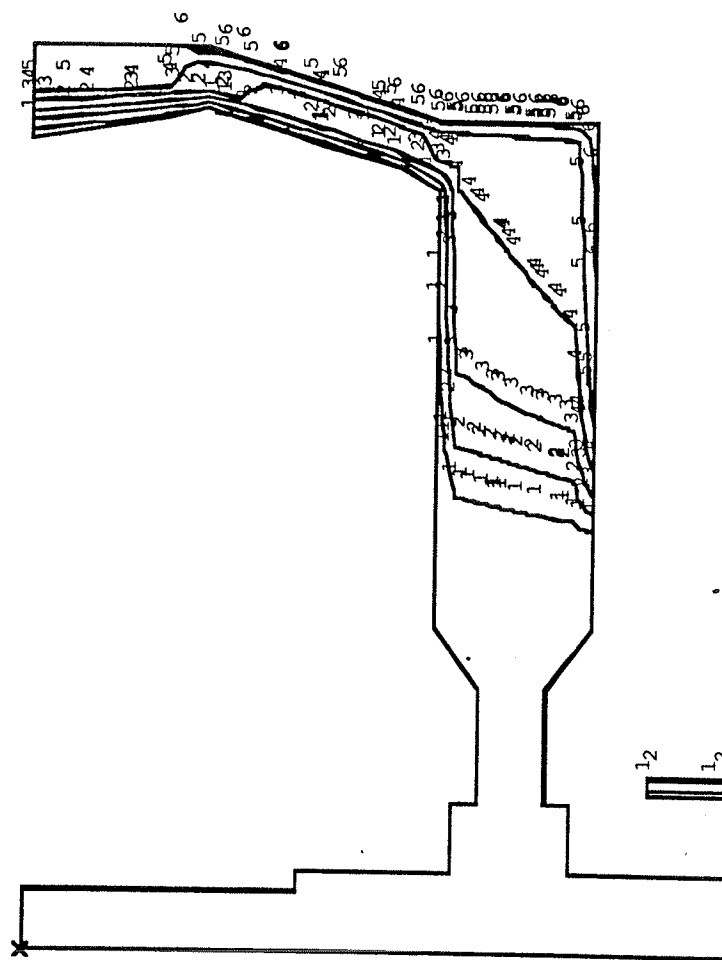
Figure 58. Metal castings with excess metal in runners and pour cup.



Baffle Height = 8.0 cm
Temperature Scale

1 - 1280 C (2330 F)	2 - 1330 C (2420 F)
3 - 1380 C (2510 F)	4 - 1430 C (2600 F)
5 - 1480 C (2690 F)	6 - 1530 C (2780 F)

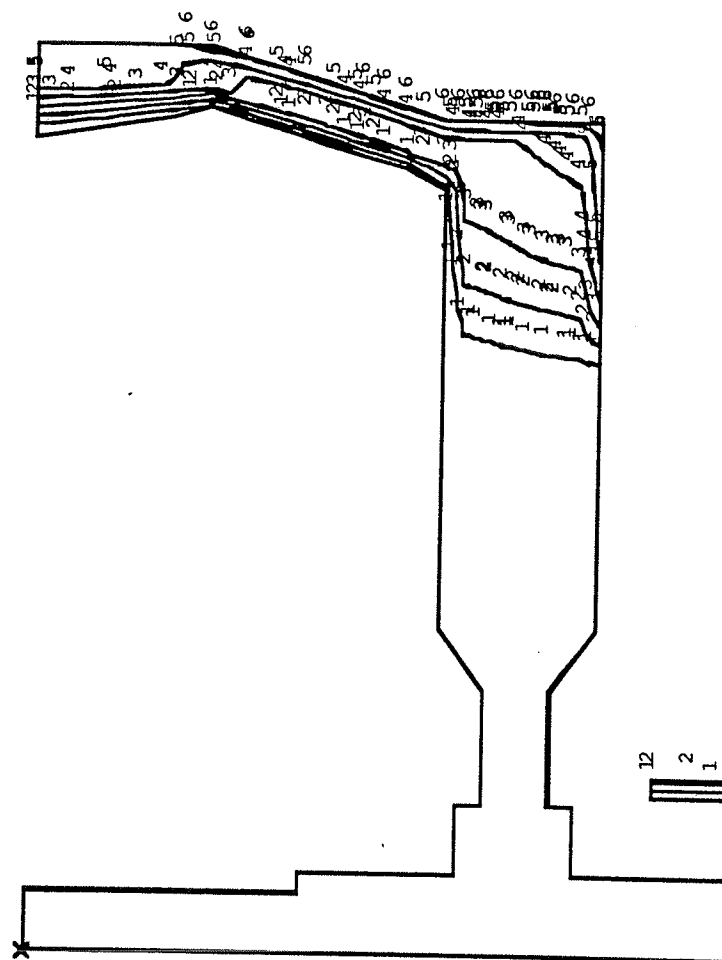
Figure 63. Temperature contour of metal and mold after 8 cm of withdrawal.



Baffle Height = 11.0 cm
Temperature Scale

- | | |
|---------------------|---------------------|
| 1 - 1280 C (2330 F) | 2 - 1330 C (2420 F) |
| 3 - 1380 C (2510 F) | 4 - 1430 C (2600 F) |
| 5 - 1480 C (2690 F) | 6 - 1530 C (2780 F) |

Figure 64. Temperature contour of metal and mold after 11 cm of withdrawal.



Baffle Height = 16.5 cm
Temperature Scale

- | | |
|---------------------|---------------------|
| 1 - 1280 C (2330 F) | 2 - 1330 C (2420 F) |
| 3 - 1380 C (2510 F) | 4 - 1430 C (2600 F) |
| 5 - 1480 C (2690 F) | 6 - 1530 C (2780 F) |

Figure 65. Temperature contour of metal and mold after 16.5 cm of withdrawal.

a very sharp incline. The addition of the feeding system in this 2D case has created an extreme in which there is no gap between the individual runners. Since the inner mold surfaces cannot see the susceptor through the top or through the sides of the molds, the model is an extreme case in which inner mold surfaces have no view of the susceptor. A 3D model using the cyclic symmetry of the cluster would be needed to model view of the mold through the gaps in the runner and mold pieces.

The results from the furnace slice model show the flexibility, accuracy and efficiency of the view factor exchange method. With the use of this modeling technique, a 2D model has come very close to matching experimental temperature data from a cylinder cast in a production foundry. These results show that the model is handling the heat flow correctly during the withdrawal process and can be a very valuable tool in investigating the directional solidification of turbine blades.

REFERENCES

- [1] M. McLean and F. Schubert, "Mechanical Properties of Directionally Solidified Superalloys and Eutectics," Third International Symposium on Superalloys, 1976, Seven Springs, PA., pp. 423-458.
- [2] F. P. Incropera and D. P. DeWitt, Fundamentals of Heat Transfer, John Wiley & Sons, Inc., 1981, p. 630.
- [3] Shogo Morimoto, Akira Yoshinari, and Eisuke Nyama, "Effects of Thermal Variables on the Growth of Single Crystals of Ni-Base Superalloys," Third International Symposium on Superalloys, 1976, Seven Springs, PA., pp. 177-184.
- [4] A. F. Giamei and J. S. Erickson, "Computer Application in Directional Solidification Processing," Third International Symposium on Superalloys, 1976, Seven Springs, PA., pp. 405-424..
- [5] L. Vermot Des Roches and J. Ch. Chevrier, "Radiation Heat Transfer Modeling in Precision Investment Casting Technology," Personnel correspondence, pp. 426-427.
- [6] R. J. Mador, M. O. Duffy, A. F. Giamei, and F. Landis, "Finite Element Simulation of the Directional Solidification process for Cylinders (2D) and Rectangular Bars (3D)," in Kou, S. and Mehrabian, R. (eds.), Modeling and Control of Casting and Welding Processes, The Metallurgical Society, Inc., PA, 1986, pp. 433-448.
- [7] A. F. Giamei, R. J. Mador, M. O. Duffy and P. M. Morris, "Simulation of Superalloy Castings," Journal of Metals, February 1988, pp. 7-10.
- [8] M. O. Duffy, P. M. Morris, and R. J. Mador, "Casting Solidification Analysis and Experimental Verification," Personnel correspondence.

- [9] A.B. Shapiro, FACET - A Radiation View Factor Computer Code for Axisymmetric, 2D Planar, and 3D Geometries with Shadowing, University of California, Lawrence Livermore National Laboratory, Rept. UCID-19887 (1983).
- [10] A.B. Shapiro, TOPAZ2D: A Two-Dimensional Finite Element Code for Heat Transfer Analysis, Electrostatic, and Magnetostatic Problems, University of California, Lawrence Livermore National Laboratory, 1986, Rept. UCID-20824, pp. 16-19.
- [11] A.B. Shapiro, TOPAZ3D: A Three-Dimensional Finite Element Heat Transfer Code, University of California, Lawrence Livermore National Laboratory, 1985, Rept. UCID-20484, pp. 23-47.
- [12] D.W. Stillman, INGRID: A Three-Dimensional Mesh Generator for Modeling Nonlinear System, University of California, Lawrence Livermore National Laboratory, UCID-20506.
- [13] Structural Dynamics Research Corporation, Investment Casting Solidification Simulation User's Manual, Milford, OH. May 4, 1987.

APPENDIX A

MODIFIED FACET SUBROUTINE DATAIN

```

C*****
C
  SUBROUTINE DATAIN (XND,NDS,KINTI,KINTO,KTOPI,KBOTI,KTOPO,KBOTO,
    X GAREA,XNG,XCG,KBLK)
C
C*****
  COMMON /BLK02/ NDIM, NUMNP, NUMEL, NDIV, MAXL, MAXA, NBLK, NCPL,
    1 NINTI, NINTO, NIBS, NOBS, ISDRC
  COMMON /BLK03/ KDA
C
  COMMON /IOBUF/ IOB(12100B)
  COMMON /IOBUF/ IOB('12100'O)
  CRAY
  VAX
  DIMENSION XND(3,1), X(4), Y(4), Z(4), NDS(6,1), GAREA(1), XNG(3,1)
    1 , XCG(3,1), KBLK(1), IX(4), XK(3), KINTI(1), KINTO(1), KTOPI(1)
    2 , KBOTI(1), KTOPO(1), KBOTO(1)
C
  DATA NOLD, KN0, NP, XK /0,0,2,0.,0.,1./
C.....INPUT AND GENERATE NODE POINT DATA
  WRITE (59,250)
10 KN=KN0
  IF (ISDRC.EQ.1) THEN
    IF (NDIM.EQ.2) THEN
      READ (5,176) N,XND(1,N),CON,XND(2,N)
      XND(1,N)=XND(1,N)*100.00
      XND(2,N)=XND(2,N)*100.00
    ELSE
      READ (5,176) N,XND(1,N),XND(2,N),XND(3,N)
      XND(1,N)=XND(1,N)*100.00
      XND(2,N)=XND(2,N)*100.00
      XND(3,N)=XND(3,N)*100.00
    KNO=0
  ENDIF
  ELSE
    READ (5,177) N,XND(1,N),XND(2,N),XND(3,N),KN0
  END IF
  IF (KN.EQ.0) KN=1
  IF (NOLD.EQ.0) GO TO 30
  NUM=(N-NOLD)/KN
  NUMN=NUM-1
  IF (NUMN.LT.1) GO TO 30
  XNUM=NUM
  DX=(XND(1,N)-XND(1,NOLD))/XNUM
  DY=(XND(2,N)-XND(2,NOLD))/XNUM
  DZ=(XND(3,N)-XND(3,NOLD))/XNUM
  K=NOLD
  DO 20 J=1,NUMN
    KK=K
    K=K+KN
  
```

```

XND(1,K)=XND(1,KK)+DX
XND(2,K)=XND(2,KK)+DY
XND(3,K)=XND(3,KK)+DZ
20 CONTINUE
30 NOLD=N
  IF (N.NE.NUMNP) GO TO 10
C.....WRITE NODE POINT DATA
  WRITE (6,178)
  DO 40 I=1,NUMNP
    WRITE (6,180) I,(XND(J,I),J=1,3)
  40 CONTINUE
C-   CALL WRABSF (IOB(520),XND,3*NUMNP,64)
C-   CALL RIOSTAT (IOB(520))
  KDA=64+3*NUMNP
  IF (NDIM.EQ.3) GO TO 45
C.....FOR 2D, WRITE BEAM ELEMENT REFERENCE DATA POINT INTO PLOT FILE
  KBEAM=NUMNP+1
C-   CALL WRABSF (IOB(520),XK,3,KDA)
C-   CALL RIOSTAT (IOB(520))
  KDA=KDA+3
C.....INPUT AND GENERATE SURFACE DATA
  45 WRITE (59,260)
  50 READ (5,190) M,(NDS(J,M),J=1,5),NMISS,INC
    NDS(6,M)=0
    IF (NDS(5,M).EQ.0) NDS(5,M)=1
    IF (NMISS.EQ.0) GO TO 80
    IF (INC.EQ.0) INC=1
    DO 70 I=1,NMISS
      L=M
      M=M+1
      IF (NDIM.EQ.3) THEN
        DO 60 J=1,4
          60 NDS(J,M)=NDS(J,L)+INC
        ELSE
          DO 65 J=1,2
            65 NDS(J,M)=NDS(J,L)+INC
          NDS(3,M)=0
          NDS(4,M)=0
        ENDIF
        NDS(5,M)=NDS(5,L)
        NDS(6,M)=0
      70 CONTINUE
      80 IF (M.LT.NUMEL) GO TO 50
C.....CALCULATE SURFACE AREA
  IF (NDIM.EQ.3) NP=4
  DO 100 J=1,NUMEL
    DO 90 JJ=1,NP
      X(JJ)=XND(1,NDS(JJ,J))
      Y(JJ)=XND(2,NDS(JJ,J))
      Z(JJ)=XND(3,NDS(JJ,J))
    90 CONTINUE
    IF (NDIM.LT.3) CALL GEOM2D(X,Y,XCG(1,J),XCG(2,J),XNG(1,J),

```

```

      X              XNG(2,J),GAREA(J),NDIM)
      IF (NDIM.EQ.3) CALL GEOM3D(X,Y,Z,XCG(1,J),XCG(2,J),XCG(3,J),
      X              XNG(1,J),XNG(2,J),XNG(3,J),GAREA(J))
100 CONTINUE
C.....WRITE SURFACE DATA
      WRITE (6,200)
      DO 130 J=1,NUMEL
        WRITE (6,210) J,(NDS(I,J),I=1,5),GAREA(J)
        IF (NDIM.EQ.3) GO TO 110
        CALL BDLINE (NDS(1,J),NDS(2,J),KBEAM,NDS(5,J))
        GO TO 130
110 DO 120 I=1,4
        IX(I)=NDS(I,J)
120 CONTINUE
        MAT=NDS(5,J)
        CALL BDPLNE (IX,MAT)
        NDS(5,J)=NDS(1,J)
130 CONTINUE
        IF (NDIM.EQ.3) CALL BDPLNE (IX,-1)
        KDA=KDA+20
C.....INPUT BLOCKING SURFACES
        IF (NBLK.LE.0) GO TO 145
        WRITE (59,270)
        WRITE (6,220)
        M=0
140 M=M+1
        READ (5,230) KBLK(M),NMISS,INC
        IF (NMISS.EQ.0) GO TO 142
        IF (INC.EQ.0) INC=1
        DO 141 I=1,NMISS
        M=M+1
        KBLK(M)=KBLK(M-1)+INC
141 CONTINUE
142 IF (M.LT.NBLK) GO TO 140
        DO 143 I=1,NBLK
        WRITE (6,240) I,KBLK(I)
143 CONTINUE
C
C.....READ IN MODIFIED SURFACE DATA
C
C.....INPUT #1 BAFFLE INTERCEPT SURFACES
145 CONTINUE
        IF (NINTI.LE.0) GO TO 150
        WRITE (59,280)
        WRITE (6,290)
        M=0
146 M=M+1
        READ (5,190) KINTI(M),NMISS,INC
        IF (NMISS.EQ.0) GO TO 148
        IF (INC.EQ.0) INC=1
        DO 147 I=1,NMISS
        M=M+1

```

```

      KINTI(M)=KINTI(M-1)+INC
147 CONTINUE
148 IF (M.LT.NINTI) GO TO 146
      DO 149 I=1,NINTI
        WRITE (6,300)I,KINTI(I)
149 CONTINUE
C
C.....INPUT #2 BAFFLE INTERCEPT SURFACES
150 CONTINUE
      IF (NINTO.LE.0) GO TO 155
      M=0
151 M=M+1
      READ (5,190) KINTO(M),NMISS,INC
      IF (NMISS.EQ.0) GO TO 153
      IF (INC.EQ.0) INC=1
      DO 152 I=1,NMISS
        M=M+1
        KINTO(M)=KINTO(M-1)+INC
152 CONTINUE
153 IF (M.LT.NINTO) GO TO 151
      WRITE (6,295)
      DO 154 I=1,NINTO
        WRITE (6,300) I,KINTO(I)
154 CONTINUE
C
C.....INPUT TOP OF #1 BAFFLE SURFACES
155 CONTINUE
      IF (NIBS.LE.0) GO TO 165
      WRITE (59,310)
      M=0
156 M=M+1
      READ (5,190) KTOPI(M),NMISS,INC
      IF (NMISS.EQ.0) GO TO 158
      IF (INC.EQ.0) INC=1
      DO 157 I=1,NMISS
        M=M+1
        KTOPI(M)=KTOPI(M-1)+INC
157 CONTINUE
158 IF (M.LT.NIBS/2) GO TO 156
C
C.....INPUT BOTTOM OF #1 BAFFLE SURFACES
      WRITE (6,320)
      M=0
161 M=M+1
      READ (5,190) KBOTI(M),NMISS,INC
      IF (NMISS.EQ.0) GO TO 163
      IF (INC.EQ.0) INC=1
      DO 162 I=1,NMISS
        M=M+1
        KBOTI(M)=KBOTI(M-1)+INC
162 CONTINUE
163 IF (M.LT.NIBS/2) GO TO 161

```

```

      DO 164 I=1,NIBS/2
        WRITE (6,340) I,KTOPI(I),KBOTI(I)
164 CONTINUE
C
C.....INPUT TOP OF #2 BAFFLE SURFACES
165 CONTINUE
      IF (NOBS.LE.0) GO TO 175
      M=0
166 M=M+1
      READ (5,190) KTOPO(M),NMISS,INC
      IF (NMISS.EQ.0) GO TO 168
      IF (INC.EQ.0) INC=1
      DO 167 I=1,NMISS
        M=M+1
        KTOPO(M)=KTOPO(M-1)+INC
167 CONTINUE
168 IF (M.LT.NOBS/2) GO TO 166
C
C.....INPUT BOTTOM OF #2 BAFFLE SURFACES
      WRITE (6,330)
      M=0
171 M=M+1
      READ (5,190) KBOTO(M),NMISS,INC
      IF (NMISS.EQ.0) GO TO 173
      IF (INC.EQ.0) INC=1
      DO 172 I=1,NMISS
        M=M+1
        KBOTO(M)=KBOTO(M-1)+INC
172 CONTINUE
173 IF (M.LT.NOBS/2) GO TO 171
      DO 174 I=1,NOBS/2
        WRITE (6,340) I,KTOPO(I),KBOTO(I)
174 CONTINUE
C
175 CALL EMPTY (6)
      RETURN
C
176 FORMAT (I5,3E13.5)
177 FORMAT (I5,5X,3E10.0,I5)
178 FORMAT (' ***** NODE DATA *****
1 *****'///' NODE',6X,'X1',10X,'X2',10X,'X3',/)
180 FORMAT (I5,1P3E12.4)
190 FORMAT (8I5)
200 FORMAT (//' ***** SURFACE DATA *****
1 *****'///
2' ELE # N1 N2 N3 N4 MAT',12X,'AREA',/)
210 FORMAT (6I5,1PE20.8)
220 FORMAT (//' ***** BLOCKING SURFACES
1 *****'///' INDEX',5X,'SURFACE',/)
230 FORMAT (3I5)
240 FORMAT (I5,5X,I5)
250 FORMAT(5X,'READING NODE DATA')

```



```

260 FORMAT(5X,'READING SURFACE DATA')
270 FORMAT(5X,'READING OBSTRUCTING SURFACES')
280 FORMAT(5X,'READING INTERCEPT SURFACES')
290 FORMAT (/ ' ***** I T E R C E P T   S U R F A C E S   *
      1*****'//,' INDEX',5X,'#1 SURFACE'/)
295 FORMAT (/ ' INDEX',5X,'#2 SURFACE'/)
300 FORMAT(I5,7X,I5)
310 FORMAT(5X,'READING BAFFLE SURFACES')
320 FORMAT (/ ' ***** # 1 B A F F L E   S U R F A C E S   *
      1S *****'//,' INDEX',5X,'TOP SURFACE',5X,'BOTTOM SURFACE'
      2/)
330 FORMAT (/ ' ***** # 2 B A F F L E   S U R F A C E S   *
      1S *****'//,' INDEX',5X,'TOP SURFACE',5X,'BOTTOM SURFACE'
      2/)
340 FORMAT(I5,8X,I5,12X,I5)
      END

```

APPENDIX B

MODIFIED FACET SUBROUTINE VIEW3D

```
SUBROUTINE VIEW3D
C
C VIEW3D- LAWRENCE LIVERMORE NATIONAL LABORATORY/ARTHUR B. SHAPIRO
C SUBROUTINE TO DETERMINE VIEW FACTOR FOR 3D GEOMETRIES
C
C MODIFICATIONS- UNIVERSITY OF ILLINOIS/DAVID D. GOETTSCHE
C MODIFIED SURFACES(BAFFLE AND INTERCEPT ELEMENTS) ARE AUTOMATICALLY
C GIVEN A VIEW FACTOR OF ZERO. THE INTERCEPT HEIGHT MATRICES ARE SENT
C TO SUBROUTINE HWRITE TO BE WRITTEN TO OUTPUT FILE.
C
CHARACTER*5 MSG
COMMON // A(1)
COMMON /BLK01/N1, N2, N2A, N2B, N2C, N2D, N2E, N2F, N3, N4, N5,
1 N6, N7, N8, N9, N10, N11, N12, N13, N14, N15, N16, N17, N18
COMMON /BLK02/ NDM, NUMNP, NUMEL, NDM, MAXL, MAXA, NBLK, NCLP,
1 NINTI, NINTO, NIBS, NOBS, ISDRC
COMMON /BLK05/ IBUG
DATA KDA,KNH,NDONE /0,0,-1/
IF (IBUG.EQ.1) WRITE(6,80)
NTOT=(NUMEL*NUMEL-NDONE)/2
NDIV2=NDIV*NDIV
C.....VIEW FACTOR ISEG LOOP
CALL TIMEUSE (CPU0,TIO0,SYS0)
DO 60 ISEG=1,NUMEL
CALL GRIDL (A(N1),A(N2),A(N4),ISEG,NDIV,MAXL)
CALL GRIDA (A(N1),A(N2),A(N6),A(N8),ISEG,NDIV,MAXA)
C.....VIEW FACTOR JSEG LOOP
DO 50 JSEG=ISEG,NUMEL
IF (ISEG.NE.JSEG) GO TO 4
CALL VIEW00 (A(N14),ISEG,JSEG)
C.....ZERO HEIGHTS IF TWO SURFACES ARE THE SAME
CALL HEIT00 (A(N16),A(N17),ISEG,JSEG)
GO TO 50
4 CONTINUE
C
C.....CHECK IF ISEG OR JSEG ARE INTERCEPT ELEMENTS OR BAFFLE ELEMENTS
C.....IF EITHER ARE, THE VIEW FACTOR AND HEIGHTS ARE ZERO.
C
NTOTAL=NINTI+NINTO+NIBS+NOBS
CALL INTERCEPT (A(N2A),NTOTAL,ISEG,JFLG,1)
IF (JFLG.EQ.0) CALL INTERCEPT (A(N2A),NTOTAL,JSEG,JFLG,1)
IF (JFLG) 6,7,6
6 CALL VIEW00 (A(N14),ISEG,JSEG)
CALL HEIT00 (A(N16),A(N17),ISEG,JSEG)
GO TO 50
7 CONTINUE
C
NDONE=NDONE+1
```

```

      CALL INTRUPT (MSG,NWR,1)
      IF (MSG.NE.'WHERE') GO TO 8
      CALL TIMEUSE (CPU1,TIO1,SYS1)
      NLEFT=NTOT-NDONE
      TLEFT=(CPU1-CPU0+TIO1-TIO0+SYS1-SYS0)*FLOAT(NLEFT)/FLOAT(NDONE)
      WRITE (59,70) ISEG,JSEG,NDONE,NLEFT,TLEFT
      8 NSET=0
C.....CAN SURFACE I SEE SURFACE J IGNORING THIRD SURFACE OBSTRUCTIONS
      CALL SEE (A(N1),A(N2),A(N10),ISEG,JSEG,ISEE)
      IF (ISEE) 20,10,20
      10 CALL VIEW00 (A(N14),ISEG,JSEG)
      CALL HEIT00 (A(N16),A(N17),ISEG,JSEG)
      GO TO 50
      20 CONTINUE
      IF (NBLK.EQ.0.AND.ISEE.EQ.1) GO TO 40
      IF (NBLK.EQ.0.AND.ISEE.EQ.-1) GO TO 30
C.....IDENTIFY THE SUBSET OF THE OBSTRUCTING SURFACES K THAT
C.....OBSTRUCT THE VIEW BETWEEN SURFACES I AND J
C..... ALSO CALCULATE INTERCEPT HEIGHTS FOR 2 BAFFLES.
      CALL OBSTR (A(N1),A(N2),A(N2A),A(N2B),A(N10),A(N11),A(N12),
      X A(N13),A(N16),A(N17),ISEG,JSEG,NSET)
      IF (NSET.EQ.0.AND.ISEE.EQ.1) GO TO 40
C.....THIRD SURFACE BLOCKAGE -- USE AREA INTEGRATION
      30 CONTINUE
      CALL GRIDA (A(N1),A(N2),A(N7),A(N9),JSEG,NDIV,MAXA)
      CALL VIEWAA (A(N1),A(N2),A(N6),A(N7),A(N8),A(N9),A(N10),A(N13),
      1 A(N14),ISEG,JSEG,NDIV2,NSET)
      GO TO 50
C.....NO THIRD SURFACE BLOCKAGE -- USE CONTOUR INTEGRATION
C.....DOES SURFACE I & SURFACE J SHARE A COMMON EDGE
      40 CALL EDGE (A(N1),A(N2),ISEG,JSEG,IEDGE)
      CALL GRIDL (A(N1),A(N2),A(N5),JSEG,NDIV,MAXL)
      IF (IEDGE.EQ.1) CALL VIEWCC (A(N4),A(N5),A(N14),ISEG,JSEG,MAXL)
      IF (IEDGE.EQ.2) CALL VIEWMS (A(N1),A(N2),A(N14),ISEG,JSEG,NDIV)
      50 CONTINUE
C.....F FOR THE ROW ISEG HAVE BEEN CALCULATED -- WRITE THEM TO DISK
      NW=NUMEL-ISEG+1
      CALL FWRITE (A(N14),NW,KDA)
      KDA=KDA+NW
      60 CONTINUE
C.....WRITE HEIGHT MATRIX OUT TO FILE
      IF ((NIBS.GT.0).OR.(NOBS.GT.0)) CALL HWRITE (A(N16),A(N17),
      X A(N2C),A(N2D),A(N2E),A(N2F))
      RETURN
C
      70 FORMAT (' CALCULATING VIEW FACTOR FOR ISEG=',I5,2X,'JSEG=',I5/
      1 I10,' VIEW FACTORS HAVE BEEN CALCULATED;',I10,' ARE REMAINING'/
      2 ' ESTIMATED COMPLETION TIME [SEC] = ',1PE12.4//)
      80 FORMAT(/' ***** (AREA) X (VIEW FACTOR) *****
      1 *****'/)
      END

```

APPENDIX C

MODIFIED FACET SUBROUTINE OBSTR

```
SUBROUTINE OBSTR (XND,NDS,KINTI,KINTO,XNG,XCG,KBLK,KSET,HI,HO,  
X ISEG,JSEG,NSET)  
C  
C OBSTR- LAWRENCE LIVERMORE NATIONAL LABORATORY/AUTHUR B. SHAPIRO  
C  
C THIS SUBROUTINE INSPECTS ALL THE SPECIFIED OBSTRUCTING SURFACES  
C AS POSSIBLE SHADOWING SURFACES BETWEEN THE CURRENT VIEW FACTOR  
C SURFACES ISEG & JSEG. A SUBSET OF OBSTRUCTING SURFACES IS  
C FORMED. WHEN THE VIEW FACTOR IS CALCULATED BETWEEN ISEG & JSEG  
C THIS SUBSET IS EXAMINED FOR THE SHADOWING SUFACES.  
C  
C MODIFICATIONS- UNIVERSITY OF ILLINOIS/DAVID D. GOETTSCH  
C  
C THE MODIFICATIONS INCLUDE A CHECK TO DETERMINE IF KSEG IS AN  
C INTERCEPT SURFACE BY CALLING SUBROUTINE INTERCEPT. IF KFLG =1 OR  
C -1, KSEG IS AN INTERCEPT SURFACE. THE SUBROUTINE SECTN WILL  
C CALCULATE IF KSEG DOES OBSTRUCT ISEG AND JSEG. IF IT DOES,  
C IFLAG = 1 AND THE SUBROUTINE HEIGHT IS CALLED TO CALCULATE THE  
C HEIGHT OF THE INTERSECTION POINT ON KSEG (ZHEIT). THE LOWEST AND  
C HIGHEST HEIGHTS ARE FOUND FROM THE HEIGHT ARRAY. THE HIGHEST HEIGHT  
C IS STORED WITH THE SURFACE WITH THE HIGHEST CENTROID. IF ISEG IS  
C HIGHER THEN SURFACE JSEG THEN THE LARGEST INTERCEPT HEIGHT IS STORED  
C IN HI(I,J) AND THE SMALLEST INTERCEPT HEIGHT IS STORED IN HI(J,I).  
C NINTI - NUMBER OF #1 INTERCEPT ELEMENTS  
C NINTO - NUMBER OF #2 INTERCEPT ELEMENTS  
C NIBS - NUMBER OF #1 BAFFLE SURFACES  
C NOBS - NUMBER OF #2 BAFFLE SURFACES  
C ZINTI - ARRAY OF INTERCEPT HEIGHTS FOR #1 INTERCEPT  
C ZINTO - ARRAY OF INTERCEPT HEIGHTS FOR #2 INTERCEPT  
C  
C KFLG = -1 #1 INTERCEPT ELEMENT  
C KFLG = 0 NOT INTERCEPT ELEMENT  
C KFLG = +1 #2 INTERCEPT ELEMENT  
C  
COMMON /BLK02/ NDIM, NUMNP, NUMEL, NDIV, MAXL, MAXA, NBLK, NCLP,  
1 NINTI, NINTO, NIBS, NOBS, ISDRG  
COMMON /BLK05/ IBUG  
DIMENSION XND(3,1), NDS(6,1), XNG(3,1), XCG(3,1), KBLK(1), KSET(1)  
1 , V(5,3), AX(3), XI(3), KINTI(1), KINTO(1), ZINTI(10), ZINTO(10)  
2 , HI(NUMEL,1), HO(NUMEL,1)  
C  
KI=0  
KO=0  
DO 10 I=1,NBLK  
KSET(I)=0  
10 CONTINUE  
DO 30 KOUNT=1,NBLK
```

```

      KSEG=KBLK(KOUNT)
      IF (ISEG.EQ.KSEG.OR.JSEG.EQ.KSEG) GO TO 30
C....CHECK TO SEE IF KSEG IS INTERCEPT ELEMENT
      CALL INTERCEPT (KINTI,NINTI,KSEG,KFLG,-1)
      IF (KFLG.EQ.0.AND.NOBS.GT.0) CALL INTERCEPT (KINTO,NINTO,
X   KSEG,KFLG,1)
C
      DOT=XNG(1,KSEG)*(XCG(1,ISEG)-XCG(1,JSEG))
X   +XNG(2,KSEG)*(XCG(2,ISEG)-XCG(2,JSEG))
X   +XNG(3,KSEG)*(XCG(3,ISEG)-XCG(3,JSEG))
      IF ((ABS(DOT).LT.1.E-06).AND.(KFLG.EQ.0)) GO TO 20
      CALL SECTN (XND,NDS,XCG,XNG,ISEG,JSEG,KSEG,IFLAG,KFLG,ZHEIT)
C
C.... IF KSEG INTERSECTS AND IS A INTERCEPT ELEMENT,(KFLG=-1 or 1 & IFLAG
C.... = 1), STORE HEIGHT BUT DO NOT STORE SURFACE AS A BLOCKING SURFACE
C.... FOR VIEW FACTOR CALCULATIONS.
C
C.... IF KSEG INTERSECTS AND IS NOT A INTERCEPT ELEMENT, (KFLG=0 & IFLAG
C.... = 1), STORE SURFACE AS BLOCKING SURFACE.
C
C....IF KSEG DOES NOT INTERSECT, (IFLAG=0),GO TO THE NEXT KSEG.
      IF (IFLAG.EQ.0) GO TO 30
      IF (KFLG) 14,20,15
14   KI=KI+1
      ZINTI(KI)=ZHEIT
      GO TO 30
15   KO=KO+1
      ZINTO(KO)=ZHEIT
      GO TO 30
20   NSET=NSET+1
      KSET(NSET)=KSEG
30   CONTINUE
C
C.... DETERMINES THE LOWEST AND HIGHEST INTERCEPT HEIGHTS FOR #1 BAFFLES.
      IF (KI.GT.0) THEN
        ZHI=ZINTI(1)
        ZLOW=ZINTI(1)
        KHI=1
        KLOW=1
        DO 35 K=2,KI
          IF (ZINTI(K).GE.ZHI) THEN
            ZHI=ZINTI(K)
            KHI=K
          END IF
          IF (ZINTI(K).LT.ZLOW) THEN
            ZLOW=ZINTI(K)
            KLOW=K
          END IF
35   CONTINUE
C
      IF (XCG(3,ISEG).GE.XCG(3,JSEG)) THEN
        HI(ISEG,JSEG)=ZINTI(KHI)

```

```

      HI(JSEG,ISEG)=ZINTI(KLOW)
      IF (IBUG.EQ.1) WRITE(6,*)'HI(I,J),HI(J,I) =',HI(ISEG,JSEG)
X      ,HI(JSEG,ISEG)
      ELSE
      HI(ISEG,JSEG)=ZINTI(KLOW)
      HI(JSEG,ISEG)=ZINTI(KHI)
      IF (IBUG.EQ.1) WRITE(6,*)'HI(I,J),HI(J,I) =',HI(ISEG,JSEG)
X      ,HI(JSEG,ISEG)
      ENDIF
      IF (KHI.EQ.KLOW) THEN
      WRITE(6,*) '** ERROR, NO HEIGHT RANGE CALC (I,J) =',ISEG,JSEG
      ENDIF
      ENDIF
C
C.....DETERMINE INTERSECT HEIGHTS FOR #2 BAFFLE
C
      IF (KO.GT.0) THEN
      ZHI=ZINTO(1)
      ZLOW=ZINTO(1)
      KHI=1
      KLOW=1
      DO 36 K=2,KO
      IF (ZINTO(K).GE.ZHI) THEN
      ZHI=ZINTO(K)
      KHI=K
      END IF
      IF (ZINTO(K).LT.ZLOW) THEN
      ZLOW=ZINTO(K)
      KLOW=K
      ENDIF
36  CONTINUE
C
      IF (XCG(3,ISEG).GE.XCG(3,JSEG)) THEN
      HO(ISEG,JSEG)=ZINTO(KHI)
      HO(JSEG,ISEG)=ZINTO(KLOW)
      IF (IBUG.EQ.1) WRITE(6,*)'HO(I,J),HO(J,I) =',HO(ISEG,JSEG)
X      ,HO(JSEG,ISEG)
      ELSE
      HO(ISEG,JSEG)=ZINTO(KLOW)
      HO(JSEG,ISEG)=ZINTO(KHI)
      IF (IBUG.EQ.1) WRITE(6,*)'HO(I,J),HO(J,I) =',HO(ISEG,JSEG)
X      ,HO(JSEG,ISEG)
      ENDIF
      IF (KHI.EQ.KLOW) THEN
      WRITE(6,*) '** ERROR, NO HEIGHT RANGE CALC (I,J) =',ISEG,JSEG
      ENDIF
      ENDIF
50  RETURN
C
      END

```

APPENDIX D

MODIFIED FACET SUBROUTINE SECTN

```

SUBROUTINE SECTN (XND,NDS,XCG,XNG,ISEG,JSEG,KSEG,IFLAG,KFLG
X,ZHEIT)
C
C SECTN- LAWRENCE LIVERMORE NATIONAL LABORATORY/ARTHUR B. SHAPIRO
C
C THIS SUBROUTINE DETERMINES IF A LINE CONNECTING THE CENTROIDS OF
C SURFACES ISEG & JSEG INTERSECTS SURFACE KSEG.
C     IFLAG=0 NO INTERSECTION
C     IFLAG=1 INTERSECTION
C
C MODIFICATIONS- UNIVERSITY OF ILLINOIS/DAVID D. GOETTSCH
C
C THE MODIFICATIONS INCLUDE A CALL TO SUBROUTINE HEIGHT IF THE SURFACE
C KSEG IS AN INTERCEPT SURFACE, (KFLG=-1 or 1). THE INTERSECTION
C HEIGHT (ZHEIT) IS PASSED OUT OF THE SUBROUTINE.
C THE CONSTRAINT ON THE FINAL CHECK FOR OBSTRUCTION HAS BEEN REDUCED
C DUE TO OBSTRUCTING INTERCEPT SURFACES NOT PASSING THE CHECK CORRECTLY
C
    DIMENSION XND(3,1), NDS(6,1), XCG(3,1), XNG(3,1), V(5,3), AX(3),
    1 XI(3)
    IFLAG=0
    N=NDS(2,KSEG)
C.....DETERMINE INTERSECTION POINT
    AX(1)=XCG(1,ISEG)-XCG(1,JSEG)
    AX(2)=XCG(2,ISEG)-XCG(2,JSEG)
    AX(3)=XCG(3,ISEG)-XCG(3,JSEG)
    C1=XNG(1,KSEG)*XND(1,N)+XNG(2,KSEG)*XND(2,N)+XNG(3,KSEG)*XND(3,N)
    TNUM=XNG(1,KSEG)*XCG(1,ISEG)+XNG(2,KSEG)*XCG(2,ISEG)
    X +XNG(3,KSEG)*XCG(3,ISEG)-C1
    TDEN=XNG(1,KSEG)*AX(1)+XNG(2,KSEG)*AX(2)+XNG(3,KSEG)*AX(3)
    IF (ABS(TDEN).LT.1.E-06) RETURN
    T=TNUM/TDEN
    XI(1)=XCG(1,ISEG)-AX(1)*T
    XI(2)=XCG(2,ISEG)-AX(2)*T
    XI(3)=XCG(3,ISEG)-AX(3)*T
C.....IS INTERSECTION POINT BETWEEN SURFACES ISEG & JSEG
    XL1=SQRT((XI(1)-XCG(1,ISEG))**2+(XI(2)-XCG(2,ISEG))**2
    X +(XI(3)-XCG(3,ISEG))**2)
    XL2=SQRT((XI(1)-XCG(1,JSEG))**2+(XI(2)-XCG(2,JSEG))**2
    X +(XI(3)-XCG(3,JSEG))**2)
    XL3=SQRT(AX(1)*AX(1)+AX(2)*AX(2)+AX(3)*AX(3))
    DIF=ABS(XL3-XL2-XL1)/XL3
    IF (DIF.GT.1.E-06) RETURN
C.....IS INTERSECTION POINT WITHIN QUADRILATERAL KSEG
    DO 10 I=1,4
    N=NDS(I,KSEG)

```

```

      V(I,1)=XND(1,N)-XI(1)
      V(I,2)=XND(2,N)-XI(2)
      V(I,3)=XND(3,N)-XI(3)
10  CONTINUE
      V(5,1)=V(1,1)
      V(5,2)=V(1,2)
      V(5,3)=V(1,3)
      ANGLE=0.
      DO 20 I=1,4
          XL1=SQRT(V(I,1)*V(I,1)+V(I,2)*V(I,2)+V(I,3)*V(I,3))
          XL2=SQRT(V(I+1,1)*V(I+1,1)+V(I+1,2)*V(I+1,2)+V(I+1,3)*V(I+1,3))
          DEN=XL1*XL2
          IF (DEN.LT.1.E-06) GO TO 30
          DOT=(V(I,1)*V(I+1,1)+V(I,2)*V(I+1,2)+V(I,3)*V(I+1,3))/DEN
          IF (DOT.GT. +1.) DOT=+1.
          IF (DOT.LT. -1.) DOT=-1.
          ADOT=ACOS(DOT)
          ANGLE=ANGLE+ADOT
20  CONTINUE
C-----
C      IF (ABS(ANGLE-6.283185308).GT.1.E-06) RETURN
C
C      IF (ABS(ANGLE-6.283185308).GT.1.E-04) RETURN
C-----
30  IFLAG=1
C
C.... IF OBSTRUCTION SURFACE IS AN INTERCEPT ELEMENT AND BLOCKS
C.... SURFACE PAIR CALCULATE INTERCEPT HEIGHT.
      IF (KFLG.NE.0) CALL HEIGHT (XND,NDS,XCG,XNG,ISEG,JSEG,KSEG
1  ,ZHEIT)
      RETURN
END

```


APPENDIX E

NEW FACET SUBROUTINE HEIGHT

```
SUBROUTINE HEIGHT (XND,NDS,XCG,XNG,ISEG,JSEG,KSEG,ZHEIT)
C
C WRITTEN BY- UNIVERSITY OF ILLINOIS/DAVID D. GOETTSCH
C
C SUBROUTINE TO DETERMINE HEIGHT OF INTERSECTION OF CENTROID LINE
C FROM SURFACES ISEG AND JSEG TO THE PLANE CREATED BY SURFACE KSEG.
C
  DIMENSION XND(3,1), NDS(6,1), XCG(3,1), XNG(3,1)
  X ,N(4),U(3),V(3)
C
C.....DETERMINE EQUATION OF LINE BETWEEN ISEG AND JSEG
C..... X = XL + DELX*T, Y = YL + DELY*T, Z = ZL + DELZ*T
  DELX=XCG(1,JSEG)-XCG(1,ISEG)
  DELY=XCG(2,JSEG)-XCG(2,ISEG)
  DELZ=XCG(3,JSEG)-XCG(3,ISEG)
C
C.....DETERMINE EQUATION OF KSEG PLANE
C..... W1(X-XP) + W2(Y-YP) + W3(Z-ZP) = 0
  DO 10 I=1,4
    N(I)=NDS(I,KSEG)
  10 CONTINUE
  DO 20 J=1,3
    U(J)=XND(J,N(2))-XND(J,N(1))
    V(J)=XND(J,N(3))-XND(J,N(1))
  20 CONTINUE
  W1=U(2)*V(3)-U(3)*V(2)
  W2=U(3)*V(1)-U(1)*V(3)
  W3=U(1)*V(2)-U(2)*V(1)
C
C.....DETERMINE Z HEIGHT OF LINE/PLANE INTERSECTION
  TTOP=W1*(XND(1,N(1))-XCG(1,ISEG))+W2*(XND(2,N(1))-XCG(2,ISEG))+
  X W3*(XND(3,N(1))-XCG(3,ISEG))
  TBOT=W1*DELX + W2*DELY + W3*DELZ
  T=TTOP/TBOT
  ZHEIT=XCG(3,ISEG) + DELZ*T
C
  RETURN
END
```

APPENDIX F

NEW FACET SUBROUTINE HWRITE

```
SUBROUTINE HWRITE (HI,HO,KTOPI,KBOTI,KTOPO,KBOTO)
C
C WRITTEN BY- UNIVERSITY OF ILLINOIS/DAVID D. GOETTSCH
C
C SUBROUTINE WRITES OUT INTERCEPT HEIGHT MATRICES FOR MODTOPAZ
C TO READ IN. THE SDRS ICSS DIVIDES ALL COORDINATES BY 100. IN
C ORDER TO HAVE THE PROPER HEIGHTS FOR THE TOPAZ RUN, WHICH USES
C THE REAL COORDINATES, THE HEIGHT MATRIX MUST BE MULTIPLIED BY
C 100.
C
COMMON /BLK02/ NDIM, NUMNP, NUMEL, NDIV, MAXL, MAXA, NBLK, NCLP,
1 NINTI, NINTO, NIBS, NOBS, ISDRS
COMMON /IOBUF/ IOB('12100'O) VAX
DIMENSION HI(NUMEL,1),HO(NUMEL,1),KTOPI(1),KBOTI(1),KTOPO(1),
X KBOTO(1),ICTRL(5)
C
KDA=0
NW=NUMEL*NUMEL
C
C
ICTRL(1)=NUMEL
ICTRL(2)=NIBS
ICTRL(3)=NOBS
ICTRL(4)=0
ICTRL(5)=0
CALL WRABSF (IOB(520),ICTRL,5,0)
CALL RIOSTAT (IOB(520))
C
KDA=5
IF (NIBS.GT.0) THEN
CALL WRABSF (IOB(520),KTOPI,NIBS/2,KDA)
CALL RIOSTAT (IOB(520))
KDA=KDA+NIBS/2
CALL WRABSF (IOB(520),KBOTI,NIBS/2,KDA)
CALL RIOSTAT (IOB(520))
KDA=KDA+NIBS/2
CALL WRABSF (IOB(520),HI,NW,KDA)
CALL RIOSTAT (IOB(520))
KDA=KDA+NW
ENDIF
IF (NOBS.GT.0) THEN
CALL WRABSF (IOB(520),KTOPO,NOBS/2,KDA)
CALL RIOSTAT (IOB(520))
KDA=KDA+NOBS/2
CALL WRABSF (IOB(520),KBOTO,NOBS/2,KDA)
CALL RIOSTAT (IOB(520))
KDA=KDA+NOBS/2
```

```
CALL WRABSF (IOB(520),HO,NW,KDA)
CALL RIOSTAT (IOB(520))
ENDIF
C
RETURN
END
```

APPENDIX G

MODIFIED TOPAZ3D SUBROUTINE RADIN3

```
SUBROUTINE RADIN3 (X,NODES,NRCOND,NCRAD,KTOPI,KBOTI,KTOPO
1 ,KBOTO,THOLE,WAVLTH,EMIS,FROW,IPVT,WORK,ARAD,ARTOPI,ARBOTI
2 ,ARTOPO,ARBOTO,AEF,HI,HO,AEBC,NBAND,NECURV,SIGMA,IRTPY,ITMAXB
3 ,TOLB,IGEOM,NUMNP,NUMEL,NRDM,NRSEG,NIBS,NOBS,WITHD1,DIST1
4 ,WITHD2,GAP,TCOLD,NECOLD,NEHOT)

C
C  RADIN3- SUBROUTINE TO INPUT ENCLOSURE RADIATION DATA
C
C  RADIN3- LAWRENCE LIVERMORE NATIONAL LABORATORY/ARTHUR B. SHAPIRO
C
C  MODIFICATIONS- STRUCTURAL DYNAMICS RESEARCH CORPORATION
C    - DESCRIPTION OF VARIABLES AND ARRAYS
C    5-NOV-86 / T. RICE / CHANGED TO DOUBLE PRECISION
C      AND PUT COMMON BLOCKS IN INCLUDE FILES
C
C  MODIFICATIONS- UNIVERSITY OF ILLINOIS/DAVID D. GOETTSCH
C    - INPUT OF INTERCEPT HEIGHT MATRICES, HI AND HO FOR
C      ENCLOSURE RADIATION USING VIEW FACTOR EXCHANGE METHOD.
C    - CALCULATION OF SURFACE AREA RATIO'S FOR MULTI-ELEMENT
C      BAFFLE SURFACES
C
C  DESCRIPTION
C
C *****
C* SUBROUTINE TO INPUT ENCLOSURE RADIATION DATA
C *****
C *****
C
C  ACCESS
C
C  INPUT PARAMETERS
C    X , REAL ARRAY    - NODAL COORDINATES
C    FROW , REAL ARRAY  - NOT USED
C    IPVT , INTEGER ARRAY - PIVOT VECTOR USED BY SGEFA/SGEDI
C    WORK , REAL ARRAY  - WORK SPACE USED BY SGEDI
C    ARAD , REAL ARRAY  - SURFACE AREA FOR ENCLO RAD BC
C    AEF , REAL ARRAY   - VIEW FACTOR MATRIX
C    AEBC , REAL ARRAY  - SURFACE AREA FOR SPECIFIED
C                        ENCLOSED RAD BC
C    NBAND , INTEGER VARIABLE - NUMBER OF RADIATION BANDS
C    NECURV, INTEGER VARIABLE - NO OF EMIS VS WAVELENGTH CURVES
C    IRTPY , INTEGER VARIABLE - RADIATION CALC TYPE (CARD 2)
C    IGEOM , INTEGER VARIABLE - TYPE OF GEOMETRY
C    NUMNP , INTEGER VARIABLE - NUMBER OF NODES
C    NUMEL , INTEGER VARIABLE - NUMBER OF ELEMENTS
C    NRDM , INTEGER VARIABLE - NO OF ENCL RADIATION SURFACES
```

```

C      NRSEG , INTEGER VARIABLE - NO OF ENCL RADIATION SURFACES
C      NIBS , INTEGER VARIABLE - NUMBER OF #1 BAFFLE SURFACES
C      NOBS , INTEGER VARIABLE - NUMBER OF #2 BAFFLE SURFACES
C
C
C
C
C      OUTPUT PARAMETERS
C      NODES , INTEGER ARRAY - NODES ASSOCIATED WITH SURFACE
C      NRCOND, INTEGER ARRAY - SURFACE PARTICIPATION FLAG
C      NCRAD , INTEGER ARRAY - CURVE NO. FOR EMISSIVITY
C      THOLE , REAL ARRAY - TEMP OF SURFACE IF NCRAD=0
C      WAVLTH, REAL ARRAY - WAVELENGTH BREAKPOINTS
C      EMIS , REAL ARRAY - EMISSIVITY VS. WAVELENGTH CURVES
C      SIGMA , REAL VARIABLE - STEFAN-BOLTZMANN CONSTANT
C      ITMAXB, INTEGER VARIABLE - MAX NO OF RADIOSITY ITERATIONS
C      TOLB , REAL VARIABLE - RADIOSITY CONVERGENCE TOLERANCE
C      KTOPI , INTEGER ARRAY - TOP SURFACE OF #1 BAFFLE SURFACE DATA
C      KBOTI , INTEGER ARRAY - BOTTOM SURFACE OF #1 BAFFLE SURF DATA
C      KTOPO , INTEGER ARRAY - TOP SURFACE OF #2 BAFFLE SURFACE DATA
C      KBOTO , INTEGER ARRAY - BOTTOM SURFACE OF #2 BAFFLE SURF DATA
C      ARTOPI, REAL VARIABLE - AREA RATIOS FOR TOP, #1 BAFFLE ELS.
C      ARBOTI, REAL VARIABLE - AREA RATIOS FOR BOT, #1 BAFFLE ELS.
C      ARTOPO, REAL VARIABLE - AREA RATIOS FOR TOP, #2 BAFFLE ELS.
C      ARBOTO, REAL VARIABLE - AREA RATIOS FOR BOT, #2 BAFFLE ELS.
C      HI , REAL ARRAY - #1 BAFFLE INTERCEPT HEIGHTS
C      HO , REAL ARRAY - #2 BAFFLE INTERCEPT HEIGHTS
C      WITHD1, REAL VARIABLE - INITIAL WITHDRAWAL RATE
C      DIST1 , REAL VARIABLE - DISTANCE TRAVELED AT WITHD1
C      WITHD2, REAL VARIABLE - FINAL WITHDRAWAL RATE
C      GAP , REAL VARIABLE - INITIAL BAFFLE HEIGHT ABOVE ORIGIN
C      TCOLD , REAL VARIABLE - TEMP. OF COOLING CHAMBER
C      NECOLD, INTEGER VARIABLE - EMISS CURVE NUMBER FOR COOLING CHAMBER
C      NEHOT , INTEGER VARIABLE - EMISS CURVE NUMBER FOR SUSCEPTOR
C
C-----END DOC
C
C=====
C      BEGINNING OF DECLARATIONS
C=====
C
C      INCLUDE 'T3DINC:IMPDP.INC /LIST'
C
C --- SUBROUTINE ARGUMENTS
C
C      INTEGER NODES(4,*), NRCOND(*), NCRAD(*), IPV(*),
C      DIMENSION X(3,*), THOLE(*), WAVLTH(*), EMIS(8,*), FROW(*),
C      $      WORK(*), ARAD(*), AEF(NRDIM,*), AEBC(*), KTOPI(*),
C      $      KBOTI(*), KTOPO(*), KBOTO(*), ARTOPI(*), ARBOTI(*),
C      $      ARTOPO(*), ARBOTO(*), HI(NRDIM,*), HO(NRDIM,*)
C
C --- LOCAL VARIABLES AND ARRAYS
C

```

```

      INTEGER ICTRL(5)
      DIMENSION DET(2)
C
C --- COMMON BLOCKS
C
      INCLUDE 'T3DINC:IOBUF.INC /LIST'
C
C --- DATA INITIALIZATION
C
      DATA ATOPI,ABOTI,ATOPO,ABOTO /0,0,0,0/
C
C
C =====
C                      END OF DECLARATIONS
C =====
C
      WRITE (59,240)
      READ (5,140) SIGMA,TOLB,ITMAXB,WTHD1,DIST1,WTHD2,GAP
      READ (5,141) TCOLD,NECOLD,NEHOT
      IF (TOLB.LT.1.E-12) TOLB=1.E-04
      IF (ITMAXB.EQ.0) ITMAXB=100
10  READ (5,150) J,(NODES(L,J),L=1,4),NMISS,INC,NRCOND(J),NCRAD(J)
      1 ,THOLE(J)
      IF (NMISS.EQ.0) GO TO 30
      DO 20 K=1,NMISS
          JM1=J
          J=J+1
          DO 15 I=1,4
              NODES(I,J)=NODES(I,JM1)+INC
15  CONTINUE
          NCRAD(J)=NCRAD(JM1)
          THOLE(J)=THOLE(JM1)
          NRCOND(J)=NRCOND(JM1)
20  CONTINUE
30  CONTINUE
      IF (J.LT.NRSEG) GO TO 10
      NBP=NBAND+1
      WAVLTH(1)=0.
      READ (5,160) (WAVLTH(I),I=2,NBP)
      DO 40 J=1,NECURV
          READ (5,160) (EMIS(I,J),I=1,NBAND)
40  CONTINUE
          WRITE (6,170)
          WRITE (6,180) SIGMA,TOLB,ITMAXB,WTHD1,DIST1,WTHD2,GAP,TCOLD,
1  NECOLD,NEHOT
          WRITE (6,190)
          DO 50 I=1,NRSEG
              WRITE (6,200) I,(NODES(L,I),L=1,4),NRCOND(I),NCRAD(I),THOLE(I)
50  CONTINUE
          WRITE (6,210)
          WRITE (6,220) (WAVLTH(I),I=2,NBP)
          WRITE (6,230)
          DO 60 J=1,NECURV

```

```

        WRITE (6,220) (EMIS(I,J),I=1,NBAND)
60 CONTINUE
    DO 70 I=1,NECURV
        DO 70 NB=1,NBAND
            IF (EMIS(NB,I).GE.1.) EMIS(NB,I)=0.9999
70 CONTINUE
C.....READ FILE FABSF FOR IN CORE ENCLOSURE RADIATION SOLUTION
    CALL RDABSF (IOB1,ICTRL,5,0,IERR)
    CALL RIOSTAT (IOB1)
C.....CHECK HAS BEEN BY PASSED IN ORDER TO USE 2D VIEW FACTORS
C    IF (ICTRL(1).NE.IGEOM) GO TO 130
    IF (ICTRL(2).NE.NRSEG) GO TO 130
    IF (ICTRL(3).NE.IRTYP) GO TO 130
    CALL RDABSF (IOB1,ARAD,NRSEG,5,IERR)
    CALL RIOSTAT (IOB1)
    KDA=5+NRSEG
C
C --- CONVERT AREAS TO DOUBLE PRECISION ARRAY
C
    CALL CNVSTD( ARAD, ARAD, NRSEG )
C
    NW=NRSEG*NRSEG
    IF (IRTP.EQ.2) NW=NBAND*NW
    CALL RDABSF (IOB1,AEF,NW,KDA,IERR)
    CALL RIOSTAT (IOB1)
C
C --- CONVERT VIEW FACTORS TO DOUBLE PRECISION ARRAY
C
    CALL CNVSTD( AEF, AEF, NW )
C
    IF (IRTP.EQ.2) GO TO 110
C.....CALCULATE VIEW FACTOR MATRIX AND STORE IN AEF
    DO 80 I=1,NRSEG
        AREA=ARAD(I)
        DO 80 J=1,NRSEG
            AEF(I,J)=AEF(I,J)/AREA
80 CONTINUE
    IF (NBAND.GT.1) GO TO 110
    IF ((NIBS.GT.0).OR.(NOBS.GT.0)) GO TO 101
C.....FOR VIEW FACTORS WITH NBAND=1 --- FORM CHI MATRIX AND THEN
C.....PSI MATRIX; STORE IN AEF
    IRTYP=3
    DO 100 I=1,NRSEG
        MATL=NCRAD(I)
        IF (MATL.EQ.0) THEN
            EPS=0.9999
        ELSE
            EPS=EMIS(1,MATL)
        ENDIF
        XMULT=(EPS-1.)/EPS
        DO 90 J=1,NRSEG
            AEF(I,J)=XMULT*AEF(I,J)

```

```

90  CONTINUE
    AEF(I,I)=1./EPS+AEF(I,I)
100 CONTINUE
    CALL SGEFA (AEF,NRSEG,NRSEG,IPVT,INFO)
    CALL SGEDI (AEF,NRSEG,NRSEG,IPVT,DET,WORK,1)
    GO TO 110
101 CONTINUE
C
C.....READ FILE HABS FOR IN CORE VIEW FACTOR EXCHANGE, ENCLOSURE
C.....RADIATION SOLUTION
    IRTYP=3
    CALL RDABSF (IOB3,ICTRL,5,0,IERR)
    CALL RIOSTAT (IOB3)
    IF (ICTRL(1).NE.NRSEG) GO TO 130
    IF (ICTRL(2).NE.NIBS) GO TO 130
    IF (ICTRL(3).NE.NOBS) GO TO 130
    KDA=5
    NW=NRSEG*NRSEG
    IF (NIBS.GT.0) THEN
        CALL RDABSF (IOB3,KTOPI,NIBS/2,KDA,IERR)
        CALL RIOSTAT (IOB3)
        KDA=KDA+NIBS/2
        CALL RDABSF (IOB3,KBOTI,NIBS/2,KDA,IERR)
        CALL RIOSTAT (IOB3)
        KDA=KDA+NIBS/2
        CALL RDABSF (IOB3,HI,NW,KDA,IERR)
        CALL RIOSTAT (IOB3)
C
C--- CONVERT AREAS TO DOUBLE PRECISION ARRAY
C
    CALL CNVSTD( HI, HI, NW )
C
    KDA=KDA+NW
    ENDIF
    IF (NOBS.GT.0) THEN
        CALL RDABSF (IOB3,KTOPO,NOBS/2,KDA,IERR)
        CALL RIOSTAT (IOB3)
        KDA=KDA+NOBS/2
        CALL RDABSF (IOB3,KBOTO,NOBS/2,KDA,IERR)
        CALL RIOSTAT (IOB3)
        KDA=KDA+NOBS/2
        CALL RDABSF (IOB3,HO,NW,KDA,IERR)
        CALL RIOSTAT (IOB3)
C
C--- CONVERT AREAS TO DOUBLE PRECISION ARRAY
C
    CALL CNVSTD( HO, HO, NW )
    ENDIF
C
C....CALCULATE AREA RATIO'S FOR #1 AND #2 BAFFLES. THE AREA RATIO
C....IS THE INDIVIDUAL ELEMENT AREA OVER THE TOTAL AREA OF THE PARTICULAR
C... BAFFLE SURFACE.

```



```

C....CALCULATE SURFACE RATIO'S FOR #1 BAFFLE
  DO 103 I=1,NIBS/2
    ATOPI = ARAD(KTOPI(I)) + ATOPI
    ABOTI = ARAD(KBOTI(I)) + ABOTI
  103 CONTINUE
  DO 104 J=1,NIBS/2
    ARTOPI(J)=ARAD(KTOPI(J))/ATOPI
    ARBOTI(J)=ARAD(KBOTI(J))/ABOTI
  104 CONTINUE
C
C....CALCULATE SURFACE RATIO'S FOR #2 BAFFLE
  DO 106 I=1,NOBS/2
    ATOPO = ARAD(KTOPO(I)) + ATOPO
    ABOTO = ARAD(KBOTO(I)) + ABOTO
  106 CONTINUE
  DO 107 J=1,NOBS/2
    ARTOPO(J)=ARAD(KTOPO(J))/ATOPO
    ARBOTO(J)=ARAD(KBOTO(J))/ABOTO
  107 CONTINUE
C
C.....CALCULATE RADIATION SEGMENT LENGTH
  110 CONTINUE
  DO 120 J=1,NRSEG
    AEBC(J)=ARAD(J)
  120 CONTINUE
  RETURN
C
C.....ERROR TERMINATION
  130 WRITE (6,250)
    WRITE (59,250)
    CALL ADIOS (2)
C
  140 FORMAT (2E10.0,I5,4E10.0)
  141 FORMAT (1E10.0,2I5)
  150 FORMAT (5I5,5X,4I5,E10.0)
  160 FORMAT (8E10.0)
  170 FORMAT (//16(5H*****)//12X,'*** ENCLOSURE RADIATI
    1 O N D A T A ***')
  180 FORMAT (// STEFAN-BOLTZMANN CONSTANT           =,1PE12
    1  .4,// RADIOSITY CONVERGENCE TOLERANCE         =,1PE12.4,/
    2  / MAXIMUM NUMBER OF RADIOSITY ITERATIONS      =,I5,
    3  // INITIAL WITHDRAWAL VELOCITY                =,1PE12.4,
    4  // INITIAL WITHDRAWAL DISTANCE                 =,1PE12.4,
    5  // FINAL WITHDRAWAL VELOCITY                  =,1PE12.4,
    6  // INITIAL BAFFLE GAP ABOVE ORIGIN             =,1PE12.4,
    7  // COOLING CHAMBER TEMPERATURE                 =,1PE12.4,
    8  // EMISS CURVE # FOR COOLING CHAMBER SURFACE   =,I5,
    9  // EMISS CURVE # FOR SUSCEPTOR SURFACE       =,I5)
  190 FORMAT (// SURF N1 N2 N3 N4 COND CODE ',
    1 'EPS CURVE HOLE TEMP')
  200 FORMAT (5I6,3X,I5,6X,I5,3X,1PE11.3)
  210 FORMAT (// RADIATION WAVELENGTH BREAKPOINTS//,5X,'1',9X,'2',9X,

```

```
1 '3',9X,'4',9X,'5',9X,'6',9X,'7',9X,'8')
220 FORMAT (1X,1P8E10.2)
230 FORMAT (/ ' BAND EMISSIVITIES'//,5X,'1',9X,'2',9X,'3',9X,'4',9X,
1 '5',9X,'6',9X,'7',9X,'8')
240 FORMAT (5X,READING ENCLOSURE RADIATION DATA')
250 FORMAT(/ ' *** ERROR*** VIEW FACTOR FILE NOT COMPATIBLE WITH TOPA
1Z INPUT.'//)
END
```

APPENDIX H

MODIFIED TOPAZ3D SUBROUTINE APLYBC

```
SUBROUTINE APLYBC (X,KM,VOLE,NDFBC,NCFBC,FBCM,AFLUX,QFLUX,NDCBC
1 ,NTINF,TINFM,NCH,HM,ACONV,QCONV,FREE,NDRAD,NRCOND,NCRAD,THOLE
2 ,WAVLTH,EMIS,FROW,EPS,FRAC,QNET,TS,ARAD,AEF,B,H,NDRBC,NTINFR
3 ,TINFM,R,NCF,FM,AEXP,BEXP,ARADBC,QRAD,CURVX,CURVY,JDIAG,TEMP,GF,GK
4 ,ATIME,KTOPI,KBOTI,KTOPO,KBOTO,ARTOPI,ARBOTI,ARTOPO,ARBOTO
5 ,RAEF,HI,HO,VFRSI,VFRSO,BAFFLE,TIME,NSTEP,ITTER)
```

```
C
C APLYBC- APPLY BOUNDARY CONDITIONS TO SYSTEM EQUATIONS
C
C APLYBC- LAWRENCE LIVERMORE NATIONAL LABORATORY/ARTHUR B. SHAPIRO
C
C MODIFICATIONS- STRUCTURAL DYNAMICS RESEARCH CORPORATION
C   - DESCRIPTION OF VARIABLES AND ARRAYS
C   - INCLUDE COMMON BLOCKS
C 15-SEP-86 / T. RICE / DOT PRODUCT CHANGED FROM FUNCTION CALL TO
C   FDOT TO BEING CALCULATED LOCALLY
C 30-OCT-86 / T. RICE / CHANGED TO DOUBLE PRECISION
C   AND PUT COMMON BLOCKS IN INCLUDE FILES
C
C MODIFICATIONS- UNIVERSITY OF ILLINOIS/DAVID D. GOETTSCH
C   - ENCLOSURE RADIATION USING VIEW FACTOR EXCHANGE METHOD
C
C DESCRIPTION
C
C BOUNDARY CONDITION SURFACE INTEGRATION IS PERFORMED USING
C LOBATTO INTEGRATION FORMULAS
C
C ACCESS
C
C INPUT PARAMETERS
C   X , REAL ARRAY - NODAL COORDINATES
C   KM , INTEGER ARRAY - ELEMENT CONNECTIVITY
C   VOLE , REAL ARRAY - ELEMENT VOLUME
C   NDFBC , INTEGER ARRAY - NODE NUMBERS WITH FLUX BC
C   (N,NSEG) - NTH OF 4 NODES FOR NSEG FLUX
C   NCFBC , INTEGER ARRAY - FLUX CURVE NUMBER
C   FBCM , REAL ARRAY - CURVE MULTIPLIERS AT 4 NODES OF
C   FLUX BC'S
C   AFLUX , REAL ARRAY - SURFACE AREA FOR SPECIFIED
C   FLUX BC
C   NDCBC , INTEGER ARRAY - NODE NUMBERS WITH CONVECTION BC
C   (N,NSEG) - NTH OF 4 NODES FOR NSEG CONVECTION BC
C   NTINF , INTEGER ARRAY - CURVE NO. FOR T-INF FOR CONV BC
C   TINFM , REAL ARRAY - CURVE MULTIPLIER FOR T-INF FOR
C   CONV BC AT 4 NODES
C   NCH , INTEGER ARRAY - CURVE NO. FOR FILM COEFFICIENT
C   HM , REAL ARRAY - CURVE MULTIPLIER FOR FILM
```

C COEFFICIENT
 C ACONV , REAL ARRAY - SURFACE AREA FOR SPECIFIED
 C CONVECTION BC
 C FREE , REAL ARRAY - FREE CONVECTION EXPONENT
 C NDRAD , INTEGER ARRAY - NODE NO. WITH ENCLO RAD BC
 C (N,NSEG) - NTH OF 4 NODES FOR NSEG ENCL RADIATION BC
 C NRCOND, INTEGER ARRAY - SURFACE PARTICIPATION FLAG
 C NCRAD , INTEGER ARRAY - CURVE NO. FOR EMISSIVITY
 C THOLE , REAL ARRAY - TEMP OF SURFACE IF NCRAD=0
 C WAVLTH, REAL ARRAY - 8 WAVELENGTH BREAKPOINTS
 C EMIS , REAL ARRAY - EMISSIVITY VS. WAVELENGTH CURVES
 C (1-8,J) - EMISSIVITY FOR EIGHT BANDS OF CURVE J
 C ARAD , REAL ARRAY - SURFACE AREA FOR ENCLO RAD BC
 C AEF , REAL ARRAY - VIEW FACTOR MATRIX
 C NDRBC , INTEGER ARRAY - NODE NO. WITH RAD BC
 C (N,NSEG) - NTH OF 4 NODES FOR NSEG RADIATION BC
 C NTINFR, INTEGER ARRAY - CURVE NO. FOR T-INF FOR RAD BC
 C TINFMR, REAL ARRAY - CURVE MULTIPLIER FOR T-INF FOR
 C RAD BC AT 4 NODES
 C NCF , INTEGER ARRAY - CURVE NO. FOR F-RAD COEFFICIENT
 C FM , REAL ARRAY - CURVE MULTIPLIER FOR R-RAD COEFF
 C AEXP , REAL ARRAY - ** NOT USED **
 C BEXP , REAL ARRAY - ** NOT USED **
 C ARADBC, REAL ARRAY - SURFACE AREA FOR SPECIFIED RAD BC
 C CURVX , REAL ARRAY - TIME/TEMP FOR ALL FUNCTION CURVES
 C CURVY , REAL ARRAY - FUNCTION VALUES OF ALL FUNCTION
 C CURVES
 C JDIAG , INTEGER ARRAY - DIAGONAL POINTERS
 C TEMP , REAL ARRAY - TEMPS AT ALPHA-TIME
 C ATIME , REAL VARIABLE - COMPUTATIONAL TIME(TIME+ALPHA*DT)
 C KTOPI , INTEGER ARRAY - TOP SURFACE OF #1 BAFFLE SURFACE DATA
 C KBOTI , INTEGER ARRAY - BOT SURFACE OF #1 BAFFLE SURFACE DATA
 C KTOPO , INTEGER ARRAY - TOP SURFACE OF #2 BAFFLE SURFACE DATA
 C KBOTO , INTEGER ARRAY - BOT SURFACE OF #2 BAFFLE SURFACE DATA
 C ARTOPI, REAL VARIABLE - AREA RATIOS FOR TOP, #1 BAFFLE ELS.
 C ARBOTI, REAL VARIABLE - AREA RATIOS FOR BOT, #1 BAFFLE ELS.
 C ARTOPO, REAL VARIABLE - AREA RATIOS FOR TOP, #2 BAFFLE ELS.
 C ARBOTO, REAL VARIABLE - AREA RATIOS FOR BOT, #2 BAFFLE ELS.
 C RAEF , REAL ARRAY - MODIFIED VIEW FACTOR MATRIX
 C HI , REAL ARRAY - #1 BAFFLE INTERCEPT HEIGHTS
 C HO , REAL ARRAY - #2 BAFFLE INTERCEPT HEIGHTS
 C WITHD1, REAL VARIABLE - INITIAL WITHDRAWAL RATE
 C DIST1 , REAL VARIABLE - DISTANCE TRAVELED AT WITHD1
 C WITHD2, REAL VARIABLE - FINAL WITHDRAWAL RATE
 C GAP , REAL VARIABLE - INITIAL BAFFLE HEIGHT ABOVE ORIGIN
 C TCOLD , REAL VARIABLE - TEMPERATURE OF COOLING CHAMBER
 C NECOLD, INTEGER VARIABLE - EMISSIVITY CURVE NUMBER FOR COOLING CH
 C NEHOT , INTEGER VARIABLE - EMISSIVITY CURVE NUMBER FOR SUSCEPTOR
 C VFRSI , REAL VARIABLE - VIEW FACTOR ROW SUM FOR #1 BAFFLE
 C VFRSO , REAL VARIABLE - VIEW FACTOR ROW SUM FOR #2 BAFFLE
 C NTAEF , INTEGER VARIABLE - MAX. NUMBER OF TIME STEPS BETWEEN
 C VIEW FACTOR REFORMATION

```

C      ITTER , INTEGER VARIABLE - PRESENT NUMBER OF ITERATIONS IN NSTEP
C      NSTEP , INTEGER VARIABLE - PRESENT NUMBER OF TIME STEPS
C      TIME , REAL VARIABLE - PRESENT TIME

```

```

C      OUTPUT PARAMETERS

```

```

C      QFLUX , REAL ARRAY - FLUX THIS STEP AT EACH FLUX BC
C      QCONV , REAL ARRAY - FLUX AT EACH CONVECTION BC
C      FROW , REAL ARRAY - VIEW FACTOR WORK SPACE
C      EPS , REAL ARRAY -
C      FRAC , REAL ARRAY -
C      QNET , REAL ARRAY - FLUX AT EACH ENCL. RADIATION BC
C      TS , REAL ARRAY - TEMPS. FOR ENCL. RAD.
C      B , REAL ARRAY -
C      H , REAL ARRAY -
C      QRAD , REAL ARRAY - FLUX AT EACH RADIATION BC
C      GF , REAL ARRAY - GLOBAL RIGHT HAND SIDE
C      GK , REAL ARRAY - GLOBAL STIFFNESS MATRIX

```

```

C-----END DOC

```

```

C      BEGINNING OF DECLARATIONS

```

```

C      INCLUDE 'T3DINC:IMPDP.INC /LIST'

```

```

C --- SUBROUTINE ARGUMENTS

```

```

C      INTEGER KM(9,*), NDFBC(4,*), NCFBC(*),
$      NDCBC(4,*), NTINF(*), NCH(*),
$      NDRAD(4,*), NRCOND(*), NCRAD(*),
$      NDRBC(4,*), NTINFR(*), NCF(*),
$      JDIAG(*), KTOPI(*), KBOTI(*),
$      KTOPO(*), KBOTO(*)

```

```

C      DIMENSION X(3,*), VOLE(*), FBCM(4,*),
$      AFLUX(*), QFLUX(*), TINF(4,*),
$      HM(*), ACONV(*), QCONV(*), FREE(*),
$      THOLE(*), WAVLTH(*), EMIS(8,*),
$      FROW(*), EPS(*), FRAC(*),
$      QNET(*), TS(*), ARAD(*), AEF(NRDIM,*), B(*), H(*),
$      TINFMR(4,*), FM(*), AEXP(*), BEXP(*),
$      ARADBC(*), QRAD(*),
$      CURVX(*), CURVY(*), TEMP(*), GF(*), GK(*),
$      ARTOPI(*), ARBOTI(*), ARTOPO(*), ARBOTO(*),
$      RAEF(NRDIM,*), HI(NRDIM,*), HO(NRDIM,*)

```

```

C --- LOCAL VARIABLES

```

```

C      INTEGER LD(4)
C      DIMENSION W(2), BCX(4,4), BCK(10), BCF(4),

```



```

C  CONVECTION  BC  -----
C
30 IF (NCBC.EQ.0) GO TO 70
   DO 60 NSEG=1,NCBC
     DO 31 I=1,4
       LD(I)=NDCBC(I,NSEG)
       BCF(I)=0.
31 CONTINUE
     DO 32 I=1,10
       BCK(I)=0.
32 CONTINUE
     ITRI=0
     IF (LD(3).EQ.LD(4)) ITRI=1
     CALL VALUE (NSEG,NTINF,CURVX,CURVY,0.,ATIME,VAL(1),1)
     TINF=VAL(1)*TINFM(1,NSEG)
     DO 33 I=1,4
       TFILM=.5*(TINF+TEMP(LD(I)))
       CALL VALUE (NSEG,NCH,CURVX,CURVY,TFILM,ATIME,VAL(I),1)
33 CONTINUE
     IF (FREE(NSEG).EQ.0.) THEN
       DO 34 I=1,4
         VAL(I)=VAL(I)*HM(NSEG)
34 CONTINUE
       ELSE
         DO 35 I=1,4
           VAL(I)=VAL(I)*HM(NSEG)*ABS(TINF-TEMP(LD(I)))**FREE(NSEG)
35 CONTINUE
       ENDIF
       DO 37 L=1,4
         CALL SHAPE2 (RG(L),SG(L),DIS,X,LD,SH,ITRI)
         F=DIS*(SH(1)*VAL(1)+SH(2)*VAL(2)+SH(3)*VAL(3)+SH(4)*VAL(4))
         K=0
         DO 36 J=1,4
           BCF(J)=BCF(J)+SH(J)*F*TINF
         DO 36 I=1,J
           K=K+1
           BCK(K)=BCK(K)+SH(I)*F*SH(J)
36 CONTINUE
37 CONTINUE
       CALL ADDBC (GK,GF,BCK,BCF,LD,JDIAG,TEMP(LD(1)),TEMP(LD(2)),
         1      TEMP(LD(3)),TEMP(LD(4)),ALPHA,ITRAN)
       QCONV(NSEG)=99999.
60 CONTINUE
C
C  RADIATION  BC  -----
C
70 IF (NRBC.EQ.0) GO TO 110
   DO 100 NSEG=1,NRBC
     DO 71 I=1,4
       LD(I)=NDRBC(I,NSEG)
       BCF(I)=0.
71 CONTINUE

```

```

DO 72 I=1,10
  BCK(I)=0.
72 CONTINUE
  ITRI=0
  IF (LD(3).EQ.LD(4)) ITRI=1
  CALL VALUE (NSEG,NTINFR,CURVX,CURVY,0.,ATIME,TINF,1)
  TINF=TINF*TINFMR(1,NSEG)
DO 73 I=1,4
  CALL VALUE (NSEG,NCF,CURVX,CURVY,TEMP(LD(I)),ATIME,VAL(I),1)
  VAL(I)=VAL(I)*FM(NSEG)*(TEMP(LD(I))**2+TINF**2)*(TEMP(LD(I))+
1 TINF)
73 CONTINUE
DO 75 L=1,4
  CALL SHAPE2 (RG(L),SG(L),DIS,X,LD,SH,ITRI)
  F=DIS*(SH(1)*VAL(1)+SH(2)*VAL(2)+SH(3)*VAL(3)+SH(4)*VAL(4))
  K=0
DO 74 J=1,4
  BCF(J)=BCF(J)+SH(J)*F*TINF
DO 74 I=1,J
  K=K+1
  BCK(K)=BCK(K)+SH(I)*F*SH(J)
74 CONTINUE
75 CONTINUE
  CALL ADDBC (GK,GF,BCK,BCF,LD,JDIAG,TEMP(LD(1)),TEMP(LD(2)),
1 TEMP(LD(3)),TEMP(LD(4)),ALPHA,ITRAN)
  QRAD(NSEG)=99999.
100 CONTINUE
C
C ENCLOSURE RADIATION -----
C
110 IF (NRSEG.EQ.0) GO TO 350
  IF (NIBS.GT.0.OR.NOBS.GT.0) GO TO 365
  GO TO (120,230,310), IRTYP
C
C VIEW FACTORS WITH NBAND>1 USED IN CALCULATIONS
C
120 CONTINUE
  DO 130 ISEG=1,NRSEG
    QNET(ISEG)=0.
    FRAC(ISEG)=1.
    IF (NCRAD(ISEG).EQ.0) THEN
      TS(ISEG)=THOLE(ISEG)
    ELSE
      TS(ISEG)=(.5*(TEMP(NDRAD(1,ISEG))**4+TEMP(NDRAD(2,ISEG))**4))**.25
    ENDIF
  130 CONTINUE
C.....LOOP ON RADIATION BANDS
  DO 210 NB=1,NBAND
    W(1)=WAVLTH(NB)
    W(2)=WAVLTH(NB+1)
    ITER=0
    ENORM1=0.

```



```

C.....DETERMINE SEGMENT EMISSIVITY
DO 140 ISEG=1,NRSEG
  IF (NCRAD(ISEG).EQ.0) THEN
    EPS(ISEG)=1.
  ELSE
    EPS(ISEG)=EMIS(NB,NCRAD(ISEG))
  ENDIF
  CALL RADFRC (IUNITS,W,TS(ISEG),FRAC(ISEG))
  B(ISEG)=0.
140 CONTINUE
C.....RADIOSITY CALCULATIONS
150 ITER=ITER+1
  IF (ITER.LT.ITMAXB) GO TO 160
  WRITE (6,360)
  CALL ADIOS (2)
160 DO 180 ISEG=1,NRSEG
C.....DETERMINE VIEW FACTORS FOR ROW ISEG
DO 170 JSEG=1,NRSEG
  FROW(JSEG)=AEF(ISEG,JSEG)
170 CONTINUE
C.....DETERMINE IRRADIATION AND RADIOSITY
C
C
C  H(ISEG)=FDOT(FROW,B,NRSEG)
C
C --- COMPUTE DOT PRODUCT LOCALLY
C
  FDOT = 0.0
  DO 115 IDOT=1,NRSEG
    FDOT = FDOT + ( FROW(IDOT) * B(IDOT) )
115 CONTINUE
  H(ISEG)=FDOT
C
C
C  B(ISEG)=EPS(ISEG)*FRAC(ISEG)*SIGMA*TS(ISEG)**4
C  1  +(1.-EPS(ISEG))*H(ISEG)
180 CONTINUE
C.....DETERMINE RADIOSITY CONVERGENCE
C
C
C  ENORM2=SQRT(FDOT(B,B,NRSEG))
C
C --- COMPUTE DOT PRODUCT LOCALLY
C
  FDOT = 0.0
  DO 125 IDOT=1,NRSEG
    FDOT = FDOT + ( B(IDOT) * B(IDOT) )
125 CONTINUE
  ENORM2=SQRT(FDOT)
C
C
C  IF (ABS(1.-ENORM1/ENORM2).LE.TOLB) GO TO 190
  ENORM1=ENORM2
  GO TO 150

```

```

C.....RADIOSITIES ARE NOW KNOWN.
C.....DETERMINE CONTRIBUTION TO STIFFNESS MATRIX AND LOAD VECTOR
190 DO 200 ISEG=1,NRSEG
    N1=NDRAD(1,ISEG)
    N2=NDRAD(2,ISEG)
    LD(1)=N1
    LD(2)=N2
CXXX    IF (IGEOM.EQ.1) CALL RADII (X,R0,R1,R2,TWOPI,N1,N2)
CXXX    QNET(ISEG)=QNET(ISEG)+TWOPI*R0*ARAD(ISEG)*(B(ISEG)-H(ISEG))
    QNET(ISEG)=99999.
C
    IF (NRCOND(ISEG).EQ.1) GO TO 200
    DET=ARAD(ISEG)/6.
    S=DET*4.*EPS(ISEG)*SIGMA*FRAC(ISEG)*TS(ISEG)**3
    BCK(1)=S*(R0+R1)
    BCK(2)=S*R0
    BCK(3)=S*(R0+R2)
    S=DET*(3.*EPS(ISEG)*SIGMA*FRAC(ISEG)*TS(ISEG)**4
1    +EPS(ISEG)*H(ISEG))
    BCF(1)=S*(R1+2.*R0)
    BCF(2)=S*(R2+2.*R0)
    CALL ADDBC (GK,GF,BCK,BCF,LD,JDIAG,TEMP(N1),TEMP(N2),ALPHA,ITRAN)
200 CONTINUE
210 CONTINUE
    GO TO 350
C
C EXCHANGE FACTORS USED IN CALCULATIONS
C
230 CONTINUE
C.....GATHER SEGMENT TEMPERATURES
DO 235 ISEG=1,NRSEG
    QNET(ISEG)=0.
    FRAC(ISEG)=1.
    IF (NCRAD(ISEG).EQ.0) THEN
        TS(ISEG)=THOLE(ISEG)
    ELSE
        TS(ISEG)=(.5*(TEMP(NDRAD(1,ISEG))**4+TEMP(NDRAD(2,ISEG))**4))**.25
    ENDIF
235 CONTINUE
C.....LOOP ON RADIATION BANDS
DO 300 NB=1,NBAND
    IF (NBAND.GT.1) THEN
        W(1)=WAVLTH(NB)
        W(2)=WAVLTH(NB+1)
    DO 237 ISEG=1,NRSEG
        CALL RADFRG (IUNITS,W,TS(ISEG),FRAC(ISEG))
    237 CONTINUE
    ENDIF
C.....LOOP ON I SURFACES
DO 290 ISEG=1,NRSEG
    N1=NDRAD(1,ISEG)
    N2=NDRAD(2,ISEG)

```

```

      LD(1)=N1
      LD(2)=N2
CXXX  IF (IGEOM.EQ.1) CALL RADII (X,R0,R1,R2,TWOPI,N1,N2)
C.....DETERMINE EXCHANGE FACTORS FOR ROW ISEG
      J=NRSEG*(NB-1)+ISEG
      DO 240 I=1,NRSEG
        FROW(I)=AEF(I,J)
      240 CONTINUE
C.....LOOP ON J SURFACES
      SUM=0
      DO 250 JSEG=1,NRSEG
        SUM=SUM+FRAC(JSEG)*FROW(JSEG)*TS(JSEG)**4
      250 CONTINUE
      SUM=SUM-FRAC(ISEG)*FROW(ISEG)*TS(ISEG)**4
C.....DETERMINE EMISSIVITY OF SEGMENT ISEG
      EPS(1)=0.
      DO 260 I=1,NRSEG
        EPS(1)=EPS(1)+FROW(I)
      260 CONTINUE
C.....DETERMINE CONTRIBUTION TO STIFFNESS MATRIX & LOAD VECTOR
CXXX  QNET(ISEG)=QNET(ISEG)+TWOPI*R0*ARAD(ISEG)*SIGMA
CXXX  1 *((EPS(1)-FROW(ISEG))*FRAC(ISEG)*TS(ISEG)**4-SUM)
      QNET(ISEG)=99999.
C
      IF (NRCOND(ISEG).EQ.1) GO TO 290
      DET=ARAD(ISEG)/6.
      S=DET*4.*SIGMA*FRAC(ISEG)*(EPS(1)-FROW(ISEG))*TS(ISEG)**3
      BCK(1)=S*(R1+R0)
      BCK(2)=S*R0
      BCK(3)=S*(R2+R0)
      S=DET*SIGMA*(3.*FRAC(ISEG)*(EPS(1)-FROW(ISEG))*TS(ISEG)**4+SUM)
      BCF(1)=S*(R1+2.*R0)
      BCF(2)=S*(R2+2.*R0)
      CALL ADDBC (GK,GF,BCK,BCF,LD,JDIAG,TEMP(N1),TEMP(N2),ALPHA,ITRAN)
      290 CONTINUE
      300 CONTINUE
      GO TO 350
C
C VIEW FACTORS WITH NBAND=1 USED IN CALCULATIONS
C
      310 CONTINUE
C.....CALCULATE SEGMENT TEMPERATURE
      DO 320 ISEG=1,NRSEG
        IF (NCRAD(ISEG).EQ.0) THEN
          TS(ISEG)=THOLE(ISEG)
        ELSE
          TS(ISEG)=(.25*(TEMP(NDRAD(1,ISEG))**4+TEMP(NDRAD(2,ISEG))**4
          1 +TEMP(NDRAD(3,ISEG))**4+TEMP(NDRAD(4,ISEG))**4)**25
        ENDIF
      320 CONTINUE
C.....CALCULATE SEGMENT RADIOSITY
      DO 330 I=1,NRSEG

```

```

      B(I)=0.
      DO 330 J=1,NRSEG
        B(I)=B(I)+AEF(I,J)*SIGMA*TS(J)**4
      330 CONTINUE
C.....CALCULATE NET RADIATION FLUX AT SEGMENT
      DO 340 ISEG=1,NRSEG
        DO 331 I=1,4
          LD(I)=NDRAD(I,ISEG)
          BCF(I)=0.
        331 CONTINUE
        DO 332 I=1,10
          BCK(I)=0.
        332 CONTINUE
        ITRI=0
        IF (LD(3).EQ.LD(4)) ITRI=1
C.....DETERMINE SEGMENT EMISSIVITY
        IF (NCRAD(ISEG).EQ.0) THEN
          EPS(1)=0.9999
        ELSE
          EPS(1)=EMIS(1,NCRAD(ISEG))
        ENDIF
C.....CALCULATE SEGMENT IRRADIATION
        H(ISEG)=(B(ISEG)-EPS(1)*SIGMA*TS(ISEG)**4)/(1.-EPS(1))
        QNET(ISEG)=ARAD(ISEG)*(SIGMA*EPS(1)*TS(ISEG)**4-EPS(1)*H(ISEG))
        IF (NRCOND(ISEG).EQ.1) GO TO 340
        F=4.*EPS(1)*SIGMA*TS(ISEG)**3
        C=3.*EPS(1)*SIGMA*TS(ISEG)**4+EPS(1)*H(ISEG)
        DO 335 L=1,4
          CALL SHAPE2 (RG(L),SG(L),DIS,X,LD,SH,ITRI)
          K=0
          DO 334 J=1,4
            BCF(J)=BCF(J)+SH(J)*C*DIS
          DO 334 I=1,J
            K=K+1
            BCK(K)=BCK(K)+SH(I)*F*DIS*SH(J)
          334 CONTINUE
          335 CONTINUE
          CALL ADDBC (GK,GF,BCK,BCF,LD,JDIAG,TEMP(LD(1)),TEMP(LD(2)),
            1 TEMP(LD(3)),TEMP(LD(4)),ALPHA,ITRAN)
        340 CONTINUE
        GO TO 350
C *****
C ENCLOSURE RADIATION (NBAND=1) WITH VIEW FACTOR EXCHANGE METHOD
C WRITTEN BY DAVID D. GOETTSCHE
C *****
      365 CONTINUE
C.....VIEW FACTOR MATRIX IS RECALCULATED AT THE FIRST ITERATION (ITTE)
C.....AFTER THE SPECIFIED NUMBER OF TIME STEPS (NTAEF).
      IF ((NSTEP.EQ.1).AND.(ITTE.EQ.1)) GO TO 367
      J=MOD(NSTEP,NTAEF)
      IF ((J.NE.0).OR.(ITTE.GT.1)) GO TO 480
      367 CONTINUE

```



```

C.....ZERO OUT MODIFIED VIEW FACTOR MATRIX
  DO 370 I=1,NRSEG
  DO 370 J=I,NRSEG
    RAEF(I,J)=0.0
    RAEF(J,I)=0.0
  370 CONTINUE
C.....CALCULATE BAFFLE HEIGHT AT PRESENT TIME
  D1=WITHD1*TIME+GAP
  IF (D1.LT.DIST1) THEN
    BAFFLE=WITHD1*TIME+GAP
  ELSE
    BAFFLE=WITHD2*(TIME-DIST1/WITHD1)+DIST1+GAP
  ENDIF
C.....DETERMINE IF BAFFLE IS WITHIN THE OBSTRUCTION HEIGHT RANGE. IF
C.....THE BAFFLE DOES OBSTRUCT, EXCHANGE VIEW FACTORS FROM ORIGINAL
C.....SURFACE PAIR TO EACH SURFACE AND THE BAFFLE. NFLAG IS USED TO
C.....DETERMINE IF VF EXCHANGE HAS TAKEN PLACE FOR EITHER THE BOTH #1
C.....AND #2 BAFFLES. THE BAFFLE AREA RATIOS, ARTOPI,ARBOTI..., ARE USED
C.....TO GIVE A UNIFORM VF (AND HEAT FLUX) OVER ALL THE ELEMENTS OF A
C.....BAFFLE SURFACE.
C
C.....NEW SURFACE ELEMENTS (INTERCEPT & BAFFLE ELS.) DO NOT GO THROUGH
C.....EXCHANGE LOGIC
  NNSEG=NRSEG-NINS-NIBS-NOBS
  DO 430 I=1,NNSEG
  DO 420 J=I,NNSEG
    NFLAG=0
C.....#1 BAFFLE VF EXCHANGE LOGIC
  IF ((HI(I,J).LT.BAFFLE).AND.(HI(J,I).GT.BAFFLE)) THEN
    DO 380 K=1,NIBS/2
      RAEF(I,KBOTI(K))=ARBOTI(K)*AEF(I,J)+RAEF(I,KBOTI(K))
      RAEF(J,KTOPI(K))=ARTOPI(K)*AEF(J,I)+RAEF(J,KTOPI(K))
      RAEF(KBOTI(K),I)=ARAD(I)/ARAD(KBOTI(K))*AEF(I,J)+RAEF(KBOTI(K),I)
      RAEF(KTOPI(K),J)=ARAD(J)/ARAD(KTOPI(K))*AEF(J,I)+RAEF(KTOPI(K),J)
    380 CONTINUE
    RAEF(I,J)=0.0
    RAEF(J,I)=0.0
    NFLAG=1
  ELSE IF ((HI(I,J).GE.BAFFLE).AND.(HI(J,I).LT.BAFFLE)) THEN
    DO 390 K=1,NIBS/2
      RAEF(I,KTOPI(K))=ARTOPI(K)*AEF(I,J)+RAEF(I,KTOPI(K))
      RAEF(J,KBOTI(K))=ARBOTI(K)*AEF(J,I)+RAEF(J,KBOTI(K))
      RAEF(KTOPI(K),I)=ARAD(I)/ARAD(KTOPI(K))*AEF(I,J)+RAEF(KTOPI(K),I)
      RAEF(KBOTI(K),J)=ARAD(J)/ARAD(KBOTI(K))*AEF(J,I)+RAEF(KBOTI(K),J)
    390 CONTINUE
    RAEF(I,J)=0.0
    RAEF(J,I)=0.0
    NFLAG=1
  ENDIF
C.....#2 BAFFLE VF EXCHANGE LOGIC
  IF (NOBS.GT.0)THEN
    IF ((HO(I,J).LT.BAFFLE).AND.(HO(J,I).GT.BAFFLE)) THEN

```

```

DO 400 K=1,NOBS/2
  RAEF(I,KBOTO(K))=ARBOTO(K)*AEF(I,J)+RAEF(I,KBOTO(K))
  RAEF(J,KTOPO(K))=ARTOPO(K)*AEF(J,I)+RAEF(J,KTOPO(K))
  RAEF(KBOTO(K),I)=ARAD(I)/ARAD(KBOTO(K))*AEF(I,J)+RAEF(KBOTO(K),I)
  RAEF(KTOPO(K),J)=ARAD(J)/ARAD(KTOPO(K))*AEF(J,I)+RAEF(KTOPO(K),J)
400 CONTINUE
  RAEF(I,J)=0.0
  RAEF(J,I)=0.0
  NFLAG=1
  ELSE IF ((HO(I,J).GE.BAFFLE).AND.(HO(J,I).LT.BAFFLE)) THEN
DO 410 K=1,NOBS/2
  RAEF(I,KTOPO(K))=ARTOPO(K)*AEF(I,J)+RAEF(I,KTOPO(K))
  RAEF(J,KTOPO(K))=ARTOPO(K)*AEF(J,I)+RAEF(J,KBOTO(K))
  RAEF(KTOPO(K),I)=ARAD(I)/ARAD(KTOPO(K))*AEF(I,J)+RAEF(KTOPO(K),I)
  RAEF(KBOTO(K),J)=ARAD(J)/ARAD(KBOTO(K))*AEF(J,I)+RAEF(KBOTO(K),J)
410 CONTINUE
  RAEF(I,J)=0.0
  RAEF(J,I)=0.0
  NFLAG=1
  ENDIF
  ENDIF
C.....IF BAFFLE HEIGHT IS NOT WITHIN OBSTRUCTION RANGE, THE ORIGINAL
C.....VIEW FACTORS ARE PLACED IN THE MODIFIED VF MATRIX
  IF (NFLAG.EQ.0) THEN
    RAEF(I,J)=AEF(I,J)
    RAEF(J,I)=AEF(J,I)
  ENDIF
420 CONTINUE
430 CONTINUE
C
C.....CALCULATE BAFFLE SURFACE VF ROW SUM
  VFRSI=0.0
  VFRSO=0.0
  DO 440 I=1,NRSEG
    IF (NIBS.GT.0) VFRSI=VFRSI+RAEF(KTOPI(1),I)
    IF (NOBS.GT.0) VFRSO=VFRSO+RAEF(KTOPO(1),I)
440 CONTINUE
C
C.....ADJUST EACH BAFFLE ELEMENT VIEW FACTOR SO THAT THEIR ROW SUM IS
C.....EQUAL TO 1. WHEN BAFFLE FALLS, IT'S ROW SUM IS ZERO.
  DO 470 I=1,NRSEG
    IF (VFRSI.GT.0) THEN
      DO 450 K=1,NIBS/2
        RAEF(KTOPI(K),I)=RAEF(KTOPI(K),I)/VFRSI
        RAEF(KBOTI(K),I)=RAEF(KBOTI(K),I)/VFRSI
450 CONTINUE
      ENDIF
    IF (VFRSO.GT.0) THEN
      DO 460 K=1,NOBS/2
        RAEF(KTOPO(K),I)=RAEF(KTOPO(K),I)/VFRSO
        RAEF(KBOTO(K),I)=RAEF(KBOTO(K),I)/VFRSO
460 CONTINUE

```

```

ENDIF
470 CONTINUE
C
480 CONTINUE
C.....INTERCEPT SURFACES HAVE NO VIEW FACTORS AND DO NOT GO THROUGH HEAT
C.....FLUX CALCULATIONS
NNSEG=NRSEG-NINS
C.....CALCULATE SEGMENT TEMPERATURE
DO 490 ISEG=1,NNSEG
IF ((NCRAD(ISEG).EQ.0).AND.(THOLE(ISEG).GT.0.0)) THEN
TS(ISEG)=THOLE(ISEG)
ELSE
TS(ISEG)=(.25*(TEMP(NDRAD(1,ISEG))**4+TEMP(NDRAD(2,ISEG))**4
1 +TEMP(NDRAD(3,ISEG))**4+TEMP(NDRAD(4,ISEG))**4)**.25
ENDIF
490 CONTINUE
ITER=0
ENORM1=0.
C.....DETERMINE SEGMENT EMISSIVITY
DO 500 ISEG=1,NNSEG
IF ((NCRAD(ISEG).EQ.0).AND.(THOLE(ISEG).EQ.0.0)) THEN
C.....DETERMINE EMISSIVITY OF COOLING CHAMBER AND SUSCEPTOR
IF (TS(ISEG).LE.TCOLD) THEN
EPS(ISEG)=EMIS(1,NECOLD)
ELSE
EPS(ISEG)=0.9999
IF (NEHOT.GT.0) EPS(ISEG)=EMIS(1,NEHOT)
ENDIF
ELSE
EPS(ISEG)=EMIS(1,NCRAD(ISEG))
ENDIF
B(ISEG)=0.
500 CONTINUE
C.....RADIOSITY CALCULATIONS
510 ITER=ITER+1
IF (ITER.LT.ITMAXB) GO TO 520
WRITE (6,360)
CALL ADIOS (2)
520 DO 540 ISEG=1,NNSEG
C.....DETERMINE VIEW FACTORS FOR ROW ISEG
DO 530 JSEG=1,NNSEG
FROW(JSEG)=RAEF(ISEG,JSEG)
530 CONTINUE
C.....DETERMINE IRRADIATION AND RADIOSITY
C
C
C H(ISEG)=FDOT(FROW,B,NRSEG)
C
C --- COMPUTE DOT PRODUCT LOCALLY
C
FDOT = 0.0
DO 535 IDOT=1,NNSEG

```



```

      FDOT = FDOT + ( FROW(IDOT) * B(IDOT) )
535 CONTINUE
      H(ISEG)=FDOT
C-----
      B(ISEG)=EPS(ISEG)*SIGMA*TS(ISEG)**4+(1.-EPS(ISEG))*H(ISEG)
540 CONTINUE
C.....DETERMINE RADIOSITY CONVERGENCE
C-----
C
C  ENORM2=SQRT(FDOT(B,B,NRSEG))
C
C --- COMPUTE DOT PRODUCT LOCALLY
C
      FDOT = 0.0
      DO 545 IDOT=1,NNSEG
        FDOT = FDOT + ( B(IDOT) * B(IDOT) )
545 CONTINUE
      ENORM2=SQRT(FDOT)
C-----
      IF (ABS(1.-ENORM1/ENORM2).LE.TOLB) GO TO 550
      ENORM1=ENORM2
      GO TO 520
C.....RADIOSITIES ARE NOW KNOWN.
C.....DETERMINE CONTRIBUTION TO STIFFNESS MATRIX AND LOAD VECTOR
550 DO 590 ISEG=1,NNSEG
      DO 560 I=1,4
        LD(I)=NDRAD(I,ISEG)
        BCF(I)=0.
560 CONTINUE
      DO 565 I=1,10
        BCK(I)=0.
565 CONTINUE
      ITRI=0
      IF (LD(3).EQ.LD(4)) ITRI=1
C.....CALCULATE SEGMENT IRRADIATION
      QNET(ISEG)=ARAD(ISEG)*(B(ISEG)-H(ISEG))
      IF (NRCOND(ISEG).EQ.1) GO TO 590
      F=4.*EPS(ISEG)*SIGMA*TS(ISEG)**3
      C=3.*EPS(ISEG)*SIGMA*TS(ISEG)**4+EPS(ISEG)*H(ISEG)
      DO 580 L=1,4
        CALL SHAPE2 (RG(L),SG(L),DIS,X,LD,SH,ITRI)
C---CONSISTENT
      K=0
      DO 570 J=1,4
        BCF(J)=BCF(J)+SH(J)*C*DIS
      DO 570 I=1,J
        K=K+1
        BCK(K)=BCK(K)+SH(I)*F*DIS*SH(J)
570 CONTINUE
580 CONTINUE
      CALL ADDBC (GK,GF,BCK,BCF,LD,JDIAG,TEMP(LD(1)),TEMP(LD(2)),
1          TEMP(LD(3)),TEMP(LD(4)),ALPHA,ITRAN)

```

```
590 CONTINUE
C
350 CONTINUE
    RETURN
C
360 FORMAT(/' *** ERROR *** RADIOSITY ITERATIONS GREATER THAN ITMAXB'
1)
END
```

APPENDIX I

ANALYTICAL 2D VIEW FACTOR CODE

PROGRAM VIEW

```
C
C WRITTEN BY DAVID D. GOETTSCH
C VIEW- 2D VIEW FACTOR CODE FOR A PLANAR MOLD SURFACE BEING WITHDRAWN
C FROM A DIRECTIONAL SOLIDIFICATION FURNACE. THE VIEW FACTORS OF THE
C MOLD SURFACE TO EACH FURNACE COMPONENT ARE CALCULATED USING
C 2D VIEW FACTOR EQUATIONS TAKEN FROM "FUNDAMENTALS OF HEAT TRANSFER",
C BY F. P. INCROPERA, 1986, P.590.
C

      REAL PFT(50),PFTB(50),PFBB(50),PFBS(50),PMB(50),PFC(50),
1 PFS(50),LS,LC,LB,HS,HB,HTC,HBC,HEC,HEB,NINC,BAFTL(50),
2 BAFBL(50)
      INTEGER I,J,INC
C***
      OPEN (UNIT = 15,FILE = 'pvfout',STATUS = 'UNKNOWN')
C***
C*** PFT( ) - PLANAR VIEW FACTORS FROM ELEMENTS TO FURNACE TOP
C*** PFTB( ) - " " " " " " " TOP BAFFLE
C*** PFBB( ) - " " " " " " " BOTTOM BAFFLE
C*** PFBS( ) - " " " " " " " BAFFLE SIDE
C*** PMB( ) - " " " " " " " MOLD BASE
C*** PFC( ) - " " " " " " " CHERRIO
C*** PFS( ) - " " " " " " " FURNACE SUSCEPTOR
C*** RS - RADIUS OF SUSCEPTOR
C*** RC - RAD. OF CHERRIO
C*** RCB - RAD. OF CLUSTER BASE
C*** RB - RAD. OF BAFFLE
C*** RM - RAD. OF MOLD
C*** HS - HEIGHT OF SUSCEPTOR
C*** HMB - HEIGHT OF CLUSTER MOLD BASE
C*** HTC - HBC - HEIGHT OF TOP & BOTTOM OF EXPOSED CHERRIO
C*** HTS - HBC - " " " " " " " SUSCEPTOR
C*** HEC - HEIGHT OF ELEMENT CENTER ABOVE CHILL PLATE
C*** HEB - HEIGHT OF ELEMENT CENTER ABOVE BAFFLE
C*** WE - WIDTH OF ELEMENT
C*** WT - WIDTH OF TOP
C*** HB - HEIGHT OF BAFFLE
C*** NINC - INCREMENT DISTANCE
C*** GAP - START-UP GAP BETWEEN CHILL PLATE & SUSCEPTOR
C***
      RS = 9.0
      RC = 10.0
      RCB = 9.0
      HS = 15.7
      HMB = 0.25
      WE = 0.5
```

```

      HB = 0.25
      GAP = 0.0
      WITHD = 11.0
C***
C**   default values
      RB = 8.0
      RM = 7.25
      HEC = 6.0
      NINC = 0.25
C**
      LS = RS - RM
      LC = RC - RM
      LB = RB - RM
      HEB = HEC - HMB - HB/2
      CON2 = HEB
      INC = WITHD/NINC
C**
      DO 10 I = 1,INC
C***
C*****
C*** VIEW FACTORS FOR FURNACE TOP
C***    $Fe-g = (Lg/Lc) * (Fg-c+ - Fg-+)$ 
C*****
      CON1 = HB/2
      CON = HS + HB/2
      HTC = YCOR(RM,HEB,RB,CON1,RS)
      IF (HTC .GT. CON) THEN
        HTC = XCOR(RM,HEB,RB,CON1,CON)
        WI = HTC - RM
      ELSE
        WI = RS - RM
      ENDIF
      WJ = (HS + HB/2) - HEB + WE/2
      F1 = ELL(WI,WJ)
      WJ = (HS + HB/2) - HEB - WE/2
      F2 = ELL(WI,WJ)
      PFT(I) = (WI/WE) * (F1 - F2)
C***
C*****
C*** VIEW FACTORS FOR EXPOSED CHERRIO
C*****
C****PLANE ELEMENT
C***** find blocking intercept in lower chamber
      IF ((HEB+WE/2) .GT. (-HB/2)) THEN
C*** element is above baffle
      CON = -HB/2
      HTC = YCOR(RM,HEB,RB,CON,RC)
      CON = -1 * (HEC - HMB - HEB)
      HBC = YCOR(RM,HEB,RCB,CON,RC)
      IF (ABS(HTC) .LT. ABS(HBC)) THEN
C*** plane face element
      WI = WE

```

```

        WJ = (HEB + ABS(HBC))*2
        F1 = EPP(WI,WJ,LC)
        WJ = (HEB + ABS(HTC))*2
        F2 = EPP(WI,WJ,LC)
        PFC(I) = (F1 - F2)/2
    ELSE
        PFC(I) = 0.0
    ENDIF
ELSE
C*** element is below baffle
C**** plane face element
        WJ = (ABS(HEB) - HB/2) * 2
        F1 = EPP(WE,WJ,LC)
        CON = -1 * (HEC - HMB - HEB)
        HBC = YCOR(RM,HEB,RCB,CON,RC)
        WJ = 2 * ABS(HBC)
        F2 = EPP(WE,WJ,LC)
        IF (F1 .GT. F2) THEN
            PFC(I) = F2 + (F1 - F2)/2
        ELSE
            PFC(I) = F1 + (F2 - F1)/2
        ENDIF
    ENDIF
C**
C***
C*****
C*** VIEW FACTORS FOR MOLD BASE
C*****
C***PLANE FACE ELEMENT
        IF (HEB .GT. -HB/2) THEN
            CON = -1 * (HEC - HMB - HEB)
            CON1 = -HB/2
C** xcor is intercept line on the mold base from element to baffle
            BASED = XCOR(RM,HEB,RCB,CON1,CON)
        ELSE
            BASED = RCB + 1.0
        ENDIF
C**
        IF (BASED .LE. RCB) THEN
            WI = BASED - RM
        ELSE
            WI = RCB - RM
        ENDIF
C**
        WJ = HEC - HMB + WE/2
        F1 = ELL(WI,WJ)
        WJ = HEC - HMB - WE/2
        F2 = ELL(WI,WJ)
        PMB(I) = (WI/WE)*(F1 - F2)
C**
C***
C*****

```

```

C*** VIEW FACTORS FOR BAFFLE
C*****
C*** plane face element
  IF ((HEB + WE/2) .GT. (HB/2)) THEN
    IF ((HEB - WE/2) .LE. (HB/2)) THEN
      WI = ABS(HEB) + WE/2. - HB/2
      F1 = ELL(WI,LS)
      F2 = ELL(WI,LB)
      PFTB(I) = F1 - F2
      BAFTL(I) = WI
    ELSE
      CONU = HEB - HB/2 + WE/2
      COND = HEB - HB/2 - WE/2
      F1 = ELL(CONU,LS)
      F2 = ELL(COND,LB)
      F3 = ELL(COND,LS)
      F4 = ELL(CONU,LB)
      PFTB(I) = (CONU*F1 + COND*F2 - COND*F3 - CONU*F4)/WE
      BAFTL(I) = WE
    ENDIF
  ELSE
    PFTB(I) = 0.0
  ENDIF
C***
  IF ((HEB-WE/2) .LT. (-HB/2)) THEN
    IF ((ABS(HEB) - WE/2) .LE. (HB/2)) THEN
      WI = ABS(HEB) + WE/2 - HB/2
      F1 = ELL(WI,LC)
      F2 = ELL(WI,LB)
      PFBB(I) = F1 - F2
      BAFBL(I) = WI
    ELSE
      CONU = ABS(HEB) - HB/2 + WE/2
      COND = ABS(HEB) - HB/2 - WE/2
      F1 = ELL(CONU,LC)
      F2 = ELL(COND,LB)
      F3 = ELL(COND,LC)
      F4 = ELL(CONU,LB)
      PFBB(I) = (CONU*F1 + COND*F2 - COND*F3 - CONU*F4)/WE
      BAFBL(I) = WE
    ENDIF
  ELSE
    PFBB(I) = 0.0
  ENDIF
C**
C***
C*****
C*** VIEW FACTORS FOR SUSCEPTOR
C*****
  IF (HEB .LT. (HB/2)) THEN
    HTC = YCOR(RM,HEB,RB,HB/2,RS)
    WI = WE

```

```

      WJ = (ABS(HEB) + HS + HB/2)*2.
      F1 = EPP(WI,WJ,LS)
      WJ = (ABS(HEB) + HTC + HB/2)*2.
      F2 = EPP(WI,WJ,LS)
      PFS(I) = (F1 - F2)/2
      IF (HTC .GT. (HS+HB/2)) PFS(I) = 0.0
    ELSE
      WJ = (HEB - HB/2)*2
      F1 = EPP(WE,WJ,LS)
      WJ = 2 * (HS + HB/2 - HEB)
      F2 = EPP(WE,WJ,LS)
      IF (F1 .GT. F2) THEN
        PFS(I) = F2 + (F1 - F2)/2
      ELSE
        PFS(I) = F1 + (F2 - F1)/2
      ENDIF
    ENDIF
  ENDIF
C***
C***
C*****
C*** VIEW FACTORS FOR BAFFLE SIDE
C*****
C*** plane face element
      WI = WE
      WJ = (ABS(HEB) + HB/2) * 2.
      F1 = EPP(WI,WJ,RB-RM)
      WJ = (ABS(HEB) - HB/2) * 2.
      F2 = EPP(WI,WJ,RB-RM)
      PFBS(I) = (F1 - F2)/2.
C*****
      HEB = HEB - NINC
10  CONTINUE

C***
C**
      WRITE(15,*)'HEB Psuc PTbaf PMbaf PBbaf Pch Psusc',
x ' PMbas '
      DO 20 I = 1,INC
        WRITE (15,1500) CON2,PFT(I),PFTB(I),PFBS(I),PFBB(I),
x PFC(I),PFS(I),PMB(I)
        CON2 = CON2 - NINC
      20 CONTINUE
1500 FORMAT (F6.3,9(2X,F6.5))
C***
      CLOSE (UNIT = 15,STATUS = 'KEEP')
      END
C*****
C***
      FUNCTION ELL(WI,WJ)
        ELL = (1. + (WJ/WI) - SQRT(1. + (WJ/WI)**2))/2.
      RETURN
      END

```

```

C***
  FUNCTION EPP(WI,WJ,RLS)
    RWI = WI/RLS
    RWJ = WJ/RLS
    CON = SQRT((RWI + RWJ)**2 + 4.)
    CON1 = SQRT((RWJ - RWI)**2 + 4.)
    EPP = (CON - CON1)/(2. * RWI)
  RETURN
END
C***
  FUNCTION YCOR(XI,YI,XB,YB,X)
    YCOR = YB - (YI - YB)*(XB - X)/(XI - XB)
  RETURN
END
C***
  FUNCTION XCOR(XI,YI,XB,YB,Y)
    XCOR = XB - (XI - XB)*(YB - Y)/(YI - YB)
  RETURN
END

```


APPENDIX J

ANALYTICAL 2D HEAT FLUX CODE

```
PROGRAM HEAT
C
C WRITTEN BY DAVID D. GOETTSCH
C
C HEAT- 2D RADIATION HEAT FLUX CODE WHICH READS IN VIEW FACTORS
C OF DIRECTIONAL SOLIDIFICATION FURNACE COMPONENTS AND
C CALCULATES THE HEAT FLUX INTO A PLANAR MOLD SURFACE.
C THE FURNACE COMPONENTS ARE GIVEN A CONSTANT TEMPERATURE
C AND THE MOLD SURFACE FOLLOWS A TEMPERATURE HISTORY.
C

      REAL PFT(50),PFTB(50),PFBB(50),PFBS(50),PMB(50),PFC(50),
      1 PFS(50),NINC,TMOLD(50),TEMP(8),HTOP(50),HSUSC(50),HTBAF(50),
      2 HBAFS(50),HBBAF(50),HCHER(50),HMBAS(50),HEC,EXD(55,2),
      3 HEIT(50),HFLOWT(50,8),WITHD(50)
      INTEGER I,J,K,INC,NTINC
C
      OPEN (UNIT = 16,FILE = 'pvfout',STATUS = 'UNKNOWN')
      OPEN (UNIT = 17,FILE = 'pheatout',STATUS = 'UNKNOWN')
      OPEN (UNIT = 18,FILE = 'pseph',STATUS = 'UNKNOWN')
      OPEN (UNIT = 19,FILE = 'ex5054',STATUS = 'UNKNOWN')
C***
C*** PFT() - PLANAR VIEW FACTORS FROM ELEMENTS TO FURNACE TOP
C*** PFTB() - " " " " " " " TOP BAFFLE
C*** PFBB() - " " " " " " " BOTTOM BAFFLE
C*** PFBS() - " " " " " " " BAFFLE SIDE
C*** PMB() - " " " " " " " MOLD BASE
C*** PFC() - " " " " " " " CHERRIO
C*** PFS() - " " " " " " " FURNACE SUSCEPTOR
C*** HEIT() - HEIGHT OF ELEMENT CENTER ABOVE BAFFLE
C*** WE - WIDTH OF ELEMENT
C*** NINC - INCREMENT DISTANCE
C*** TSUSC - TEMP OF SUSCEPTOR ** 2850 - 3200 F
C*** TTOP - TEMP OF SUSCEPTOR TOP ** 2600 - 3000 F
C*** TTBAF - TEMP OF TOP OF BAFFLE ** 1000 - 2850 F
C*** TBAFS - TEMP OF BAFFLE SIDE ** 60 - 2850 F
C*** TBBAF - TEMP OF BOTTOM OF BAFFLE ** 200 - 2000 F
C*** TCHER - TEMP OF CHERRIO ** 60 - 1000 F
C*** TMBAS - TEMP OF MOLD BASE ** 60 - 2850 F
C***
C*** TWITHD - TOTAL WITHDRAWAL DISTANCE
C*** HEC - HEIGHT OF ELEMENT ABOVE CHILL PLATE
C*** WITHD() - WITHDRAWAL DISTANCE THROUGH THE PROCESS
C*** NTINC - NUMBER OF TEMPERATURE VARIATIONS TO SEE DEVIATION
C*** TEMPINC - TEMP. INCREMENT THAT WILL BE ADD TO THE BASE TEMP.
C**
C**      stef - bolt constant (Btu/sec-in2-R4)
```

```

      SBC = 3.35648E-15
      TWTHD = 11.0
      HEC = 6.0
      NINC = 0.25
C** ELEMENT WIDTH IN INCHES
      WE = 0.5
      NTINC = 5
      TEMPINC = -500.0
      EMISS = 1.0
C***
      TSUSC = 2850 + 459.7
      TTOP = 2850 + 459.7
      TTBAF = 2850 + 459.7
      TBBAF = 60 + 459.7
      TBAFS = 2850 + 459.7
      TCHER = 60 + 459.7
      TMBAS = 60 + 459.7
C**
      INC = TWTHD/NINC
C*
C*
C*****
C*** READ IN WITHDRAWAL HEIGHTS,VIEW FACTORS AND EXPERIMENTAL
C*** TEMPERATURE DATA IN FILE EX5054 FOR THE MOLD WALL TEMP.
C*****
      DO 20 I = 1,INC
        READ (16,*)HEIT(I),PFT(I),PFTB(I),PFBS(I),PFBB(I),PFC(I),
x        PFS(I),PMB(I)
      20 CONTINUE
C**
      DO 30 I = 1,53
        READ(19,*) EXD(I,1),EXD(I,2)
      30 CONTINUE
C*
C*
C*****
C*** TAKE EXPERIMENTAL DATA ARRAY AND INTERPOLATE SO VALUES
C*** CORRESPOND TO THE SIMULATION WITHDRAWAL DISTANCE.
C*****
      TMOLD(1) = EXD(1,2) + 459.7
      WITHD(1) = 0.0
      DO 40 I = 2,INC
        J = 1
        WITHD(I) = ABS(HEIT(1) - HEIT(I))
45      IF (WITHD(I) .LE. EXD(J,1)) THEN
        CON = (EXD(J,2) - EXD(J-1,2))*(WITHD(I)-EXD(J-1,1))
        TMOLD(I) = CON/(EXD(J,1) - EXD(J-1,1)) + EXD(J-1,2)
        TMOLD(I) = TMOLD(I) + 459.7
      ELSE
        J = J + 1
      GO TO 45
      ENDIF

```

```

40  CONTINUE
C*
C*
C*****
C*** CALCULATE HEAT FLOW FROM EACH FURNACE PIECE TO THE ELEMENT
C*** USING THE EXPERIMENTAL TEMPERATURE FOR THE ELEMENT AND
C*** VARYING ONE OF THE TEMPERATURE OF A FURNACE PIECE. THEN
C*** CALCULATE THE % DEVIATION FROM THE VARYING TEMPERATURE.
C*****
DO 50 I = 1,NTINC
C.... IN ORDER TO VARY SURFACE TEMPERATURES, TEMP(I) MUST BE SET
C....EQUAL TO THE FURNACE COMPONENT VARIABLE IN NEXT LINE.
TEMP(I) = TTOP
DO 55 J = 1,INC
TM = TMOLD(J)
CON = SBC * EMISS
HTOP(J) = CON * PFT(J) * (TM**4 - TTOP**4)
HSUSC(J) = CON * PFS(J) * (TM**4 - TSUSC**4)
HTBAF(J) = CON * PFTB(J) * (TM**4 - TTBAF**4)
HBAFS(J) = CON * PFBS(J) * (TM**4 - TBAFS**4)
HBBAF(J) = CON * PFBB(J) * (TM**4 - TBBAF**4)
HCHER(J) = CON * PFC(J) * (TM**4 - TCHER**4)
HMBAS(J) = CON * PMB(J) * (TM**4 - TMBAS**4)
HFLOWT(J,I) = HTOP(J) + HSUSC(J) + HTBAF(J) + HBAFS(J)
HFLOWT(J,I) = HFLOWT(J,I) + HBBAF(J) + HCHER(J) + HMBAS(J)
55  CONTINUE
C** increment the temperature
C....THE VARIABLES BELOW MUST ALSO BE SET TO THE FURNACE COMPONENT
C....NAME IN ORDER TO INCREMENT TEMPERATURES.
TTOP = TTOP + TEMPINC
50  CONTINUE
C**
C**
C*****
C*** PRINT OUT STATEMENTS FOR GRAPHING
C*****
DO 70 K = 1,NTINC
TEMP(K) = TEMP(K) - 459.7
70  CONTINUE
C**
C**
WRITE(18,*) 'height HTOP HSUSC HTBAF HBAFS',
1 ' HBBAF HCHER HMBAS'
WRITE(17,*) 'height',(TEMP(I), I=1,NTINC)
DO 80 K = 1,INC
WRITE(17,170) HEIT(K),(HFLOWT(K,I), I=1,NTINC)
WRITE(18,180) HEIT(K),HTOP(K),HSUSC(K),HTBAF(K),HBAFS(K),
1 HBBAF(K),HCHER(K),HMBAS(K)
80  CONTINUE
C**
170  FORMAT(2X,F7.4,6(4X,F10.8))
180  FORMAT(F6.3,7(2X,F8.6))

```

```
CLOSE (UNIT = 16,STATUS = 'KEEP')  
CLOSE (UNIT = 17,STATUS = 'KEEP')  
CLOSE (UNIT = 19,STATUS = 'KEEP')  
CLOSE (UNIT = 18,STATUS = 'KEEP')  
END
```